# *Long-term Reactivity Transient Analysis in an Extended Loss of all AC Power at the Koeberg Nuclear Plant*

By Neil Foster
March 2021

Supervisor : Professor David Aschman

University of Cape Town • iYunivesithi yaseKapa • Universiteit van Kaapstad

Mini-dissertation submitted in partial fulfilment of the requirements for
a degree of Master of Engineering
in the Faculty of Engineering and the Built Environment,
University of Cape Town

## Declaration

I declare that the entirety of work contained herein is my own original work,
that I am the authorship owner thereof (unless to the extent explicitly otherwise stated), and
that I have not previously submitted it for obtaining any qualification, in its entirety or in part.

Signed by candidate

Neil Andrew Sean Foster
*Submitted: 15 March 2021*
*Examiner's comments addressed: 7 November 2021*

I know the meaning of plagiarism and declare that all the work in the document, save for that which is properly acknowledged, is my own. This thesis/dissertation has been submitted to the Turnitin module and I confirm that my supervisor has seen my report and any concerns revealed by such have been resolved with my supervisor.

The copyright of this thesis vests in the author. No quotation from it or information derived from it is to be published without full acknowledgement of the source. The thesis is to be used for private study or non-commercial research purposes only.

Published by the University of Cape Town (UCT) in terms of the non-exclusive license granted to UCT by the author.

University of Cape Town

## Abstract

This study investigates, through neutronics and thermodynamic modelling of the Koeberg Nuclear Station, a 900 MW pressurized water reactor (PWR), whether extended loss of all AC power (ELAP) scenarios will result in an uncontrolled return to criticality. The purpose is to determine whether re-criticality can be avoided without performing plant modifications, or significantly adjusting the existing procedures to depressurize the primary system. The concern is that many currently proposed solutions introduce the risk of further complications, such as a loss of reactor coolant accident (LOCA).

The Fukushima Daiichi accident in 2011 was caused by a tsunami that resulted in an extended loss of all AC power at the power station, causing a major nuclear accident, highlighting the importance of introducing measures to deal with ELAP scenarios over and above the short-term AC power loss scenarios previously catered for. The immediate concern in an ELAP is to ensure sufficient removal of heat from the primary system. This is achieved by providing adequate secondary side feed-water and steam-evacuation capability from the steam generators, and maintaining an adequate volume of borated water in the primary system, to prevent overheating of the reactor core. However, in the ELAP scenario, a long-term reactivity concern develops as additional reactivity is introduced into the core by the cooling of the moderator (during the course of recovery actions) which is compounded by the decay of neutron poisons in the core.

The xenon isotope $^{135}Xe$ is a significant neutron poison which accumulates in the fuel of an operating nuclear reactor. Its presence in the fuel of a recently-tripped reactor initially helps to maintain sub-criticality, but this eventually decays away. This depletion starts at about 8 hours after a reactor trip, gradually adding more reactivity to the core. If borated water cannot be injected into the primary system to compensate for this, the reactor could return to criticality in an uncontrolled manner. Although this would be self-limiting (due to re-heating of the moderator and fuel), and not catastrophic in itself, the undesired generation of additional nuclear power in the reactor would, by consuming already limited supplies of cooling water, decrease the time available for recovery before the fuel in the reactor core overheats and melts.

Utilities have made proposals to maintain sub-criticality in an ELAP scenario, which do not require AC power. They involve introducing boron into the primary system. They are often costly, and some proposals require the operator to open the primary system relief valves, introducing an additional risk of a failure of the relief valves to close, leading to a loss of coolant accident, and a core melt.

The primary aim of the study was to determine, in an ELAP scenario, whether it is necessary to provide additional boron injection (over and above the existing accumulator inventory) to maintain the reactor sub-criticality. This was achieved using neutronics and thermodynamic modelling of Koeberg Nuclear Power Station. Another area of focus was to confirm that the existing cooldown strategies to mitigate ELAP events, are sufficient to maintain sub-criticality. After modelling and assessing the ELAP scenario over four different stages of the fuel cycle, it was concluded that, with best estimate assumptions, the selected reactivity acceptance criteria were met. However, with assumptions that envelope the majority of fuel cycle variances and code uncertainty (i.e. greater than 97.5% of cases), meeting the acceptance criteria for the latter part of the fuel cycle could not be demonstrated. Some potential solutions to ensure long-term sub-criticality are proposed.

## Table of Contents

Abstract ..... 2
I. Introduction ..... 5
II. Reactivity Concepts and Reactivity Balance Calculations ..... 8
Reactivity Concepts ..... 8
Reactivity Balance Calculations ..... 8
III. Reactivity Acceptance Criteria ..... 11
Design Extension Conditions Shutdown Margin Acceptance Criteria ..... 12
IV. Extended Loss of all AC Power (ELAP) Transient ..... 14
Description of a Generic ELAP Transient ..... 15
Worldwide Station Black-out Events ..... 18
Maanshan Station Blackout ..... 18
Notable Differences in the Design and Operation of 3-loop 900 MW PWRs ..... 19
ELAP Thermodynamic Analysis ..... 19
Overview of ELAP Reactivity Transient ..... 25
V. ELAP Reactivity Analysis ..... 27
Koeberg Neutronics Codes ..... 27
ELAP Transient Reactivity Analysis ..... 27
Integrated Control Rod Worth Including Power Defect Reactivity Analysis ..... 29
Cooldown Reactivity Analysis ..... 33
Additional Borated Water Insertion Reactivity Analysis ..... 35
Consolidation of Reactivity Results ..... 41
Neutronics Code Uncertainties ..... 42
Consolidation of all Significant Reactivity Contributors ..... 43
VI. Conclusion ..... 51
Potential Solutions ..... 53
Areas for Further Study ..... 53
VII. Acknowledgements ..... 54
VIII. References ..... 55
Appendix A: Reactivity Concepts ..... 57
Reactivity ..... 57
Excess Reactivity ..... 57
Reactivity Coefficients ..... 58
Control Rod Worth ..... 59
Moderator Temperature Co-efficient ..... 59
Fuel Temperature Co-efficient ..... 60
Void Content ..... 61
Power Co-efficient and Power Defect ..... 61
Boron Worth ..... 61

Uncontrollable Neutron Poisons ..... 62
Appendix B: Development of Accident Analysis in PWRs ..... 65
General Design Criteria for PWRs ..... 65
SL-1 Accident ..... 65
Three Mile Incident ..... 65
Chernobyl Accident ..... 66
Fukushima Accident ..... 66
Appendix C: SBO or Near SBO Events that have occurred at NPPs ..... 68
Appendix D: Integrated Control Rod Worth ..... 70
Appendix E: Power Defect ..... 74
Appendix F: Reactivity Reduction due to Reactor Trip ..... 75
Appendix G: Reactivity Change during Cooldown from Hot Shutdown down to RRA Conditions ..... 76
Appendix H: Koeberg Simulator Benchmarking of Maanshan Event ..... 80
List of Acronyms ..... 82

# I. Introduction

As a consequence of the Fukushima nuclear accident of 11 March 2011, involving four General Electric boiling water reactor (BWR) units on the Japanese coast, it became evident that all reactors should be capable of withstanding a long-term loss of electrical power. While such accidents give rise to many concerns, the focus of this mini-dissertation is specifically to confirm that in a long-term loss of all power to a 3-loop pressurized water reactor (PWR), the reactor will remain sub-critical without any additional boron injection, besides the existing passively injected accumulator volumes.

The Fukushima Daiichi accident (IAEA, 2015a) was initiated by a 9.0 $M_w$ (moment magnitude) earthquake off the Japanese coast, which induced a series of tsunami waves, the highest reaching 15 m above mean sea level at the site. The earthquake initially destroyed the offsite power supplies to all the units, which were only totally restored 11 days after the earthquake struck. Of the six boiling water reactors (BWR) at the site, three were in outage and three were operational. The three operational units were automatically tripped, and all of their emergency diesel generators successfully started, supplying the essential electrical power required to remove the residual decay heat in the operational units. At this point, the reactors were still well controlled.

Approximately 40 minutes later, the first tsunami wave struck. This, and subsequent waves, inundated the turbine hall, electrical switchboards and the emergency diesel generators, resulting in the loss of all AC power to Units 1 to 4. Unit 5 and 6 which were still in outage were powered by a sole surviving air cooled emergency diesel generator (EDG) which had been installed at a higher level. At this stage, all AC power sources had been lost on Units 1 to 4, a condition commonly termed a station blackout (SBO).

On some units, batteries designed to provide DC power for operating the control systems of the steam-driven emergency reactor cooling systems for eight hours were drained in a few minutes through immersion in sea-water. Limited power was restored by means of car batteries, but the major safety systems were disabled for several days by the extended loss of all AC power (now commonly referred to as ELAP). Due to the loss of electrical power, Unit 1 lost all core cooling within one hour of the tsunami. Both Units 2 and 3 had steam-driven cooling pumps, and core cooling continued, sometimes intermittently, for around four days until the steam-driven pumps were eventually lost. This, together with associated complications, ultimately resulted in the core melting in the three reactors.

Although BWR and pressurized water reactor (PWR) designs are different, they have similar vulnerabilities in an ELAP. The initial reactor trip (often termed *SCRAM*) will lead to the control rods inserting to provide significant sub-criticality. However, the cooldown of the reactor, together with the decay of xenon (a short-lived fission product normally present in the fuel of recently tripped reactors) could result in the reactor becoming critical again at some time after the initial trip if no means of introducing another neutron poison (e.g. boron) can be provided. This mini-dissertation assesses whether long-term sub-criticality can be maintained in a PWR, such as the two Koeberg reactors, with only passive injection of borated water by the existing accumulators during the expected cooldown and depressurization of the reactor by means of the existing steam generators, with no need to provide additional means of injecting borated water or intentionally opening the pressurizer relief valves to depressurize the primary system.

In an ELAP transient affecting a PWR, the immediate concern is to ensure that there is adequate feed-flow to, and steam evacuation from, the steam generators in order to remove core decay heat for a period of several days. Maintaining adequate primary system coolant is also necessary to ensure core cooling by transfer of heat from the primary system to the steam generators through natural circulation. As the primary system cools down, the moderator (water in the primary coolant) becomes denser and reactivity is inserted into the core. In addition, the concentration of $^{135}Xe$ (hereafter simply referred to as xenon), a fission product of nuclear fission (with a very large neutron

absorption cross section) which acts as a neutron absorber reaches a maximum concentration within the first 10 hours of the reactor tri., The Xenon then subsequently decays away, thus gradually resulting in additional reactivity insertion in the core. Without any additional boron injection into the primary system, the reactor could eventually become critical again in an uncontrolled manner, due to the loss of electrical power to normal boron injection systems.

Any uncontrolled return to criticality is undesirable, but it need not be catastrophic. As nuclear energy is generated in the core by nuclear fission, the moderator will heat up, thus lowering the reactivity of the reactor core. The increased moderator temperature will, in turn, result in more heat removal via the steam generators, and a new quasi-static thermal state will be attained with core power being limited to approximately 10% of the normal operating level. While this, in itself, may not be intolerable in the short term, evacuating this heat via the steam generators will cause more rapid depletion of limited supplies of emergency feed-water, and thereby hasten the onset of a core-melt accident. The aim of this mini-dissertation is to examine the long-term reactivity response in an extended loss of all AC power transient. The purpose is to confirm that a 3-loop PWR reactor, such as the Koeberg units, will remain sub-critical until a long-term safe steady state condition has been established, i.e. until a tolerable constant primary system pressure and temperature has been achieved, with essentially all xenon build-up having decayed out of the core.

To maintain sub-criticality under such conditions, nuclear utilities are investigating whether to provide additional boron injection systems. This includes proposals to either inject existing higher concentrated borated sources into the primary system, or to investigate methods of providing additional boron mixing capability that will operate in ELAP conditions. In addition, EDF are considering whether to relieve primary system pressure through the intentional early opening of pressurizer relief valves. This would rapidly reduce the primary pressure to below 4.2 MPa to induce the passive injection of borated water (contained in the three accumulators) into the primary system. This, however, carries the risk of inducing a loss of coolant accident (LOCA) if the pressurizer relief valves should fail to re-close when required, potentially complicating the ELAP scenario and increasing the likelihood of eventually melting the reactor core.

This study investigates whether it is necessary to provide additional boron injection, over and above the existing inventory in the accumulator, for an ELAP scenario, at Koeberg. This study also considers whether existing cool down strategies to mitigate SBO (or ELAP) events (where all on-site and off-site AC power sources are lost), relying only on cooling and depressurizing the primary system by means of the steam generators, are sufficient to maintain sub-criticality.

This analysis consists of quantifying the changes in the critical reactivity co-efficients for numerous fuel cycles, in an ELAP transient. Additional neutronics calculations were performed using SCIENCE a neutronics code (US-NRC, 1999) in order to determine the integrated control rod worth with all control rods inserted, as well as the moderator temperature effect during a postulated controlled cooldown using steam-generators. Other reactivity co-efficients were determined using either pre-existing reactivity calculations or existing plant data from previous fuel cycles. Key primary system input parameters such as primary system temperature and pressure during the ELAP transient were obtained using the Koeberg operator training simulator.

Confidence in the simulator modelling of an ELAP transient was gained by benchmarking the existing Koeberg model against an actual Three hour station black-out event that occurred in 2011, at Maanshan Nuclear Power Station, also a 3-loop 900 MWe reactor. Good correlation of the key parameters of interest was obtained between the simulations of an event at Koeberg, and the event that occurred at Maanshan.

After this introduction, a brief refresher on the key reactivity definitions and concepts that are important to this analysis follows. This includes defining reactivity, the separate contributors that

affect reactivity and how they combine to affect the overall reactivity in the reactor core. It also highlights the particular reactivity contributors in a PWR.

Then a description of typical extended loss of all AC power events on a PWR follows. A brief overview and simple description of actual SBO events that have occurred at other nuclear power plants around the world, including the Maanshan event, is presented. The event that occurred at Maanshan Nuclear Power Plant (NPP), which is a Westinghouse 900 MW, 3-loop unit is of particular interest, because that plant's reactor and primary system is similar in design and operation to the Koeberg plant, and provides a useful benchmark reference for at least the initial stage of a SBO transient. While the Maanshan event was limited to a total of around three hours, it provides a good benchmark to establish whether the simulator model is a reasonable tool to establish the thermo-hydraulic transient analysis. The ELAP transient, modelled using the Koeberg simulator as an ELAP occurring on one of the Koeberg units, is then presented. This ELAP transient analysis provides critical input such as primary system pressure, temperature and water inventory, during the transient, required for the reactivity calculations.

A discussion of what is considered reasonable acceptance criteria for sub-criticality for this analysis follows. This is necessary as the conservatism and modelling assumptions should comply with international norms and regulations. The ELAP scenario does not fall under classical design basis analysis, but falls into a category known as beyond design basis accidents (BDBA) which are modelled with less conservative methods than are used for design base accidents (DBAs). It entails multiple simultaneous failures, but cannot be practically eliminated from consideration and therefore now falls into a new, recently defined category of accidents, commonly referred to as design extension conditions (DECs). The section defines rules of performing DEC analyses that are different to the original DBA and touches on the evolution of the acceptance criteria for both design basis and design extension conditions.

The computation and calculations performed in this mini-dissertation to determine the reactivity change from each of the reactivity components is then presented, including combining them to quantify the overall reactivity changes expected to occur during the transient. It includes analyses to ensure that the variation in core reload patterns, as well as cycle duration are considered, covering numerous previous cycles that are representative of the existing and expected future core load configurations. Different phases of the cycle are considered as well as the effects on the different contributors to reactivity change over the fuel cycle. One of the challenges has been that there is not any obvious point in the cycle that can be assumed to be bounding. Therefore the full cycle range is considered, as taking any overly conservative approach is anticipated to result in unnecessarily penalizing results.

Finally, there is a discussion of the results, including the limitations of the study and recommendations for further work.

# II. Reactivity Concepts and Reactivity Balance Calculations

## Reactivity Concepts

Reactivity (ρ) is a measure of the fractional change in neutron population in a nuclear core, between neutron generations (NAoNT, 2014). Reactivity is used as a measure of a reactor's relative departure from criticality. It measures the deviation of an effective multiplication factor from unity. For critical conditions the reactivity is equal to zero, and becomes negative if the reactor is sub-critical, and positive if super-critical.

Mathematically, reactivity is a dimensionless number, but is expressed by various units. The usual units for commercial power reactors are pcm (1 pcm = ρ x $10^{-5}$) or %ΔK/K (Δk/k% = 1% x ρ = 1000 pcm). In many LWRs, including Koeberg) the typical measure in per cent mille (pcm), or one thousand of a percent ($10^{-3}$ x $10^{-2}$). Pcm is used as the unit of measure, as the reactivity insertion values are generally quite small and pcm allows reactivity to be written in whole numbers.

The reactivity in a core is dynamic and is therefore time dependent. In a PWR it changes in response numerous parameter including fuel and moderator temperature fluctuation, control rod positions, and reactor power level. A brief recapitulation of applicable reactivity related topics in nuclear physics necessary to follow this study is provided Appendix A. These include:

- Reactivity
- Excess Reactivity
- Reactivity Co-efficients
- Control Rod Worth
- Moderator Temperature Co-efficient
- Fuel Temperature Co-efficient
- Void Content
- Power Coefficient and Power Defect
- Uncontrollable Neutron Poisons (e.g. $^{135}$Xe, $^{139}$Sm)

For each of these parameters, there is a discussion of relevance to PWRs including an indication of the applicable range of values for PWRs.

## Reactivity Balance Calculations

In order to determine the reactivity changes in the core during an ELAP, a reactivity balance calculation will be performed. Such calculations are typically done on nuclear power plants to determine estimated critical positions, estimated critical boron concentrations and shutdown margins, and for the analysis of reactivity anomalies. These types of reactivity calculation are also suited to determining the reactivity of the plant during an ELAP transient.

There are two methods that are typically used to perform reactivity calculations for PWRs (US-NRC, 2011). These are the Δρ (delta rho) method and the reactivity balance method. The basis of both calculations relies on the fact that core reactivity is equal to zero when the reactor is critical. However, in order to apply the Δρ method a previous critical condition must be known.

Because this analysis focuses on the at-power transient, the reactor would initially be critical and assumed to be at constant power before the reactor trip. Hence, the sum of the reactivity contributions to the previous critical condition (net reactivity) must equal zero. The reactivity calculations in this study apply the Δρ method, as most of the input reactivity data is readily obtained or calculated.

The existing control-rod worth data is conservatively calculated assuming the highest worth control rod fully out of the core, as is conventional for design basis accident analysis. As part of this mini-dissertation it was necessary to re-calculate the integral control rod worth for all control rod assemblies inserting, using a neutronics code, to avoid unduly conservative results. The power defect, for the twelve core reload considered, could be sourced from the existing Koeberg Physics Databooks (ESKOM, PDBs), as well as the evolution reactivity effects of both xenon and samarium.

As there was no existing reactivity data for a cooldown from an initial shutdown condition, all of this reactivity data due to the cooldown to cold-shutdown conditions had to be calculated. The reactivity insertion from the accumulators injecting boron is determined by initially calculating the volume of borated water that is inserted, and the resultant primary system concentration, and then using the boron worth data from the Koeberg Physics Databooks (ESKOM, PDBs).

All the reactivity calculations that were required for this mini-dissertation were performed using the SCIENCE code package (see Section V for more details).

## *Adaptation of the Delta Rho (Δρ) Method to Determine Sub-criticality in ELAP*

In this method, the overall net reactivity, $\rho_{net}$ , is represented as the algebraic sum:

[1] -- $\rho_{net} = \rho_{pwr} + \rho_{rods} + \rho_{tmp} + \rho_{bor} + \rho_{xe} + \rho_{sm}$

where:

$\rho_{net}$ = net initial core reactivity;
$\rho_{pwr}$ = reactivity contribution due to power defect;
$\rho_{rods}$ = reactivity contribution due to control rods;
$\rho_{tmp}$ = reactivity contribution due to moderator temperature;
$\rho_{bor}$ = reactivity contribution due to boron concentration;
$\rho_{xe}$ = reactivity contribution due to xenon-135 concentration; and
$\rho_{sm}$ = reactivity contribution due to samarium-149 concentration.

The reactor is assumed to be at stable full power ($k_{eff}$ = 1) before the transient, referred to as the initial critical condition (designated with subscript '*1*'), so:

[2] -- $\rho_{net1} = \rho_{pwr1} + \rho_{rods1} + \rho_{tmp1} + \rho_{bor1} + \rho_{xe1} + \rho_{sm1}$

Since the net reactivity for the critical condition to be calculated during the transient (designated with subscript '*2*') must also be the sum of its core reactivity components, it can be expressed as:

[3] -- $\rho_{net2} = \rho_{pwr2} + \rho_{rods2} + \rho_{tmp2} + \rho_{bor2} + \rho_{xe2} + \rho_{sm2}$

Subtracting Equation [2] from Equation [1] we obtain:

[4] -- $\rho_{net2} - \rho_{net1} = (\rho_{pwr2} - \rho_{pwr1}) + (\rho_{rods2} - \rho_{rods1}) + (\rho_{tmp2} - \rho_{tmp2}) + (\rho_{bor2} - \rho_{bor1}) + (\rho_{xe2} - \rho_{xe1}) + (\rho_{sm2} - \rho_{sm1})$

For the initially critical reactor, $\rho_{net1} = 0$ and thus:

[5] -- $\rho_{net2} = (\rho_{pwr2} - \rho_{pwr1}) + (\rho_{rods2} - \rho_{rods1}) + (\rho_{tmp2} - \rho_{tmp2}) + (\rho_{bor2} - \rho_{bor1}) + (\rho_{xe2} - \rho_{xe1}) + (\rho_{sm2} - \rho_{sm1})$

Or, more simply:

[6] -- $\rho_{net2} = \Delta\rho_{pwr} + \Delta\rho_{rods} + \Delta\rho_{tmp} + \Delta\rho_{boron} + \Delta\rho_{xe} + \Delta\rho_{sm}$

where:

$\Delta\rho_{pwr}$ = change in reactivity contribution due to power defect;
$\Delta\rho_{rods}$ = change in reactivity contribution due to control rods;
$\Delta\rho_{tmp}$ = change in reactivity contribution due to moderator temperature;
$\Delta\rho_{bor}$ = change in reactivity contribution due to boron concentration;
$\Delta\rho_{xe}$ = change in reactivity contribution due to xenon concentration; and
$\Delta\rho_{sm}$ = change in reactivity contribution due to samarium concentration

Samarium is not a significant contributor, and it gradually increases after shutdown, leading to a gradual increase in shutdown margin, Therefore, for this reactivity analysis, $\Delta\rho_{sm}$ is disregarded as being negligible, leading to slightly conservative results. So finally:

[7] -- $\rho_{net2} = \Delta\rho_{pwr} + \Delta\rho_{rods} + \Delta\rho_{tmp} + \Delta\rho_{boron} + \Delta\rho_{xe}$

The reactivity change arising from each of these contributors will be calculated independently, and then summed to determine the cumulative impact on reactivity. Two significant sources of uncertainty will be considered specifically the variation over the different fuel cycles in order to ensure the results will envelop most core configurations and the code or calculation uncertainties.

However before we embark on the calculation, we must first define the technical acceptance criteria that must be met to ensure that the intent of this mini-dissertation can be achieved.

## III. Reactivity Acceptance Criteria

The US-NRC initially developed general design criteria (GDC) into their code of federal regulation for nuclear power plants, as documented in 10-CFR-50 Appendix A (US-NRC, 2017). They establish the minimum requirements for the principal design criteria for light water reactors in the USA. These GDC formed the basic design rules for all reactors built in the USA since the 1960s. As both PWRs and BWRs were initially developed in the USA, this set of design criteria forms the foundation for both of these reactor design basis. These GDC include requirements regarding the treatment of reactivity, as well as fundamental nuclear design concepts such as the "single failure" criterion. This criterion is to ensure that given a postulated initiating event (e.g. transient or accident), the failure of any individual component will not prevent the mitigation of the accident.

In response to nuclear power plant accidents, these design rules (and in certain case operating rules) have evolved over time to cater for new emerging concerns. Subsequent to the original development of the GDC, there have been significant nuclear accidents at certain commercial nuclear power plants, leading the regulators (including the US-NRC, the IAEA, and the South African NNR) to supplement their GDC with additional rules and safety tools, such as Probabilistic Safety Assessment (PSA).

In response to the Fukushima accident, there was a renewed focus on external hazards and the potential of underestimating them and their consequences. This renewed focus highlighted the subsequent loss of multiple safety systems, the impact of multiple units being affected simultaneously, and the need to analyze and mitigate prolonged accidents. It sped up the introduction of the concept of Design Extension Conditions (IAEA, 2019), which is a move away from the assumption that very unlikely events were not plausible.

New accidents, rather than being considered implausible or "beyond design basis", are now being grouped into a new class of accidents referred to as Design Extension Conditions (DEC). DECs can be assessed using best-estimate methodologies (IAEA, 2019) instead of the traditionally conservative methods employed for design basis accidents. The state of knowledge and the capabilities of analysis codes and design codes are now significantly better than when the general design codes were originally developed, so that best-estimate methods can be employed with a greater level of confidence. Appendix B provides more detail on the impact of various nuclear accidents influenced the analysis and mitigation of nuclear accident on PWRs.

ELAP, like an SBO, would be classified as a DEC as it is design basis accidents combined with multiple safety systems failures (IAEA, 2019). The Fukushima accident demonstrated that nuclear power plants need to consider accidents that last beyond 24 hours, and that prolonged loss of all electrical power was a real possibility. These factors are now being incorporated into the accident mitigation strategies of nuclear power plants.

## Design Extension Conditions Shutdown Margin Acceptance Criteria

This section defines the necessary margin of sub-criticality required in beyond design basis accidents, now referred to as DECs. The latest revision of IAEA standard for nuclear plant design (IAEA, 2016) defines four distinct plant operational states that should be considered in the design of a nuclear reactor, based on the frequency of occurrence, namely:

- Normal operation;
- Anticipated operational occurrences;
- Design basis accidents;
- Design extension conditions.

The first three have typically been identified during the design of the plant, but the latter plant state has been identified after the plant has been built and operated. Design extension conditions are derived for the purpose of further improving the safety of the nuclear power plant by enhancing the plant's capabilities to withstand, without unacceptable radiological consequences, accidents that are either more severe than design basis accidents or that involve additional failures (IAEA, 2016). Both SBO and ELAP events fall in to this category of design extension conditions. They are both anticipated operational occurrences combined with multiple failures of safety systems, i.e. the loss of off-site power combined with the failure of the emergency diesel generators and all alternative emergency power supplies.

Acceptance criteria for deterministic accident analysis should be established at two levels (IAEA, 2019):

(1) High level (radiological) criteria: relate to radiological consequences of plant operational states or accident conditions. They are usually expressed in terms of dose or activity levels, and are typically defined by regulatory requirements or law;

(2) Detailed technical criteria: relate to the integrity of barriers and releases of radioactive material (e.g. the fuel matrix, fuel cladding, reactor coolant system pressure boundary and containment). These are either defined in regulatory requirements, or proposed by the designer, and applied as part of the plant's safety demonstration.

Technical acceptance criteria are set in terms of the parameters that govern the physical processes that could impact on the integrity of a barrier. It is common engineering practice to use surrogate variables relating to the integrity of the barriers to establish an acceptance criterion, or a combination of criteria, to ensure the integrity of the barrier (IAEA, 2019). Sub-criticality would be considered as a surrogate acceptance criterion for integrity of the reactor core in SBO and ELAP.

Sub-criticality limits for the neutron multiplication factor, k-effective ($k_{eff}$), are typically used in commercial reactors to ensure adequate safety margin to uncontrolled criticality. For normal operation and design basis accidents, the criterion is a k-effective of less than or equal to 0.95 is widely employed worldwide for design base accident conditions. In the UK (Venner, 2003), k-effective must not exceed 0.95, except for systems where the uranium enrichment is less than 5% $^{235}U$ where a limit of 0.98 is applied, which would apply to a commercial PWR. However, in practice, in the UK, a value of 0.95 is often adopted for low enriched systems for normal conditions with 0.98 for contingency conditions, although there is no clear justification for this approach.

It is acceptable practice to use realistic modelling, assumptions and computer codes for Design Extension Conditions (IAEA, 2019), as opposed to the conservative analysis originally performed for design basis accidents. In recent submittals to the US-NRC, by plant such as North Anna (Dominion Energy, 2015), specifically for ELAP scenarios a shutdown margin acceptance criterion of $\Delta k/k\%=1\%$ (1 000pcm) has been used.

Ideally, the margin of sub-criticality calculated for the criticality safety assessment should be proportionate to the risks involved. The consequence of a return to criticality is limited to a return to power that will stabilize at less than 10%. This would still be within the design and capacity of the heat removal systems still available in an ELAP scenario, namely emergency steam dump from the steam generators to atmosphere and the feed-flow of the emergency turbine driven feed-water pump[1]. While a return to criticality will require an additional cooling water inventory, the event itself is not envisaged to result in any form of fuel damage or radioactive release.

It is therefore considered reasonable to adopt an acceptance criterion of $\Delta k/k\% = 1\%$, or 1000 pcm, for sub-criticality for ELAP as it would be defined as a Design Extension Condition. This was further supported by Dr. S. Steyn a reactor fuel engineering specialist at Koeberg, who in discussion, also independently suggested the acceptance criterion of 1000 pcm, for non-design basis reactivity accidents.

[1] This information come from a reference that is potentially propriety and for this reason is not explicitly referenced.

## IV. Extended Loss of all AC Power (ELAP) Transient

When commercial reactors were originally designed they did not consider the total loss of all AC power to be a credible scenario. Although the loss of offsite power, on its own, was considered a credible accident, redundant onsite EDGs to power the cooling safety systems, with battery back-ups for the DC control systems, were incorporated into the plant design. However, in principle, commercial reactors were designed to withstand single failures, so simultaneous failure of the off-site and on-site emergency electrical supplies was not considered a design requirement.

As a result of the Fukushima nuclear accident, the industry was faced with having to consider an accident scenario it had previously discounted: a prolonged loss of all AC power that could last for days. Previously, most loss of AC power accident analysis had been limited to less than a day, as it was assumed that the power supplies, either off-site or on-site emergency supplies, could be recovered within that time. The extended loss of AC power (ELAP), presents additional challenges including long-term cooling water supply, limited control and instrumentation power and, the focus of this dissertation, the risk of re-criticality due to cooling of the moderator and xenon depletion.

The normal operation of a PWR reactor is discussed extensively in the literature, such as *Introduction to Nuclear Engineering* (Lamarsh, 2001). A simplified diagram of the key features required for this dissertation is shown in Figure 1 below. The diagram shows one loop of the 3-loop plant for simplicity. The reactor core (1) is situated in the reactor vessel (2). Water, heated by the core, passes through the hot leg to the steam generators (SGs) (3). The primary water then flows through the U-tube bundles in the SGs, and exchanges its heat to the secondary side. The cooled water then flows to the primary pumps (4), and then back to the reactor vessel via the cold leg, down the down-comer (2a) to the bottom of the core. The pressurizer (6), situated on one of the loops maintains the primary pressure during normal operation, and each loop has an accumulator (5). In an SBO, heat is removed from the secondary side via the atmospheric steam dump (8), and the SGs inventory is replenished from the emergency condensate tank (9) using a steam-driven turbine pump (7). This tank will have to be replenished, which will eventually be achieved using a back-up water reservoir (10).

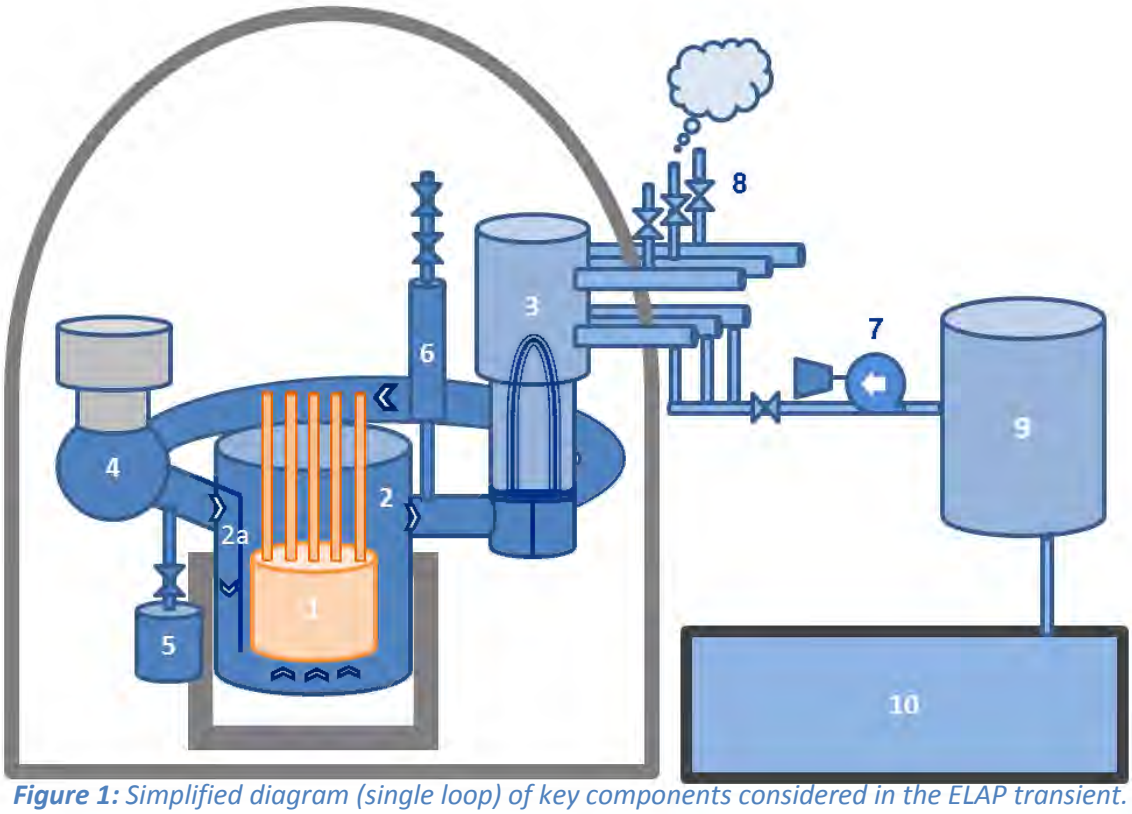


***Figure 1:*** *Simplified diagram (single loop) of key components considered in the ELAP transient.*

While the emergency condensate (ASG) tank has around 12 hours of water, it is assumed in this analysis that adequate make-up to the tank will be available, as a back-up water reservoir will be installed to provide water for over a week, for both units.

A general description of an SBO transient is described below, which will eventually evolve into an ELAP scenario, if power cannot be restored within a few hours.

## *Description of a Generic ELAP Transient*

In the event of a loss of off-site power on a PWR reactor, all control rods will fall into the core under the influence of gravity, as a result of loss of power to the control rod drive mechanism. Power to the primary reactor coolant pumps that provide forced circulation in normal operation will be lost, and they will coast down over a period of 10 minutes. When secondary side feed flow and steam-dump capability are established to the steam generators, the hot primary coolant will flow from the top reactor core (located at a lower elevation than the water-tubes of the steam generators) where the primary water is cooled. This is achieved by the evaporation of secondary side water in the steam generators (shell side). As the primary coolant temperature reduces it becomes denser and returns to the bottom of the reactor core, which is at a lower elevation. PWRs are specifically designed to be able to use this process, referred to as 'natural circulation', which is capable of transferring decay heat from the reactor to the steam generators in accident conditions, when forced circulation fails.

The normal secondary side feed-water supply to the SGs will be lost, as it is not backed-up with emergency power supplies. The units are equipped with an emergency feed-water supply, which consists of two electrically powered feed-water pumps and a single turbine powered feed-water pump. If, in addition to off-site power supplies, the on-site EDGs are also lost, then a steam-powered auxiliary feed-water pump is the only feed-water supply to the SGs. It takes suction from a tank that contains enough water to last about 12 hours, without additional make-up. This feed-water pump is powered by the steam still being generated from the residual heat of the reactor core. Heat removal in these circumstances is achieved through the secondary side SG steam-dump valves that open directly from the steam generators to the atmosphere. The control systems of the steam-driven pump and the actuators of the steam-dump valves are designed to operate using a combination of DC power and compressed air, but this equipment can be operated by hand if required. At Koeberg, it is currently not possible to inject water into the primary system to make up any significant primary water loss, without AC power.

In order to endure a prolonged SBO, or ELAP, it is necessary to maintain the power that has to be removed within the capability of the heat removal systems, ideally by keeping the reactor sub-critical, and to minimize the consumption of cooling water. While re-criticality will lead to more power production, the power will be inherently limited by the subsequent primary system coolant heat-up. The power level remains within the capacity of the steam-driven auxiliary feed pump and the SG steam dump system. However, it will significantly increase the rate at which the available cooling water inventories will be depleted, and thus hasten the onset of a core-melt accident.

In order to ensure that natural circulation continues to remove the core residual energy to the secondary system and ultimately to atmosphere, the core must remain covered, so the primary system's coolant inventory must be maintained. The most significant risk to losing primary water

inventory is through the reactor coolant system (RCP) pump seals[2]. With the loss of electrical power, seal injection will be lost and the seal could leak or rupture, leading to a significant loss of primary coolant. While Koeberg does have a small seal injection powered by a dedicated power supply, this system is not designed to withstand most external hazards.

With the loss of primary water inventory natural circulation will eventually stall. This will eventually lead to the primary system heating up and re-pressurizing and eventually reaching the safety valve set-point. At this point primary water inventory, in the form of steam via the safety valves will be lost. When sufficient primary inventory is lost, the core will be uncovered, leading to core melt.

In order to eliminate this risk, Koeberg is in the process of procuring recently developed RCP pump passive shutdown seals, specifically designed for this type of transient. This analysis assumes that these are installed and therefore does not consider the RCP pumps seal as a leak path. Another potential significant primary system inventory loss path could be the failure of a pressurizer relief valves to close, if they were to open. One of the aims of this mini-dissertation is ideally to demonstrate that there is no need to open the primary system relief valve to induce rapid injection borated water by the accumulators, thus significantly reducing the risk of inventory loss through this pathway.

Another important consideration is preventing the injection of non-condensable gases into the primary system. This could lead to a build-up of non-condensable gases in the top of the SG tubes, which would prevent natural circulation. The primary concern here involves the injection of the nitrogen that is used as a pressure blanket in the accumulators. The existing design does not allow for the accumulators to be isolated in an SBO scenario, as the existing accumulator isolation valves are powered by AC power. If the primary system pressure drops too low, the nitrogen in the top of the accumulators could be injected into the primary system. This is currently prevented by procedurally limiting SG depressurization, thus maintaining the primary system pressure above the pressure that would result in nitrogen injection from the accumulators.

Finally, as was the case at Maanshan, it must be taken into consideration that the reactor may be tripped as a precaution before the onset of a classic SBO, especially in the case of a gradually decaying electrical system. This has the benefit of reducing the residual decay heat that needs to be removed by the time all AC power is lost. However, because in such scenarios the decay of xenon will have progressed to some extent by the time the SBO begins, such a situation may be more likely to give rise to a return to criticality than a complete and immediate SBO.

This makes a time dependent reactivity analysis, as was originally envisaged, limited in terms of the conclusions reached. Therefore the analysis initially focuses on the ELAP transient without the xenon and samarium contribution which are time-dependent. The enveloping (limiting) reactivity contribution of the two nuclides is dealt with last, considering the worst case, i.e. the total decay of both neutron poisons, in order to ensure that the analysis envelopes all the potential cooldown scenarios.

[2] Koeberg has been modified to provide an emergency seal injection system that is powered by a small diesel generator that also provides electrical supply to essential battery chargers. It was not designed specifically to cope with external hazards such as occurred at Fukushima. For the purpose of retaining generality of the conclusions of this study, this emergency seal injection system was disabled in the Koeberg simulator, but it was assumed that no coolant would be lost through the seals. Thus, the model used for the analysis corresponds to a Koeberg-type reactor with no emergency seal injection system but with shutdown seals installed. Because these assumptions do not consider the addition of borated water through the seals, the results are conservative in regard to criticality, but should not be taken as a full investigation of an SBO at Koeberg in its current configuration.

To summarize, the evolution of a typical ELAP transient applying the SBO emergency operating procedure (ECA-0.0) is as follows. The plant will initially trip, or be tripped by the operator, and will automatically stabilize at hot shutdown, while the assessment of the availability of key safety systems is made. This takes the operators approximately 30 minutes, based on personal observations in reactor operator training in an SBO. With the loss of all power, most active system will not be operable, with the notable exception of a turbine-driven emergency feed-water pump. This pump is powered by some of the secondary steam, being generated by the residual heat.

However the plant is designed with battery supplies, to power the indication and control systems that should last for around two to six hours. This time can be extended using, if available, a separate back-up SBO diesel (distinct from the emergency diesel generators which are assumed to have failed in an SBO or ELAP scenario, but has a very limited power output) or the key parameter of interest could be measured locally using portable equipment. The only available safe-guard equipment will be the turbine driven auxiliary feed-water pump used to feed the SGs, and the SGs steam dump to atmosphere relief valves. The plant will stabilize with cooling being provided via the secondary side, using steam dump to atmosphere. The turbine driven auxiliary feed-water pump is used to maintain the SG water levels. With cooling being provided by the SGs, the primary system which no longer has power supplies for the primary system recirculation pumps, will automatically set-up natural circulation to transfer heat from the core to the atmosphere via the SGs. The operator will stop depressurizing the secondary side once it reaches 1.7 MPa, in accordance with the SBO procedures (ESKOM, 2017), in order to ensure that nitrogen is not injected into the primary system from the accumulators.

There are two particular parameters of interest for this reactivity analysis. The first is the primary system temperature, or more specifically the coolant temperature in the core, which is a measure of the moderator temperature. This will affect the reactivity insertion due to the cooldown of the primary system moderator. The second is the primary system pressure as it dictates the quantity of borated water that will be injected from the accumulators into the primary system.

The cooldown and depressurization of the primary system, by dumping steam from the SGs affects both of these parameters. Until the cooldown is initiated the primary pressure and temperature are automatically maintained by the plant's control systems at hot shutdown conditions (ESKOM, 2019), i.e., 15.4 MPa and 286 $^{o}$C. The SG cooldown will start removing energy (in excess of that which the core is producing from residual heat) from the primary system, reducing its temperature and causing shrinkage of the primary system inventory. As a consequence, the pressure in the primary system will then reduce as long as the primary water is still sub-cooled. However, as the plant is without power, there is no primary pressure control and at some point the primary pressure drops to where the temperature at the top of the core reaches saturation temperature. At this stage, a pressure bubble forms under the reactor head which keeps the primary system pressurized, causing the primary system pressure to drop more slowly than the reducing secondary pressure.

The primary system pressures impacts on the moderator density (which is not that significant in a PWR) and more importantly on the rate that the accumulators inject borated water into the primary system. The impact on reactivity from the boron injection is very pronounced at the end-of-life (EOL) when the boron is essentially totally diluted from the primary system as there is little excess reactivity remaining in the core.

## Worldwide Station Black-out Events

Even before the Fukushima accident, there were a few events where nuclear reactors have lost all of their power supplies. Appendix C provides a list of SBO events, including near SBO conditions, which have been reported in the nuclear power industry up to 2014.

This experience demonstrates that loss of off-site power can be initiated by grid-related, switchyard-related, plant-centered, and external hazard-related events. However natural external events, such as weather-related and seismic events, can have a significant effect on the ability to restore off-site power, as well as posing a threat to the on-site power supplies, as occurred at Fukushima.

With the notable exception of Fukushima, all total loss of all power events have been limited in duration to a few hours (i.e. SBO events). One SBO event of particular interest for this study occurred at Maanshan Nuclear Power Station in Taiwan, in 2001, and is discussed in some detail below.

## Maanshan Station Blackout

The SBO event that occurred at Maanshan is essentially the first stage of an ELAP. Because Maanshan and Koeberg are of very similar design, this event provides a very good historical event to benchmark the simulator model against, at least for the first few hours of the simulated ELAP transient.

Both Maanshan units, in Taiwan, are 3-loop Westinghouse PWRs with a similar thermal capacity to Koeberg, a 3-loop Framatome PWR design. In 2001, Maanshan Unit 1 experienced an SBO event (US-NRC, 2013). On 17 March, the plant experienced a loss of all the main offsite lines power due to salt-laden sea mist, leading to grid instability. The units were tripped and power supply was initially swapped over to the alternative back-up off-site power supply, but at 00:45 am the next morning this too was lost. The emergency electrical trains automatically swapped over to the redundant emergency diesel generators (EDGs). However, on Unit 1, both EDGs failed to start, one due to a bus grounding fault, and the other due to a loss of power to the alternator exciter. This led to a loss of all AC power to unit 1, plunging it into an SBO. The so-called *swing diesel*, an EDG that can be lined up to replace any of the two EDGs on either unit for the purpose of performing maintenance, eventually restored power to one train of safeguard equipment 02:54 am, ending the blackout event just over two hours later. The duration of the event, starting with loss of off-site power, was approximately two hours.

The primary systems of the Maanshan units (Westinghouse 3-loop Model 54F, 2950 $MW_t$ design) are essentially identical to those of Koeberg (Framatome Model CPY, 2775 $MW_t$ design). The Framatome CPY plants were in fact based on the same Westinghouse 3-loop PWR design. Although the Westinghouse emergency core cooling systems (ECCS) are not identical to the Framatome CPY plants, these are unpowered and thus disabled during ELAP or SBO transients, and therefore any differences between these are irrelevant to this study. Only the two safeguard systems that did not require electrical supplies were available, namely the turbine-driven feed-water pump, and the accumulators, which are similar in both designs.

A summary of the simulator model benchmarking is provided in Appendix H, which concludes that the current simulator predicted the actual transient reasonably well.

## Notable Differences in the Design and Operation of 3-loop 900 MW PWRs

Koeberg has adopted accident procedures developed by Westinghouse, and now managed by the PWR owner group (PWROG). Both Koeberg and the US utilities operating PWRs are generally implementing the accident procedure changes proposed by the PWROG, in order to cater for an ELAP. This involves the augmentation of the existing Station Black-out accident procedure (ECA-0.0), with additional Functional Support Guidelines (FSGs). These FSGs generally involve the pre-staging of mobile equipment, battery load-shedding, but do not change the existing cooldown and depressurization strategy employed in ECA-0.0 accident procedure, for Station Black-out (SBO). The strategy still involves using the SG steam dump valves, to relieve secondary side steam to atmosphere (as used in the current SBO procedure) to remove the residual heat. Many nuclear plants have installed (or are installing) passive shutdown seals on their primary pumps, which eliminates any water inventory leakage from the primary seals. This is the approach most operators of PWR plants appear to have adopted, with the notable exception of EDF's French fleet.

To maintain long-term sub-criticality, EDF intended to ensure that the existing borated accumulators will inject into primary system, thereby introducing additional neutron poison into the reactor system. As the primary system is cooled down and depressurized without pressure control due to the loss of pressurizer spray and heaters, the primary system eventually becomes saturated. As the top of the core is the hottest part of the system, this leads to steam formation at the top of the core which displaces the water in the top of the reactor vessel, creating a steam bubble in the reactor head, which tends to hold up the reactor pressure above the injection pressure of the accumulators.

In response to the Three Mile Island (TMI) accident, Westinghouse developed which they referred to as *symptom-based procedures*. They are actually a blend of event-based and symptom-based procedures. While they employ a similar strategy As such, the reactor and secondary plant operator have separate procedures that are specific to the part of the plant they are each responsible for. By contrast, the PWROG's emergency accident suite has a single procedure that is employed by the whole control room operator crew. EDF are also currently proposing to open their plant's pressurizer relief valves (SEBIMs) to reduce the primary system directly. This is to ensure that the accumulator will inject, and that they are capable of injecting additional water with a dedicated low pressure primary system injection pump that can operate in SBO conditions. This is primarily as a result of EDF's regulator requiring two independent strategies to deal with the ELAP scenario. However, this has two negative impacts. The first is the loss of primary system water inventory, when all conventional injection sources are unavailable, and the second is the possibility of the relief valves failing to re-close when required. This would eventually result in the loss of primary water leading to the core becoming uncovered and melting even through steam-generator feed-water and steam-evacuation capability may still be available.

EDF's pressurizer relief valves have been modified and are equipped with dual relief paths, each consisting of a pair of SEBIM valves placed in series. SEBIM valves can open and close without AC power if battery power is available, and two SEBIMs would have to fail on a single line in order to incur a LOCA. Koeberg still has the original design where each relief line is equipped with a pilot-operated relief valve (PORV), which can close without AC power, in series with a motor-operated isolation valve which cannot. Thus, both Koeberg, and other reactors of similar design in the USA that have similar pressurizer relief arrangements, are more vulnerable than EDF plants in SBO scenarios if a single PORV should fail to close when required. Therefore, EDF's depressurization strategy of deliberately opening relief valves is not an ideal solution for all PWR operators.

## ELAP Thermodynamic Analysis

In order to determine the reactivity insertion due to the cool down, and the reactivity reduction from the injection of borated water from the accumulators, it is important to ascertain certain key

parameters during the ELAP transient. The two of particular interest are the coolant/moderator temperature in the reactor core and the primary pressure (which determines the quantity of borated water injected into the primary system due to depressurization that is caused by the cooldown).

The initial intention was to use RELAP (a design basis thermal hydraulic modelling tool) to model the transient, but it was found that the Koeberg RELAP did not model all the key elements required to perform the analysis. Another alternative considered was MAAP (a simplified thermal hydraulic tool designed primarily to calculate severe accident consequences), but initial runs indicated that it did not adequately model the formation of a bubble in the reactor head during the cool down. This is important as the formation of a steam bubble in the reactor head holds up the primary system pressure during the cool down, significantly delaying the injection of boron from the accumulators. As a final alternative, the Koeberg simulator was used.

While not an engineering tool, the simulator model does consider and provide a reasonable representation of the key elements required for the transient. The one challenge was that the simulator is only typically run for three hour operator training sessions, and many of the non-significant code modules, which typically modelled the secondary side systems, including the turbine and it support systems, failed to run for the full duration of the analysis. They either caused the prematurely termination the transient run or resulted in the simulator getting caught in an endless loop. These were hence systematically deactivated (as they were discovered) by the simulator maintenance staff. The analysis involved numerous transient runs to achieve a stable Koeberg model on the simulator that could be run beyond 24 hours. The final transient analysis was eventually run over a period of four days.

The ELAP transient modelling done for this dissertation involved, de-energizing all off-site and on-site electrical power sources, including the five on-site safeguard diesel generators, the off-site backup supply and house load. This left any safety systems requiring electrical power de-energized, except those that could be powered by batteries. For this analysis, it will be assumed the battery supplies will be supplemented before they are depleted. The control rods automatically insert due to the loss of power to the control rod drive mechanism power system. Essentially, all safety systems are lost with the exception of the auxiliary feed water pump (which is powered by a steam turbine) and the atmospheric steam dump valves(which will be powered by DC batteries and back-up air tanks). If necessary both of these systems can be controlled manually locally. On the reactor-trip signal the secondary side will be isolated and the turbine power steam-turbine will automatically inject cooling water into the three steam generators at full flow, and steam will automatically be released to control the SGs pressure at 7.03 MPa (ESKOM, 2019).

Without electrical power to power the main reactor coolant pumps which gradually coast-down, the primary system establishes natural circulation, which, in conjunction with the auxiliary feed-water pump and steam-dump, is adequate to remove the decay heat. While the operator stabilizes the rest of the plant, the primary system remains stable in the hot shutdown conditions, with the primary temperature at 286$^{o}$C, and primary pressure at 15.4 MPa (ESKOM, SAR 2019).

Based on personal observation during operator training exercises, the operator action to initiate cool down on the secondary side by opening the steam dump valves to atmosphere on the SGs, at a cooldown rate of 55$^{o}$C/hour, after 30 minutes as per the existing SBO emergency operating procedure (ECA 0-0). Once the SG levels have recovered, the feed flow to the SGs is throttled. This is achieved by periodically reducing the flow from the feed-water pump to the SGs in a stepwise fashion, resulting in all the SG levels dropping and recovering, between a SG narrow range level of +1 m to +1.5 m, in a few cycles, as shown in Figure 2. This is necessary as the core residual heat is continuously reducing, requiring less steam production to remove the decay heat over time. The stepwise reduction in the feed-water flow was adopted as it is easier to model and does not impact

on the primary system cooldown rate, provided substantial coverage of the SG tube bundle is maintained.

A scenario summary of the ELAP transient used to determine these key thermohydraulic events on the simulator are provided in Table 1. An end-of-life (EOL) core was used in order to maximize residual heat, and should provide a reasonably conservative representative across the full fuel cycle. The green text indicates user inputs, where the blue text denotes the calculated consequences of the scenario modelled.

| | Time | | Comment |
|---|---|---|---|
| $T_{SBO}$ | 0.0 hrs | 1 min | Initiate Station Blackout (EOL), minimum (i.e. no) RCP pump seal leakage |
| $T_{CD}$ | 0.5 hrs | 30 min | Initiate ECA-0.0 Cooldown at primary system cooldown @ ~50 °C Cooldown Rate (ECA-0.0, Step 23) |
| $RH_{BF1}$ | 1.3 hrs | 80 min | Steam bubble formation in reactor vessel head |
| $T_{CDt}$ | 2.1 hrs | 125 min | Stop cooldown and depressurization when 1.7 MPa reached in SGs (secondary side) |
| $T_{RFF1}$ | 2.2 hrs | 134 min | Reduce ASG flow (reduce manual control valve 10%) to match GCT flow, to prevent SG overfilling |
| $T_{RFF2}$ | 11.7 hrs | 700 min | Further reduce ASG Flow (manual control valve 6%) to allow SG levels to reduce and recover |
| AI | 12.5 hrs | 750 min | Accumulator Start to Inject |
| $RH_{BC}$ | 23.0 hrs | 1 380 min | Bubble in Reactor Head Collapses |
| $RH_{BF2}$ | 26.1 hrs | 1 567 min | Bubble re-formation in Reactor Head |
| $P_{RF}$ | 26.2 hrs | 1 572 min | Pressuriser starts to fill |
| PC | 30 hrs | 1 800 min | RCP pressure reasonably constant at 2.2 MPa (or 22 bar) |

***Table 1:*** *ELAP scenario description -ECA-0.0 controlled cooldown to 1.7MPa*

In normal operation, the reactor SG levels are controlled at 0m, on the narrow range level, which if on-range, are more accurate than the wide range level indication. However the wide range indication does provides a better overview of the actual level in the SGs, as indicated in the SG diagram in Figure 2.

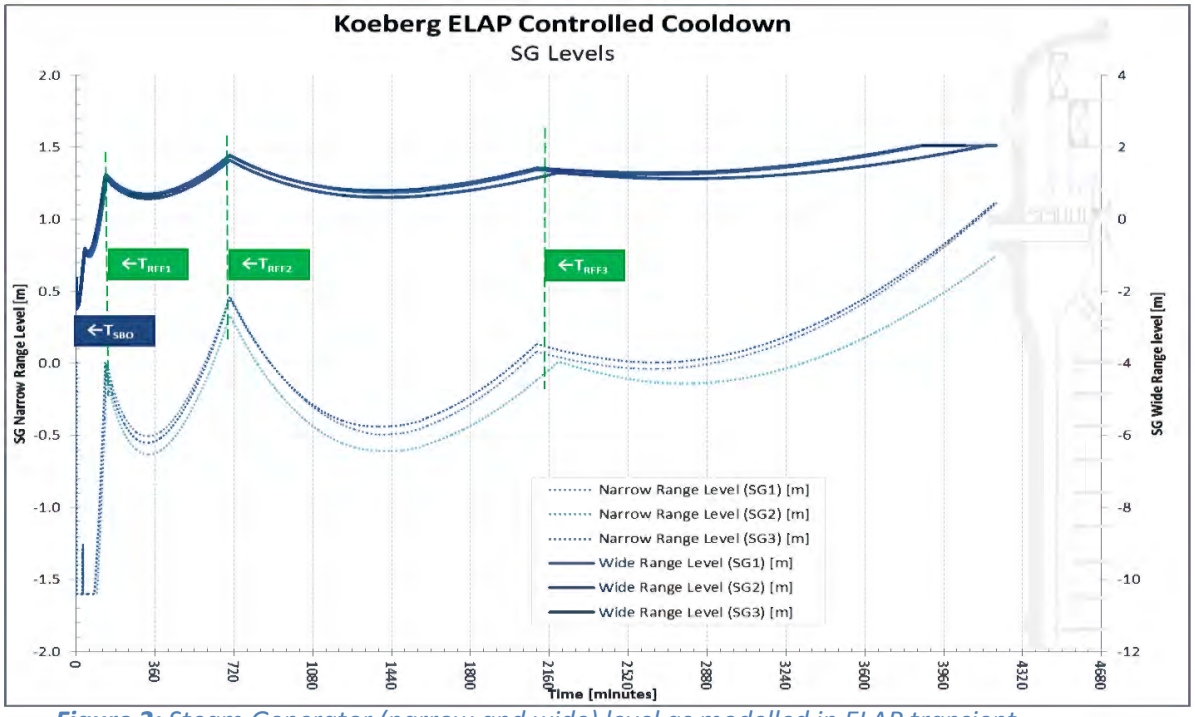


***Figure 2:*** *Steam Generator (narrow and wide) level as modelled in ELAP transient*

Once the pressure of the secondary side of the SG has been reduced to 1.7 MPa, the cooldown and depressurization is terminated by reducing the steam flow rate through the SGs to maintain a constant secondary side pressure, which is maintained for the remainder of the transient[3].

This results in the depressurization of the primary system while it cools down, as the primary system water volume shrinks. As the pressurizer heaters and reactor coolant pump (which provides pressurizer spray) are de-energized the primary system pressure cannot be controlled using the pressurizer and the primary system will become saturated. This leads to a steam bubble forming in the reactor vessel head, as described previously, during the cooldown which now keeps the primary pressure elevated at around 6 MPa, above the accumulator injection pressure of 4.2 MPa, as can be observed in Figure 3, at approximately 80 minutes ($RH_{BF1}$).

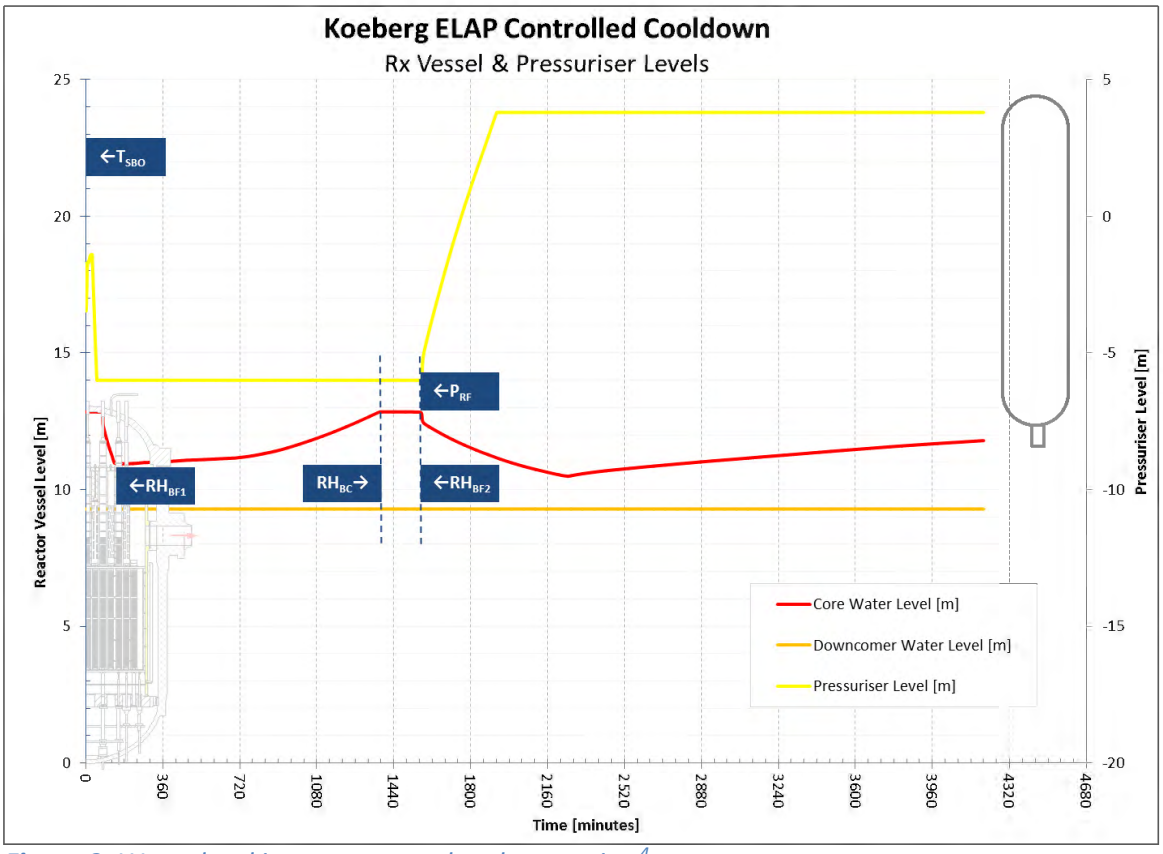


***Figure 3:*** *Water level in reactor vessel and pressuriser*[4]

The reactor head gradually cools, as a function of the thermal conductivity of the head and surrounding structure and equipment. The primary system then gradually depressurizes in a slower, uncontrolled fashion. There is a lot of uncertainty regarding this cooldown rate, as it is dictated by the thermal inertia of the structures and equipment surrounding the reactor vessel head. Hence the predicted depressurization rate should be treated with some caution. However, from the benchmarking with the Maanshan event, it would appear that, in the existing simulator modelling, the rate of primary system depressurization is probably slower than in an actual event (see benchmarking in Appendix H) and for this mini-dissertation it would be considered as conservative. This is because the accumulator injection rate will be slow due to the primary system pressure hold-up, delaying the boron injection from the accumulators (a negative reactivity insertion), while reactivity insertion from the reduced moderator temperature is unaffected.

[3] *The diagrams of the components are inserted to provide a sense of the levels being measured, but are strictly a visual aid. While care was taken to scale them appropriately, they may not be perfectly accurately to scale.*

[4] *The left axis 0m is bottom of reactor vessel, and is used for reactor vessel related levels i.e. core and down-comer water level. The right axis provides a reference for the pressuriser level, with the 0m level representing the normal operating pressuriser level. The relative scales for both axes are the same.*

The primary parameter of interest required for the reactivity calculation is the moderator temperature. This is firstly used to calculate the reactivity insertion due to the moderator temperature reduction. However it also plays a key role in controlling the primary pressure which, in turn, affects both the accumulator boron injection rate and volume of boron injected.

These key parameters of interest (which are required as input for the reactivity analysis) are presented in Figures 4, 5 and 6. The first, Figure 4, shows the pressure evolution of both the primary and secondary systems. The temperature evolution of the primary system is provided in Figure 5, and the primary inventory levels and accumulator injected volumes in Figure 6.

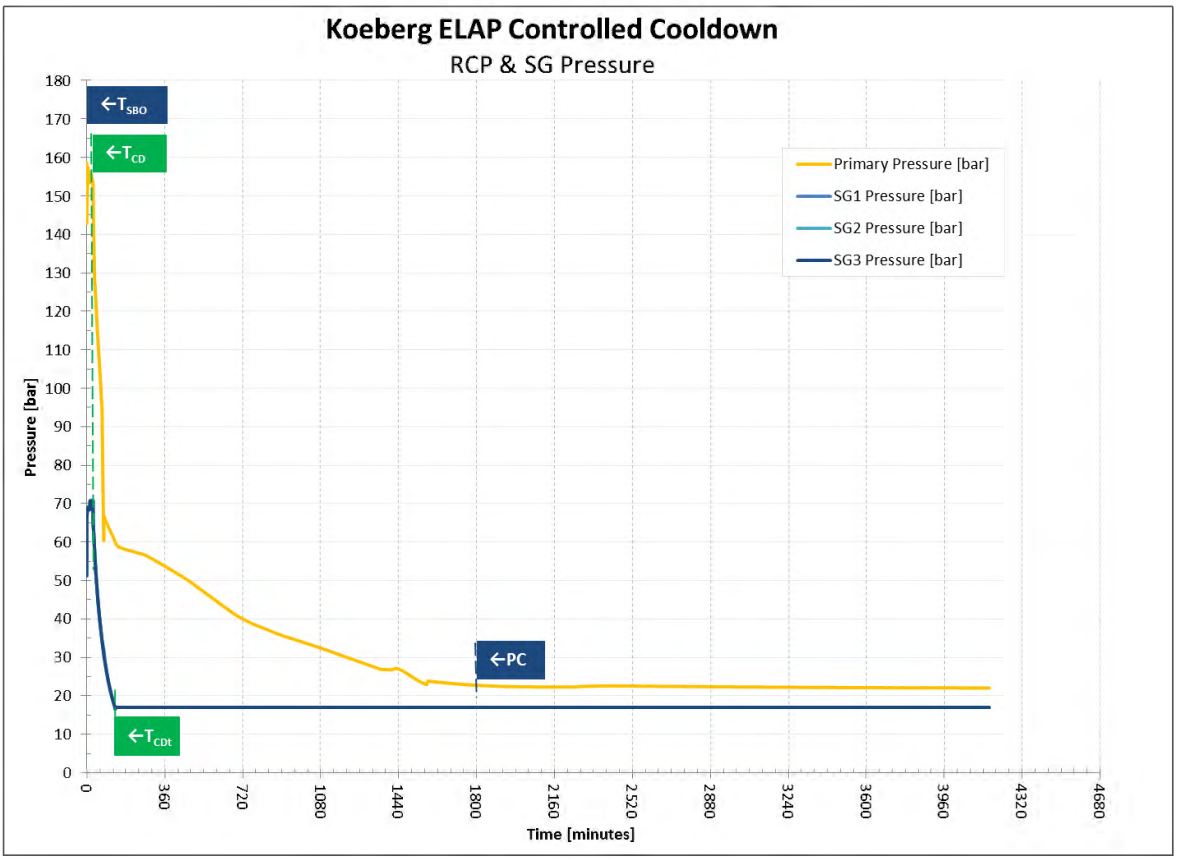


***Figure 4:*** *Primary system and secondary side depressurization as a result of the ELAP cooldown.*

Figure 4 shows both the primary and secondary side pressure reduction due to the cooldown initiated by the operator after 30 minutes. The three SGs are de-pressurized at the same rate so the three SG pressure profiles are all represented by the blue line. The secondary side depressurization is stopped by the operator at 1.7 MPa, and controlled at this pressure. The primary pressure follows the secondary side depressurisation, until the primary system becomes saturated and the steam bubble forms in the reactor head. This stalls the primary pressure reduction at just over 6 MPa, but this pressure gradually decreases as the reactor head cools. This delays the accumulator injection until after 750 minutes. At this stage, the accumulator gradually injects until eventually a constant pressure differential evolves between the primary and secondary side, which the simulator predicts will be achieved at around 30 hours (1 800 minutes). The time taken is dictated by the thermal energy required to be removed for the primary system. Based on the benchmarking with the Maanshan event this would probably occur earlier than the simulation suggests.

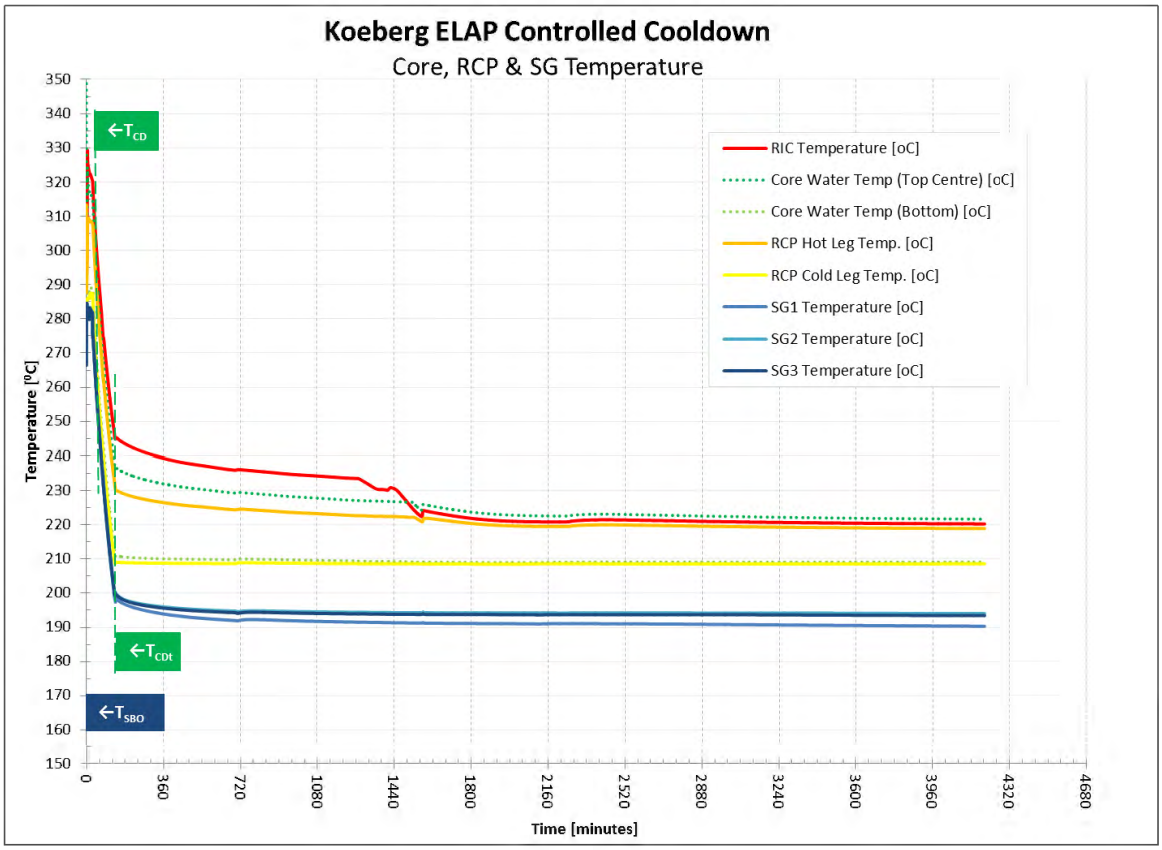


***Figure 5:*** *Primary system temperature evolution as a result of ELAP cooldown.*

During the cooldown, the primary temperature drops rapidly, but the cooldown rate is procedurally limited to 55 °C/hour (ESKOM, 2017). As indicated in Figure 5, above, the core water temperature entering the core decreases to around 210 °C by the end of the cooldown, and is maintained there for the remainder of the transient. After the cooldown, the moderator temperature of the coolant at the top of the core initially decreases to around 235°C, and thereafter gradually decreases to 220 °C as the core's residual heat decays. Therefore the average moderator temperature over the core ranges from 210 °C to 235 °C, after the cooldown, with the temperature at the top of the core gradually dropping to around 225 °C after a day. The average core temperature at this stage is around 215 °C to 220 °C. However, being unable to quantify the uncertainty of the core temperature the coldest core moderator temperature of 210 °C is conservatively assumed for the reactivity calculations to maximize the reactivity increase by the cooling moderator.

Finally, Figure 6 provides an indication of the increased primary system water mass due the injection from the accumulator, as the primary pressure decreases. The three accumulators inject at the same rate so the accumulator masses are all represented by the blue line.

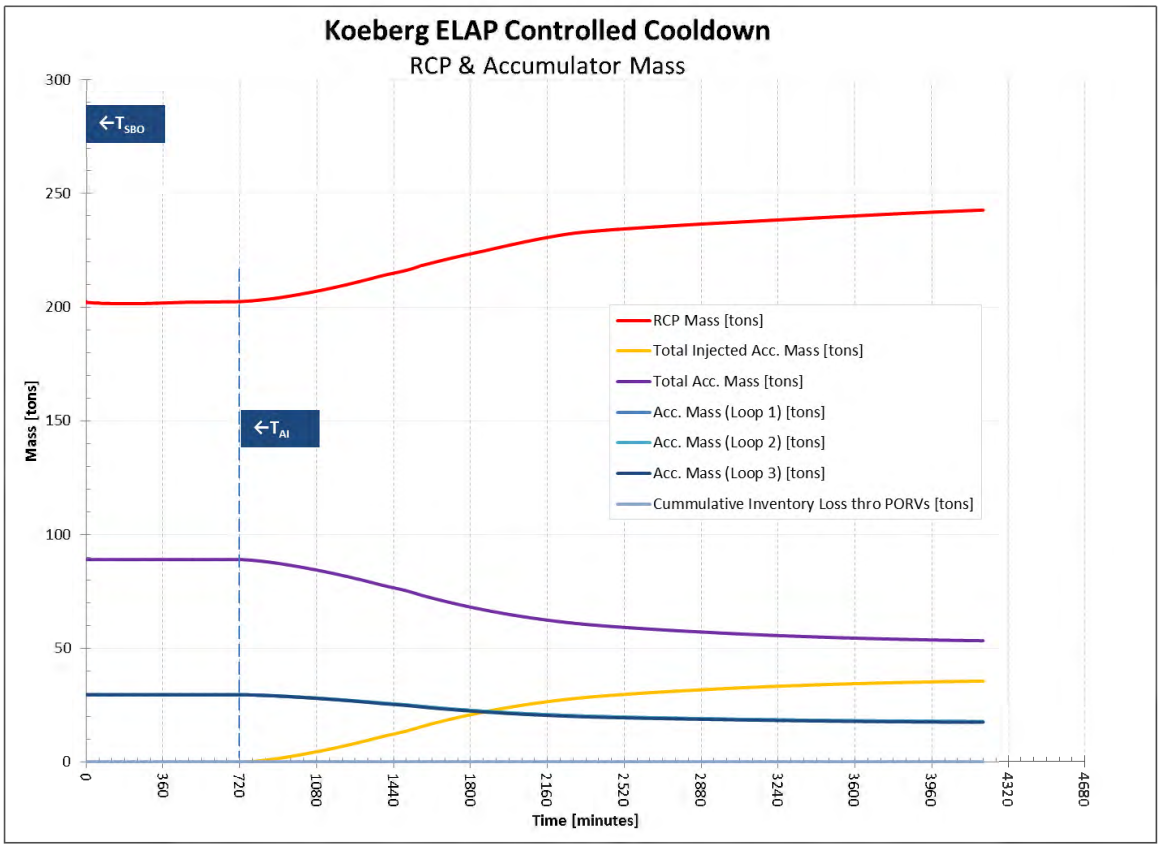


***Figure 6:*** *Primary system and accumulator inventory*

The simulator predicts that the accumulators start injecting after 12 hours, which, based on the Maanshan benchmarking, is probably conservative, so can be treated as the worst case. It predicts that the total mass of the accumulator injection will be just less than 40 $m^3$ by the end of the fourth day.

## *Overview of ELAP Reactivity Transient*

In order to focus on the dominant sources of the reactivity changes during the ELAP transient, it is easiest to split the reactivity changes into three phases. While these phases are not totally distinct, it allows the evolution of the reactivity change to be presented more clearly.

The first phase is the reactivity response due to the reactor trip. The reactor trips automatically on a loss of offsite power. The insertion of control rods provides the dominant reduction in the reactor's reactivity, and is what makes make the reactor sub-critical. This sub-criticality significantly reduces the reactor power, reducing the temperature of the fuel and moderator. As PWRs are designed with a negative fuel and moderator temperature co-efficient, this power reduction causes an almost immediate reactivity insertion (negative power defect). The controls rods typically have a reactivity worth of around - 8 000 pcm, while the reactivity insertion due to the change in power defect is around 2 000 pcm. This leaves a net initial reactivity of around - 6 000 pcm, but this is dependent on where the reactor is in the fuel cycle.

After around 30 minutes, the second phase is entered. In this phase the operator will begin depressurizing the primary system mainly to reduce the risk of losing primary system inventory through the shaft seals of the reactor coolant pump, or through any other leak path caused by a failure. As normal primary system pressure control has been lost, the only available way to depressurize the primary system is to cool the secondary system. Due to the negative moderator temperature co-efficient of the PWR design, the cooldown has the drawback of inserting additional reactivity. However, the plant is designed with three accumulators which cannot be isolated in a

SBO. When the primary pressure decreases below 4 MPa, the accumulators will inject borated water into the system, which will reduce the reactivity.

The magnitude of both reactivity changes is highly dependent on the initial boron concentration of the primary system at the start of the transient. This, in turn, depends mainly on how far through the fuel cycle the reactor is when the transient occurs. There is also a limit on the pressure the primary system can be reduced to, due to the potential of inadvertently injecting the nitrogen gas, used to pressurize the accumulators. Inadvertently injecting the nitrogen into primary system will result in the accumulation of the non-condensable nitrogen into the top of the steam generator's inverted U-tubes. This could stall the primary system natural circulation, which is the only available core heat removal mechanism left, and would result in core melt.

Finally, once the cooldown is terminated (when the SG secondary side pressure reaches 1.7 MPa (g)), the third phase is reached. This takes around two hours with the SGs reaching a saturation temperature of around 207 $^{o}$C, as the cooldown will be limited to 55$^{o}$C/hour. At this stage the target is to maintain the SG secondary side pressure at 1.7 MPa (g) (ESKOM, 2017).

As the primary side is the heat source, it can be concluded that as long as the plant is operated in accordance with the accident procedure, the primary side will remain above 207 $^{o}$C. This provides a useful lower bound for the temperature of the primary coolant or moderator, when determining the maximum reactivity insertion due to the cooldown reactivity. There are two phenomena that must be considered in this latter phase. The first is the production and decay of fission products, which is a function of time after the reactor trip, which will, after approximately a day, result in a significant reactivity addition of around 3 000 pcm, due to the decay of xenon.

The second concerns the insertion of the borated water from the accumulators. While the secondary side will be fully depressurized at the end of the second phase, the pressure transient in the primary system is more complicated. The primary side pressure will initially decrease due to shrinkage caused by the density change of the primary water as the primary water temperature decreases. However at around 7 MPa the primary system loses sub-cooling, and water in the top of the core will become saturated, leading to steam accumulation in the reactor head. This steam bubble in the reactor head will act as an uncontrollable second pressurizer. The pressure in the primary system will then gradually reduce as the residual heat reduces, and the vessel head cools. The timing of this is not simple to determine as it is both a function of the residual heat and rate of heat dissipation from the reactor vessel. This results in the accumulator injection being somewhat delayed and it is likely that the accumulators will only start to inject into the primary system sometime into the third phase.

# V. ELAP Reactivity Analysis

## *Koeberg Neutronics Codes*

To determine the reactivity margin that remains after an ELAP, both existing cycle reactivity data sources (ESKOM, PDBs) as well as the SCIENCE neutronics code was utilized. At Koeberg both SCIENCE (developed by Framatome) and BEACON (developed by Westinghouse) are used for reactivity analysis. However both unit cores and fuel load patterns were not modelled within the BEACON code.

SCIENCE (Version 1.29) was adopted in this study as the tool of choice, as it provided the most comprehensive set of readily available core reloads, over the particular period of interest. It is an integrated code package specifically designed for performing nuclear analysis of PWRs. The SCIENCE package consists of core neutronics and physics codes for two-dimensional (2D) lattice calculations and three-dimensional (3D) core calculations. The set of codes consists of two core physics codes APOLLO2-F and SMART, with additional code (which serves as the user interface), called COPILOTE. The APOLLO2-F and SMART codes contain the reactor code models. APOLLO2-F is based on APOLLO2, which was developed by the Commissariat a l'Energie Atomique (CEA), and has been modified by Framatome to meet its design needs. (US-NRC, 1999).

At Koeberg, existing reactivity studies and routine reactivity calculations predominantly focus either on power operation, or determining an enveloping conservative shutdown margin analysis for the design base accidents. Typically, for reactivity, this enveloping case is a main steam line break at hot shutdown at the end of the fuel cycle for PWRs. This is due to reactivity insertion caused by the rapid primary system cooldown experienced in this transient. However this routine analysis of this transient is limited to assessing the short-term effects due to the initial uncontrolled cooldown. These calculations are also performed conservatively, i.e. making conservative assumptions such as that the highest-worth control rod does not insert.

In order to determine the variability of control rod worth between cycles, previous fuel cycles which are considered the most representative of the current and future fuel enrichment, burnable poisons and core load patterns were used as input data. After discussions with Koeberg Reactor Fuel Engineering it was concluded that the fuel cycles from fuel cycle 18 (x18, where ‘x’ represents either Unit 1 or Unit 2) to fuel cycle 23 (x23), for both units, would provide the best representation of the current and future core designs. This was based on the expected similarity between current, and future, core load patterns and fuel enrichment. From fuel cycle 18, a stable fuel enrichment of 4.4% (ESKOM, PDBs) has been used for both units. It should be noted that there is some variability in the burnable poisons used depending on the manufacturer who supplied the fuel assemblies. This is reflected is the change in integrated control rod worth, for those cycles containing Westinghouse fuel, which was gradually introduced onto Unit 1, from cycle 120. This provides a sample size of twelve historical fuel cycles, considered to be the most representative models of current and future core reloads.

It should be noted that Koeberg is considering thermal power uprating. If this is done, Koeberg may move to 4.6% enrichment, and, while large discrepancies are not anticipated, it is an area for future study when more details become available.

## *ELAP Transient Reactivity Analysis*

For an ELAP transient we are interested in the long-term reactivity impact, which is not a typical reactivity study performed at PWRs. A total transient duration of four days was adopted, as the xenon would have essentially been depleted after this interval. Reactivity data for two particular reactivity contributors of interest were not available from the standard historical reactivity calculations performed for Koeberg and typically documented in the Koeberg Physics Databooks

(ESKOM, PDBs). The first is the total integrated control rod worth of all control rods inserting including the associated power defect. The second is the reactivity impact of the subsequent cooldown of the primary system that is dictated by the ELAP procedure, as described previously (in section IV).

For this study additional neutronics calculations were performed in order to determine the integrated control rod worth, for all control rods inserted, as well as the moderator temperature effect during the primary system cooldown. Standard design basis reactivity analysis requires the most penalizing single failure to be taken into account. This is represented by assuming the control rod with the most worth fails to insert, and is therefore not credited. However, ELAP is considered a DEC, rather than a DBA. It was not part of the initial set of design base accidents, and as it is a transient that involves multiple failures and has a frequency low enough that it will not be classified as a DBA. The conservative DBA assumption of assuming a stuck control rod is over penalizing when performing best estimate analyses, which is more appropriate for analysis supporting design extension conditions (IAEA, 2019).

As the reactivity effects of the fuel and the moderator will change during the cycle all of the reactivity calculations are performed for four key phases during the fuel cycle: beginning of life (BOL), the beginning of life after xenon concentration has stabilized (BLX), middle of life (MOL) and end of life (EOL),. While the choice of beginning (BOL), middle (MOL) and end of life (EOL) are reasonably obvious, the second phase (BLX) is specifically assessed as it is at this point in the cycle that the neutron poison (predominantly $^{135}$Xe and $^{149}$Sm) build-up in the fuel has stabilized. Until the point where the neutron poison has stabilized, there are significant adjustments made to the moderator boron concentration. For the initial stage of the cycle up to BLX, the boron dilution rate is significantly higher than the remainder of the fuel cycle.

Koeberg performs stretch-out operation at the end of the fuel cycle. This is when the plant boron concentration is essentially depleted (less than 15 ppm), and the lack of excess reactivity results in a reduction of the reactor power. In stretch-out, 100% power is no longer achievable and the boron concentration remains constant, so there is reasonable confidence that the EOL result should envelope stretch-out.

The SCIENCE code was set-up using the six previous fuel cycles (cycles x18 to x23, for both Koeberg units) employing the pre-existing cycle burn-up models. These are typically predictive models, but are updated during the cycle to reflect the actual burn-up readings, within certain tolerances.

The assessment of the reactivity evolution over that transient is split into four phases.

1. The first phase is the initial (essentially instantaneous) reactivity insertion of the reactor trip caused by both the control rod insertion and the associated power defect;
2. The second phase is the reactivity reduction due to the decrease in the moderator temperature caused by the controlled cooldown, initiated around 30 minutes after the initial trip (based on a review of operator performance in a station black-out transient);
3. The third phase is the reactivity insertion due to the gradual increase in the moderator's boron concentration resulting from the passive insertion of high concentration borated water from the three un-isolated accumulators, as the primary pressure reduces. As pressure control of the primary system is lost (due to the loss of power to both the pressurizer heaters and the pressurizer sprays), the primary system pressure gradually reduces as the primary system water temperature and density reduces.
4. The fourth phase is the change in reactivity due to the change in concentration of uncontrollable neutron poisons (predominantly $^{135}$Xe) in the fuel. Specifically, the initial increase and then their gradual depletion, which eventually (after 22 hours) leads to a

time-dependent reactivity insertion. (See Appendix A for more details on the decay processes of xenon and samarium.

Below, each of these phases are first independently assessed, and then combined to determine their cumulative impact on the core reactivity.

## Integrated Control Rod Worth Including Power Defect Reactivity Analysis

In order to determine the variation in reactivity across the different fuel loads and during the fuel cycle, the integrated control rod worth and associated power defect are calculated using the SCIENCE neutronics core models at full power operation. First, the power defect is calculated for each cycle, at the four significant cycle milestones (BOL, BLX, MOL, and EOL) by reducing the power to essentially zero (0.00001%), with the associated fuel and moderator temperature reduction. The primary system pressure is maintained at 15.5 MPa, but the primary system flow rate is reduced from 63 225 $m^3$/hour to 1 957 $m^3$/hour. This is to represent the reduced coolant flow (due to loss of the primary system pumps) which changes the primary system from forced flow to natural circulation. The flow-rate in the primary system is reduced to 3% of normal forced flow, based on results from the Koeberg training simulator. Subsequent sensitivity studies concluded that the reactivity results appeared to be insensitive to the flow rate, so further refinements were not necessary for this analysis. The difference between the $k_{eff}$ provides the contribution of reactivity insert due the power defect, at that stage of the fuel cycle.

General design criteria 23 in 10-CFR-50, states that all DBA analyses should conservatively assume that one control rod bank does not get inserted into the core. This assumption is penalizing regarding reactivity calculations. Especially in an ELAP where there is no primary system rupture, significant pressure or temperature transient that the core or reactor vessel will be exposed to, before and during a reactor shutdown or trip. The probability of a stuck control rod assembly is very low, based on international operating experience. It is therefore considered reasonable not consider the single failure assumption in this analysis and to assume that all control rods will insert into the core. This is consistent with the treatment of best-estimate analysis assumption recommended for design extension conditions.

These analyses were then augmented by inserting all the control rods. The integral control rod worth (of all control rods), is determined as the difference in reactivity considering only the power defect (with all the rods withdrawn) and augmented case with all the control rods inserted. This provides the reactivity insertion from the insertion control rods only, referred to as the integral control rod worth. These calculations were repeated for all twelve fuel cycles, at the four different phases of the fuel cycle to provide input to ascertain the mean reactivity change, as well as the variation (standard deviation) across the different fuel cycles.

### *Integral Control Rod Worth*

In order to determine integral control rod worth, the input data from twelve cycles were used. The total control rod worth (i.e. for 48 control assemblies) was calculated using the SCIENCE neutronics code, with the support of Koeberg Reactor Fuel Engineering group. The calculations were done, from the beginning of the fuel cycle to the end of the cycle (burn-up of ~16 000 MWd/t), with no stretch-out, in order to ensure no intra-cycle anomalies.

From these predicted integral control rod data, the predicted mean and the range of total control rod worth over the twelve cycles were determined. The variation of the integrated control rod worth over the twelve cycles is reflected in Figure 7 and Table 2. The mean reactivity reduction caused by the control rod insertion starts at around – 7 826 pcm and decreases to – 8 418 pcm at EOL. The variation between the different fuel cycles (all in the order of 350 pcm to 370 pcm) is reflected by the sample standard deviation provided in Table 2, which remains reasonably constant

over the cycle . The data for these four fuel cycle stages are indicated in the following graphs. The trend-lines are to provide some guidance regarding how the overall trend of these parameters changes over the cycle.

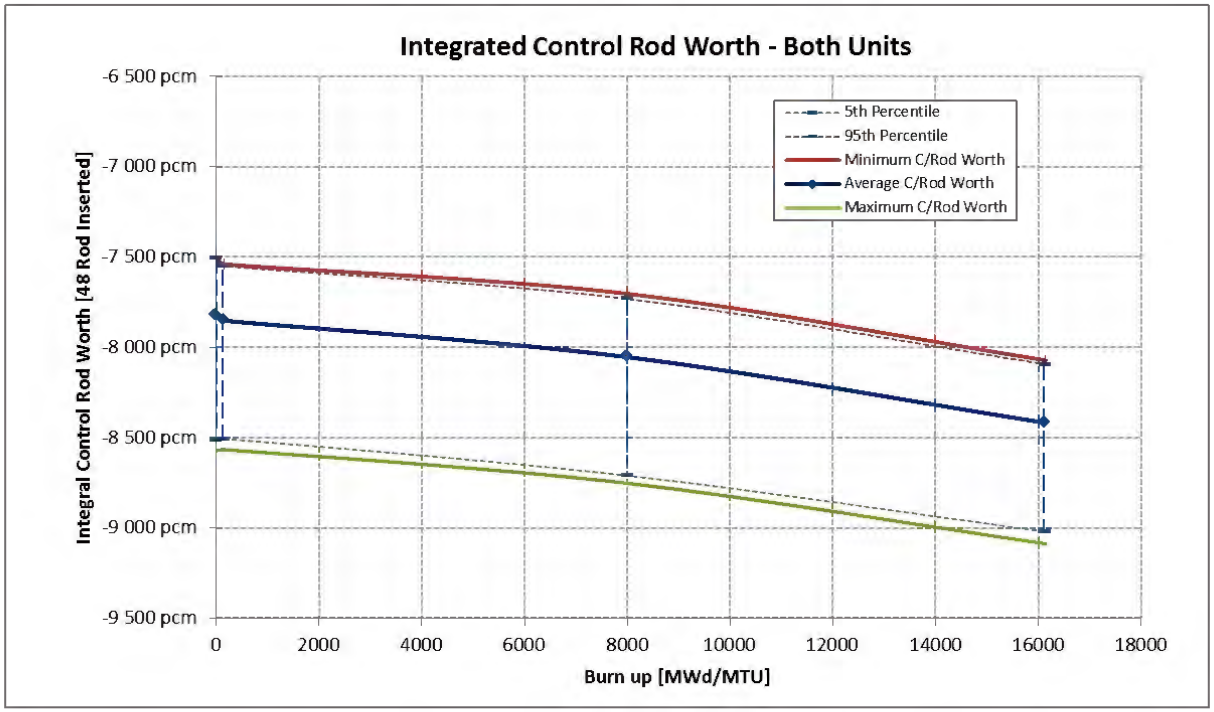


**Figure 7:** Integral Control Rod Worth for 12 Koeberg Fuel Cycles with 4.4% enriched fuel

| Fuel Cycle | Statistical Results of 14 Fuel Cycles | Fuel Cycle stage and the mean Fuel Cycle Burn-up (MWd/MTU) | | | |
|---|---|---|---|---|---|
| | | BOL | BLX | MOL | EOL |
| | | 0 | 150 | 8000 | 16142 |
| 4.4% Enrichment Cycles for Both Units | **Maximum C/Rod Worth** | -8 573 pcm | -8 566 pcm | -8 752 pcm | -9 087 pcm |
| | **5th Percentile** | -8 512 pcm | -8 506 pcm | -8 710 pcm | -9 020 pcm |
| | **95th Percentile** | -7 504 pcm | -7 549 pcm | -7 732 pcm | -8 094 pcm |
| | **Minimum C/Rod Worth** | **-7 500 pcm** | **-7 539 pcm** | **-7 703 pcm** | **-8 072 pcm** |
| | **Average C/Rod Worth** | -7 826 pcm | -7 852 pcm | -8 054 pcm | -8 418 pcm |
| | *Standard Deviation* | *372 pcm* | *354 pcm* | *366 pcm* | *369 pcm* |

**Table 2:** Integral Control Rod Worth for 12 Koeberg fuel cycles with 4.4% enriched fuel

The initial position of the control rod also has to be taken into account to confirm that the full integrated control rod worth can be credited. The predicted total integrated control-rod worth are based on the all the control rods initially being at 225 step. After the reactor trip or shutdown the control rods are assumed to be at 5 steps. There are however two operational factors which could lead to a deviation from this initial assumption that requires consideration. Firstly, in order to ensure that the impact of a reactor trip is rapid, the control bank (control bank D, i.e. the first control rod bank to respond to operating transients) is not fully withdrawn to 225 steps for the full cycle. During operation, it is left slightly inserted, at a height that ensures that as soon as it moves there will be a reactivity change, which is also referred to as it having "*bite*". This is typically at around 214 steps for the first 10 000 MWd/t of the fuel cycle, and then withdrawn to around 222 steps thereafter.

Therefore, by definition, the bank D bite insertion has a negligible reduction in total control rod worth.

Finally Koeberg operates with a *rod wear programme*, to reduce wear of the control rod tubing due to fretting against the control support plates. This rod wear program varies the operating height of all the control rods in different cycle to either 222, 225 or 228 steps. The initial height of 225 steps, assumed in this study will envelope when the control rods are withdrawn to 228 steps, but not those (a third of the fuel cycles) in which all of control rod are withdrawn to only 222 steps. Again the traditional shutdown margin calculations either incorporate this change or provide a conservative penalizing - 500 pcm adjustment to the shutdown margin. This adjustment only impacts around a third of the cycles, and some limited review and sensitivity studies indicated that a more realist adjustment would be in the order of - 100 pcm to - 200 pcm. For this study an additional 200 pcm penalty is considered.

## Power Defect

Table 3, below, provides the results of the neutronics analysis performed using the SCIENCE neutronics code, by reducing the reactor power to zero. This was performed for the last twelve Koeberg fuel cycles, and for each of the four-cycle milestones, in order to quantify the power defect, or the reactivity insertion due to reduction in power. An estimated trend of the change in the power defect range over a full fuel cycle is presented in Figure 8. This increases from a mean reactivity insertion of 1371 pcm at the beginning of life, to 2 515 pcm at the end of life, due to a power reduction from 100% to 0%.

While the results show the expected increase in power defect, the range of reactivity insertion at any particular point in the cycle appears to reasonably constant over the full cycle. At BOL, the power defect ranges from 1 332 pcm to 1 488 pcm and at EOL the range is 2460 pcm to 2613 pcm. The spread of power defect does not represent a normal distribution and, therefore, using a normal distribution statistic is not appropriate. However the calculated standard deviation is in the order of 50 pcm, as indicated in Table 3 below. Based on the results shown in the table, it appears that this asymmetry is related to the different fuel suppliers. This could be as a result of the more exotic burnable poisons introduced into the fuel by Westinghouse, only on Unit 1.

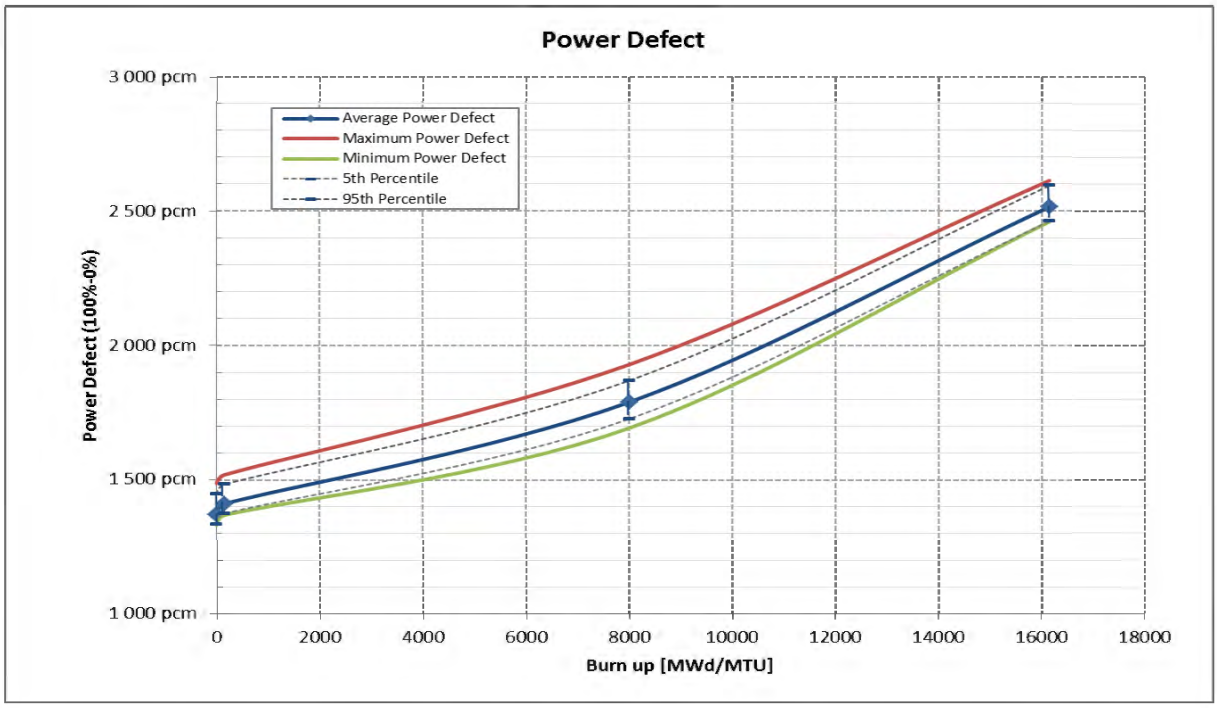


***Figure 8:*** *Reactivity reduction due to 100% power reduction of power over Fuel Cycle*

| Statistical Results of 14 Fuel Cycles | Fuel Cycle stage and the mean Fuel Cycle Burn-up (MWd/MTU) | | | |
|---|---|---|---|---|
| | BOL | BLX | MOL | EOL |
| | 0 | 150 | 8000 | 16142 |
| **Minimum Power Defect** | **1 332 pcm** | **1 369 pcm** | **1 693 pcm** | **2 460 pcm** |
| **5th Percentile** | 1 334 pcm | 1 375 pcm | 1 727 pcm | 2 462 pcm |
| **95th Percentile** | 1 446 pcm | 1 483 pcm | 1 869 pcm | 2 594 pcm |
| **Maximum Power Defect** | 1 488 pcm | 1 519 pcm | 1 929 pcm | 2 613 pcm |
| **Average Power Defect** | 1 371 pcm | 1 411 pcm | 1 789 pcm | 2 515 pcm |
| ***Standard Deviation*** | ***46 pcm*** | ***44 pcm*** | ***55 pcm*** | ***53 pcm*** |

***Table 3:*** *Reactivity Reduction due to the reduction of power from 100% for zero power*

By taking the power defect analysis cases performed above, and augmenting them by inserting all the control rods, we obtain the cumulative effect of both the control rod insertion and the power defect caused by a reactor trip from full power. The result of the cumulative impact is presented below in Figure 9, and Table 4. Figure 9 provides the mean and 95$^{th}$ percentiles, as well as the maximum and minimum reactivity reduction generated by the reactor trip. The four data points selected across the cycle provides an indication of how the total reactivity changes due to the reactor trip over the fuel cycle as the burnable poisons are lost, as well as the range of the reactivity decrease due to the different fuel and reload patterns.

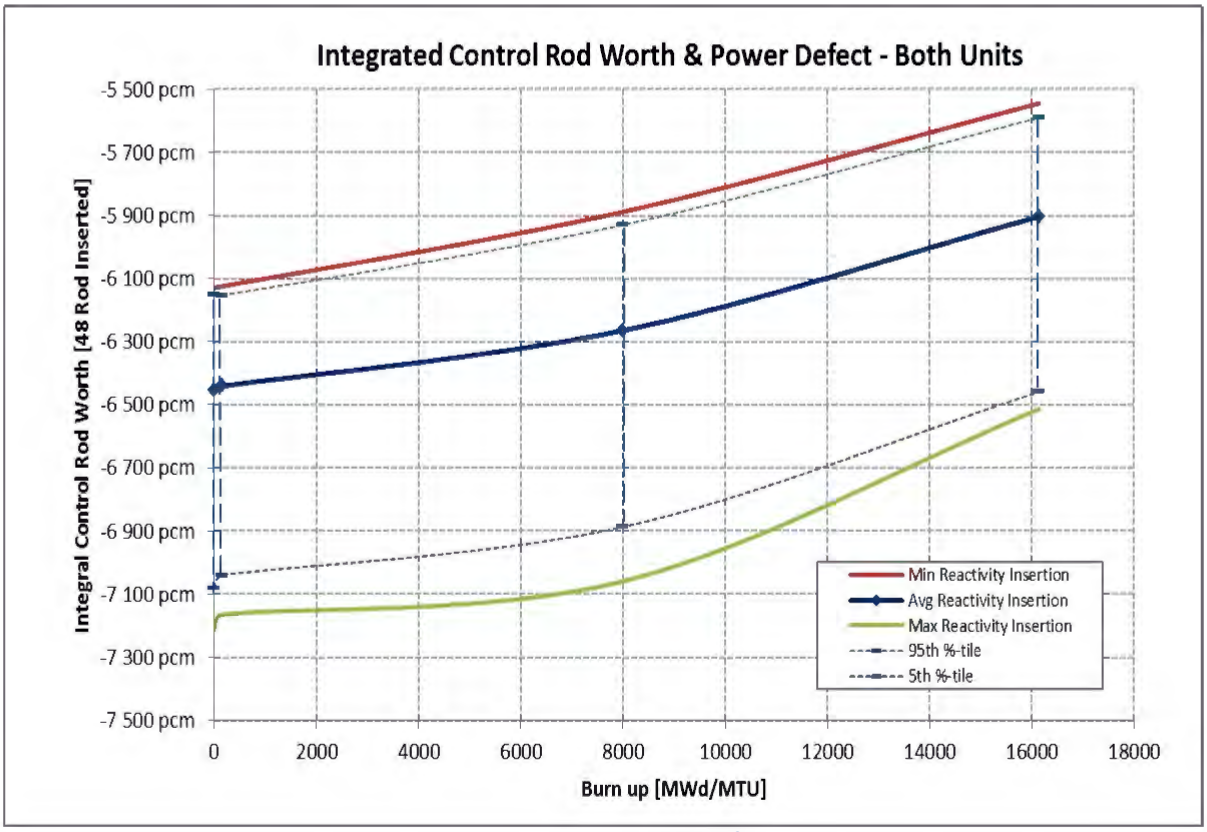


***Figure 9:*** *Reactivity insertion due to reactor trip over the fuel cycle*

| Statistical Results of 14 Fuel Cycles | Fuel Cycle stage and the mean Fuel Cycle Burn-up (MWd/MTU) | | | |
|---|---|---|---|---|
| | BOL | BLX | 8000 | EOL |
| | 0 | 150 | 8000 | 16142 |
| **Avg. Reactivity Insertion** | -6 455 pcm | -6 441 pcm | -6 265 pcm | -5 903 pcm |
| **Max Reactivity Insertion** | -7 214 pcm | -7 165 pcm | -7 060 pcm | -6 513 pcm |
| **Min Reactivity Insertion** | **-6 129 pcm** | **-6 124 pcm** | **-5 888 pcm** | **-5 544 pcm** |
| **5th %-tile** | -7 083 pcm | -7 040 pcm | -6 887 pcm | -6 458 pcm |
| **95th %-tile** | -6 152 pcm | -6 153 pcm | -5 930 pcm | -5 590 pcm |
| *Standard Deviation* | *347 pcm* | *331 pcm* | *367 pcm* | *328 pcm* |

***Table 4:*** *Reactivity insertion due to both control rod insertion and power defect*

## Cooldown Reactivity Analysis

After the reactor trips the average primary temperature will automatically stabilizes at 286°C (hot shutdown conditions), with the primary system pressure initially being controlled at 15.4 MPa. Initially the operator focuses on stabilizing the plant, while establishing the state of the plant, but after around 30 minutes, the primary system is cooled down and depressurized in accordance with procedures. The amount of reactivity inserted by the cooldown of the moderator is the focus of this section.

The plant is designed with three accumulators that in a SBO or ELAP will remain un-isolated, owing to the loss of the AC power to the actuators. When the primary pressure eventually decreases below 4 MPa, these will inject additional borated water into the system, which will further reduce the reactivity. The depressurization is limited to 1.7 MPa(g) to prevent the accumulators from injecting nitrogen into the primary system which could stall natural circulation. This effect of the boron insertion on the reactivity is discussed in the next section. From the simulator run, it was observed that the cold leg temperature stabilizes at 208.5 °C, with the moderator temperature fractionally above that as it enters the bottom of the core. The temperature of the moderator rises as flows up through the core, at a rate related to the core residual heat, which is continuously decreasing. To simplify the reactivity calculation the lowest core moderator temperature will be conservatively assumed to be the cold leg temperature of 208.5 °C.

As there was no previous assessment of the impact of a primary system cooldown on the reactivity below normal power operating temperature, additional reactivity calculations were performed using the SCIENCE code. The reactivity calculations were performed down to 155 °C, which is significantly below the minimum cold leg temperature of 208.5 °C at 1.7 MPa. The calculations were performed for each cycle stage in 10°C increments.

The range of moderator temperatures for which the calculations were performed was extended down to 155 °C, to facilitate the consideration of potential solutions. For example, a consideration could be that the accumulator could potentially be isolated with portable power, possibly eliminating the current restriction limiting the depressurization to 1.7 MPa. The range was extended down to 155 °C, which equates to a saturation pressure of around 0.5 MPa. This is to have the data to investigate the impact on reactivity, of lower primary system temperatures and pressures, in order to assess alternative mitigation strategies, if necessary.

In addition to the reactivity change due to control rod insertion, the reactivity insertion due to the subsequent primary cooldown needs to be taken into consideration. After the reactor has tripped and the control rods are fully inserted, the unit is in a plant state referred to as hot

shutdown, in which the primary system average temperature is automatically maintained at 286 °C, even during SBO. The loss of electrical power results in the loss of both pressurizer spray and pressurizer heater. As a result there is loss of primary pressure control during the subsequent cooldown, and the primary system will eventually lose sub-cooling and saturate. As the heat transfer is from the core to the secondary side, via the primary system, the primary coolant is hotter the secondary side, so the primary coolant (moderator) temperature will always remain higher than the secondary side of 204 °C. This can be seen in Figure 5, where the RCP cold leg temperature, the coolest part of the primary system, drops to around 208.5 °C once the cooldown is compete, which is indicative of the potential maximum temperature reduction in the primary system, which will result in a conservative estimate of the maximum reactivity insertion in the core. As the reactivity analysis was performed in 10 °C steps from 285 °C, the closest calculations which are below 208.5°C are those calculated for 205 °C, which will also provide a little more conservativism regarding primary temperature for the rest of the moderator temperature related reactivity calculations. The average core temperature is somewhat higher, as can be seen in figure 5, but the conservative lower temperature provides some compensation for the lack of uncertainty data.

The change in reactivity due to the cooldown was calculated for the four fuel cycle phases. The traditional cycle phases are defined by the fuel burn-up, which is largely, although not exactly correlated to moderator boron concentration. This is the dominant cause of the relative variation across the fuel cycles, due to the moderator, or primary system cooldown. This is clearly illustrated by the EOL condition where there is little or no variation in the boron concentration at EOL between the different fuel cycles. Further work could be done to perform this moderator temperature reactivity analysis using constant boron concentration for the different cycle phases, in order to reduce the variability across the fuel cycles assessed. These detailed results are documented in Appendix D, and summarized in Figure 10 below.

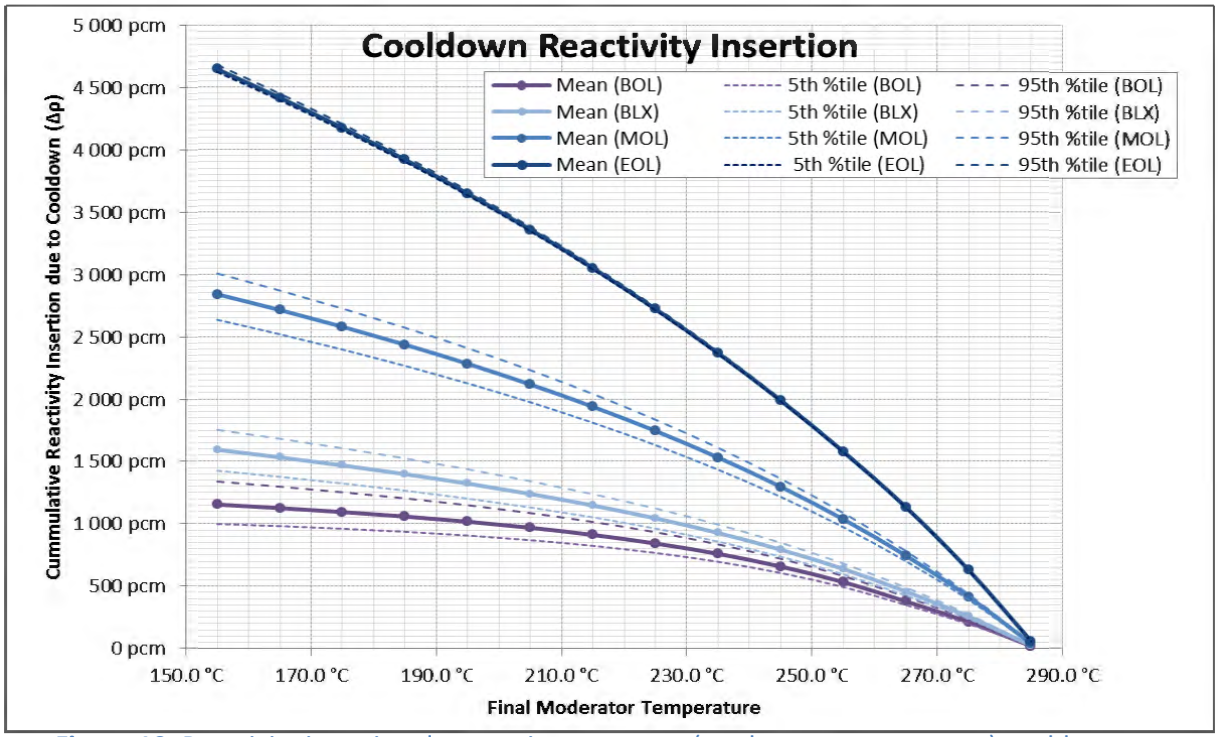


**Figure 10:** Reactivity insertion due to primary system (moderator temperature) cooldown

In summary, if we assume that the primary system cooldown will be limited to 210 °C, the most conservative reactivity insertion occurs at EOL and will be around 3 250 pcm. This reduces to around 2 000 pcm at MOL, and around 1 200 pcm at BLX and 1 000 pcm at BOL.

The overall aim of this part of the study is to determine an upper bound (95$^{th}$ percentile) of the reactivity insertion due to the cooldown down to 210 $^{o}$C. The dashed lines indicate the variation in the calculated reactivity data across the fuel cycles.

A key challenge that arose was the fact that the cycle phases for the two units ended up using different assumptions regarding the boron concentration. This occurred due to the unexpected unavailability of the SCIENCE neutronics code. As a result the cooldown reactivity insertion for the Unit 1 cycles (118-123), using the actual boron concentration, whereas for the Unit 2 cycles, a constant average boron concentration for each phase for all the cycles was assumed. The initial intention was to use the actual boron concentration for all cycles. However, while processing the first reactivity calculation, on Unit 1, it became obvious that using a varying boron concentration (at the different stages of the fuel cycle) introduced an unnecessary variable into the moderator temperature related reactivity calculation. This was clearly dominating the variation between the cycles. This is best illustrated by the reduction of variance toward the end of life where the boron is essentially depleted. It was therefore decided to rather perform the calculation keeping the boron concentration constant across the cycles, for the moderator temperature related reactivity calculation. This was performed for the Unit 2 cycles, but due to lack of availability of the neutronics code these runs could not be repeated for the Unit 1 cycles, as originally intended. This has led to an inconsistency between the Unit 1 and Unit 2 cooldown reactivity insertion data. As such, rather than assuming a normal distribution for the data from both units, it is assumed that the distribution is not known.

If the fuel cycle variation can be described as a normal distribution then the mean plus two standard deviations represents the 97.5$^{th}$ percentile (as we are considering only one side of the distribution tail). However if the distribution is unknown the Chebyshev's inequality can be used to determine an upper-bound with a particular confidence level. It is weaker than the 68-95-99.7 rule for a normal distribution. To illustrate: Chebyshev's inequality states that a minimum of 75% of values lie within two standard deviations of the mean, and 89% within three standard deviations. This was conservatively chosen because the distribution of the data could not be established.

In order to address this issue it was decided to conservatively include the Unit 1 data. This data included the variability in the boron concentration which conservatively maximizes the standard deviation across the cycles. Then assume an unknown distribution type, 3σ was used to determine the 94$^{th}$ percentile (considering only one side distribution of the tail). As the boron concentration would be fixed during most of the cooldown, and because the fuel cycle data is a blend of both fixed and varying concentrations, this uncertainty is still anticipated to be grossly over-estimated, although does not significantly affect to the overall results.

## Additional Borated Water Insertion Reactivity Analysis

The plant is designed with three accumulators, one on each primary system loop. The accumulators each contain 30 m$^3$ of a 2 500 ppm solution of boron in water.

During an ELAP, or SBO, they cannot be isolated, so when the primary pressure eventually decreases to below 4 MPa, they will inject a portion of their contents into the primary system, which will reduce the reactivity. The depressurization of the secondary side is procedurally limited to 1.7 MPa(g) to prevent the accumulators from injecting nitrogen into the primary system which could stall natural circulation.

In order to calculate the reactivity change due to the injection of boron, both the quantity of boron injected, and the resultant reactivity change due to the changes in boron concentration (termed differential boron worth) needs to be determined.

## *Differential Boron Worth*

The differential boron worth is the differential change in reactivity in response to any change in the boron concentration. This gradually increases (becomes more negative) over the fuel cycle due to the boron concentration reduction, and increases due to the cooldown. The Koeberg Physics Databook (ESKOM, PDBs) provide formulas to calculate the boron worth for both full power and hot shutdown conditions (at 286 $^{o}$C), for each fuel cycle. As the reactor is initially sub-critical and expected to remain so during the transient, the data for hot shutdown is used. This will also provide a bounding estimate of the boron worth at the lower moderator temperature, because the differential worth becomes more negative, as the temperature decreases.

The initial system boron concentration is the pre-trip concentration (or at power), but is dependent on where the reactor is in the fuel cycle. Obviously, the associated $K_{eff}$ = 1, as the reactor is initially critical (before the reactor trip). While the reactor trip will make the reactor sub-critical, the boron concentration will still remain constant, until there is any injection from the accumulators. The differential boron worth is also calculated for the four stages of the fuel cycle, but only for the potential range of applicable boron concentrations (i.e. both before and after accumulator injection). This is presented in Table 5, and is limited to covering the range that the primary system concentrations are credible, both before and after accumulator injection.

| Boron Con-centration | Average Differential Boron Worth [Δpcm/Δppm] | | |
|---|---|---|---|
| [ppm] | Mean | σ | Plant State |
| 0 | -8.3 | ±0.1 (±1%) | EOL |
| 100 | -8.3 | ±0.1 (±1%) | EOL |
| 200 | -8.3 | ±0.1 (±1%) | EOL |
| 300 | -8.2 | ±0.1 (±1%) | EOL |
| 400 | -8.2 | ±0.1 (±1%) | EOL |
| 500 | -8.1 | ±0.1 (±1%) | EOL |
| 600 | -8.1 | ±0.1 (±1%) | EOL |
| 700 | -7.4 | ±0.1 (±1%) | EOL |
| 800 | -7.4 | ±0.1 (±1%) | EOL |
| 700 | -8.0 | ±0.1 (±1%) | MOL |
| 800 | -8.0 | ±0.1 (±1%) | MOL |
| 900 | -7.4 | ±0.1 (±1%) | MOL |
| 1000 | -7.3 | ±0.1 (±1%) | MOL |
| 1100 | -7.3 | ±0.1 (±1%) | MOL |
| 1200 | -7.2 | ±0.1 (±2%) | MOL |
| 1300 | -7.2 | ±0.1 (±2%) | MOL |
| 1400 | -7.0 | ±0.2 (±2%) | BLX |
| 1500 | -7.0 | ±0.2 (±2%) | BLX |
| 1600 | -7.0 | ±0.2 (±2%) | BLX |
| 1700 | -6.9 | ±0.2 (±3%) | BLX |
| 1800 | -6.9 | ±0.2 (±3%) | BOL |
| 1900 | -6.8 | ±0.3 (±4%) | BOL |
| 2000 | -6.8 | ±0.3 (±4%) | BOL |
| 2100 | -6.8 | ±0.3 (±4%) | BOL |

***Table 5:*** *Differential Boron Worth over the range of applicable boron concentrations in the core*

The uncertainty provided covers the variation of differential boron worth over the different fuel cycles under consideration. The figures in brackets indicate the standard deviation expressed as a percentage of the mean.

Based on the initial primary system concentration, the range of interest differs depending on which part of the fuel cycle is being assessed. At the beginning of the cycle (BOL), the primary system boron concentration is typically between 1 800 ppm and 1 900 ppm. With an accumulator boron concentration of 2 500 ppm, the potential resultant primary system concentration will lie somewhere between 1 800 ppm and 2 100 ppm, depending on the injected volume from the accumulators. Over this boron concentration range the differential boron worth is around - 6.8 pcm/ppm. This becomes slightly more negative over the range of interest for BLX, where the initial primary circuit boron concentration has been reduced to around 1 500 ppm. It further decreases, in mid-cycle (MOL), to around - 7.3 pcm/ppm. By the end of the cycle (EOL) the differential boron worth is around - 8.2 pcm/ppm, but the resultant increase in change reactivity will be significantly higher due to the more substantial boron concentration change for the same volume of boron solution injection.

The differential boron worth gradually becomes more negative over the fuel cycle, so different differential boron worth's are applied at different stages of the fuel cycle. The variation due to changing boron concentration can be seen to be no more than 0.3 pcm/ppm over the applicable range of concentration change due to the boron injection. In order to simplify the calculation the least negative figure for each of the fuel cycle stages was adopted, which is slightly conservative, as it minimized the favourable effects of the born injection. The spread in the differential boron worth across the twelve different fuel cycles, was always less than ±0.2 pcm/ppm, and is considered to be relatively negligible compared with the uncertainties regarding the quantity of accumulator injection, so this bounding uncertainty figure was adopted.

### *Accumulator Boron Injection*

Each of the three accumulators has a total volume of 41 $m^3$, and contains a 2 500 ppm boron solution with a volume maintained at between 28.9 $m^3$ and 30.6 $m^3$, during normal operation. It is assumed for this study that the accumulator liquid volume is in the mid-range of 29.7 $m^3$. The remaining volume is filled with nitrogen with a resultant volume of 12.1 $m^3$, to pressurize each accumulator to 4.2 MPa. The maximum total injectable volume of boron solution is 89.1 $m^3$.

In a transient with a rapid depressurization, the accumulators would initially undergo adiabatic expansion, but in this particular case the injection takes place over a period of many hours. As the injection will occur over a long period of time and the accumulator temperature will equalize with the containment temperature, isothermal expansion is probably a more realistic assumption regarding the volume of water ultimately injected. However, in the accident analysis used to support the accident procedures (which although generally conservative, are more realistic than traditional design base accident analyses), a polytropic expansion process for the nitrogen in the accumulators is assumed, with a polytropic index of 1.25. This accumulator nitrogen expansion model is based on recommended expansion models and parameters used to support the emergency operating procedures. This provides a more realistic assumption, as the goal for that analysis was to maximize water injection, while preventing nitrogen injection, which is similar to this study. In reality, the actual depressurization would lie somewhere between the polytropic and isothermal expansion, but the polytropic expansion model results in less accumulator injection. Although conservative, the polytropic nitrogen expansion model was applied, to ensure that the reactivity insertion would not be overly optimistic.

As stated previously, to prevent nitrogen injection, which could stall the primary system's natural circulation, the secondary side cooldown and depressurization is stopped at 1.7 MPa. This ensures that the primary system pressure cannot drop below 1.7 MPa. This is illustrated, in Figure 4,

which shows that the primary pressure finally stabilizes at around 2.2 MPa, after the first 24 hours, once the core and reactor head have cooled sufficiently.

All three accumulators eventually depressurize down to 2.2 MPa. This terminates the accumulator injection, which results in an injection a total of 24.6 $m^3$ of boron solution, assuming the polytropic expansion. Table 6, below, shows the increasing volumes of boron solution injected by the accumulators, as the primary system is depressurized, for the three different nitrogen expansion models. As can be seen from the table below, the estimated boron solution injected from the accumulator is 24.6 $m^3$, using the polytropic expansion assumption, but could be as high as 33.1 $m^3$ if an isothermal expansion is assumed.

| Pressure | Single Accumulator $N^2$ Expansion | | | Single Accumulator Injecting | | | All Accumulators Injecting | | |
|---|---|---|---|---|---|---|---|---|---|
| | Adiabatic | Polytropic | Isothermal | Adiabatic | Polytropic | Isothermal | Adiabatic | Polytropic | Isothermal |
| [Mpa] | $PV^Y = const$ | $PV^Y = const$ | $PV = const$ | [$m^3$] | [$m^3$] | [$m^3$] | [$m^3$] | [$m^3$] | [$m^3$] |
| 4.2 MPa | 12.1 m3 | 12.1 m3 | 12.1 m3 | 0.0 m3 | 0.0 m3 | 0.0 m3 | 0.0 m3 | 0.0 m3 | 0.0 m3 |
| 4.1 MPa | 12.3 m3 | 12.4 m3 | 12.4 m3 | 0.2 m3 | 0.2 m3 | 0.3 m3 | 0.6 m3 | 0.7 m3 | 0.9 m3 |
| 4.0 MPa | 12.5 m3 | 12.6 m3 | 12.7 m3 | 0.4 m3 | 0.5 m3 | 0.6 m3 | 1.3 m3 | 1.4 m3 | 1.8 m3 |
| 3.9 MPa | 12.8 m3 | 12.9 m3 | 13.1 m3 | 0.7 m3 | 0.7 m3 | 0.9 m3 | 2.0 m3 | 2.2 m3 | 2.8 m3 |
| 3.8 MPa | 13.0 m3 | 13.1 m3 | 13.4 m3 | 0.9 m3 | 1.0 m3 | 1.3 m3 | 2.7 m3 | 3.0 m3 | 3.8 m3 |
| 3.7 MPa | 13.3 m3 | 13.4 m3 | 13.8 m3 | 1.1 m3 | 1.3 m3 | 1.6 m3 | 3.4 m3 | 3.9 m3 | 4.9 m3 |
| 3.6 MPa | 13.5 m3 | 13.7 m3 | 14.1 m3 | 1.4 m3 | 1.6 m3 | 2.0 m3 | 4.2 m3 | 4.8 m3 | 6.1 m3 |
| 3.5 MPa | 13.8 m3 | 14.0 m3 | 14.5 m3 | 1.7 m3 | 1.9 m3 | 2.4 m3 | 5.1 m3 | 5.7 m3 | 7.3 m3 |
| 3.4 MPa | 14.1 m3 | 14.4 m3 | 15.0 m3 | 2.0 m3 | 2.2 m3 | 2.9 m3 | 5.9 m3 | 6.7 m3 | 8.6 m3 |
| 3.3 MPa | 14.4 m3 | 14.7 m3 | 15.4 m3 | 2.3 m3 | 2.6 m3 | 3.3 m3 | 6.8 m3 | 7.7 m3 | 9.9 m3 |
| 3.2 MPa | 14.7 m3 | 15.1 m3 | 15.9 m3 | 2.6 m3 | 2.9 m3 | 3.8 m3 | 7.8 m3 | 8.8 m3 | 11.4 m3 |
| 3.1 MPa | 15.1 m3 | 15.5 m3 | 16.4 m3 | 2.9 m3 | 3.3 m3 | 4.3 m3 | 8.8 m3 | 10.0 m3 | 12.9 m3 |
| 3.0 MPa | 15.4 m3 | 15.9 m3 | 17.0 m3 | 3.3 m3 | 3.7 m3 | 4.8 m3 | 9.9 m3 | 11.2 m3 | 14.5 m3 |
| 2.9 MPa | 15.8 m3 | 16.3 m3 | 17.6 m3 | 3.7 m3 | 4.2 m3 | 5.4 m3 | 11.0 m3 | 12.5 m3 | 16.3 m3 |
| 2.8 MPa | 16.2 m3 | 16.8 m3 | 18.2 m3 | 4.1 m3 | 4.6 m3 | 6.1 m3 | 12.2 m3 | 13.9 m3 | 18.2 m3 |
| 2.7 MPa | 16.6 m3 | 17.3 m3 | 18.9 m3 | 4.5 m3 | 5.1 m3 | 6.7 m3 | 13.5 m3 | 15.4 m3 | 20.2 m3 |
| 2.6 MPa | 17.1 m3 | 17.8 m3 | 19.6 m3 | 5.0 m3 | 5.7 m3 | 7.5 m3 | 14.9 m3 | 17.0 m3 | 22.4 m3 |
| 2.5 MPa | 17.6 m3 | 18.4 m3 | 20.4 m3 | 5.4 m3 | 6.2 m3 | 8.2 m3 | 16.3 m3 | 18.7 m3 | 24.7 m3 |
| 2.4 MPa | 18.1 m3 | 19.0 m3 | 21.2 m3 | 6.0 m3 | 6.8 m3 | 9.1 m3 | 17.9 m3 | 20.5 m3 | 27.3 m3 |
| 2.3 MPa | 18.6 m3 | 19.6 m3 | 22.1 m3 | 6.5 m3 | 7.5 m3 | 10.0 m3 | 19.5 m3 | 22.5 m3 | 30.0 m3 |
| 2.2 MPa | 19.2 m3 | 20.3 m3 | 23.1 m3 | 7.1 m3 | 8.2 m3 | 11.0 m3 | **21.3 m3** | **24.6 m3** | **33.1 m3** |
| 2.1 MPa | 19.9 m3 | 21.1 m3 | 24.2 m3 | 7.8 m3 | 9.0 m3 | 12.1 m3 | 23.3 m3 | 26.9 m3 | 36.4 m3 |
| 2.0 MPa | 20.6 m3 | 21.9 m3 | 25.5 m3 | 8.5 m3 | 9.8 m3 | 13.3 m3 | 25.4 m3 | 29.5 m3 | 40.0 m3 |
| 1.9 MPa | 21.4 m3 | 22.9 m3 | 26.8 m3 | 9.2 m3 | 10.7 m3 | 14.7 m3 | 27.7 m3 | 32.2 m3 | 44.0 m3 |
| 1.8 MPa | 22.2 m3 | 23.9 m3 | 28.3 m3 | 10.1 m3 | 11.8 m3 | 16.2 m3 | 30.2 m3 | 35.3 m3 | 48.5 m3 |
| 1.7 MPa | 23.1 m3 | 25.0 m3 | 29.9 m3 | 11.0 m3 | 12.9 m3 | 17.8 m3 | 33.0 m3 | 38.6 m3 | 53.5 m3 |
| 1.6 MPa | 24.1 m3 | 26.2 m3 | 31.8 m3 | 12.0 m3 | 14.1 m3 | 19.7 m3 | 36.1 m3 | 42.3 m3 | 59.1 m3 |
| 1.5 MPa | 25.3 m3 | 27.6 m3 | 33.9 m3 | 13.2 m3 | 15.5 m3 | 21.8 m3 | 39.5 m3 | 46.5 m3 | 65.4 m3 |
| 1.4 MPa | 26.6 m3 | 29.2 m3 | 36.4 m3 | 14.4 m3 | 17.1 m3 | 24.2 m3 | 43.3 m3 | 51.2 m3 | 72.7 m3 |
| 1.3 MPa | 28.0 m3 | 31.0 m3 | 39.2 m3 | 15.9 m3 | 18.9 m3 | 27.0 m3 | 47.7 m3 | 56.6 m3 | 81.1 m3 |
| 1.2 MPa | 29.7 m3 | 33.0 m3 | 42.4 m3 | 17.5 m3 | 20.9 m3 | 30.3 m3 | 52.6 m3 | 62.7 m3 | 90.9 m3 |
| 1.1 MPa | 31.6 m3 | 35.4 m3 | 46.3 m3 | 19.4 m3 | 23.3 m3 | 34.2 m3 | 58.3 m3 | 69.8 m3 | 102.5 m3 |
| 1.0 MPa | 33.8 m3 | 38.2 m3 | 50.9 m3 | 21.7 m3 | 26.1 m3 | 38.8 m3 | 65.0 m3 | 78.3 m3 | 116.4 m3 |
| 0.9 MPa | 36.4 m3 | 41.6 m3 | 56.6 m3 | 24.3 m3 | 29.4 m3 | 44.4 m3 | 72.9 m3 | 88.3 m3 | 133.3 m3 |
| 0.8 MPa | 39.6 m3 | 45.7 m3 | 63.6 m3 | 27.5 m3 | 33.5 m3 | 51.5 m3 | 82.5 m3 | 100.6 m3 | 154.5 m3 |
| 0.7 MPa | 43.6 m3 | 50.8 m3 | 72.7 m3 | 31.5 m3 | 38.7 m3 | 60.6 m3 | 94.4 m3 | 116.1 m3 | 181.8 m3 |
| 0.6 MPa | 48.7 m3 | 57.5 m3 | 84.8 m3 | 36.5 m3 | 45.4 m3 | 72.7 m3 | 109.6 m3 | 136.1 m3 | 218.2 m3 |
| 0.5 MPa | 55.4 m3 | 66.5 m3 | 101.8 m3 | 43.3 m3 | 54.4 m3 | 89.7 m3 | 129.9 m3 | 163.2 m3 | 269.1 m3 |

***Table 6:*** *Volume of injection of borated water from accumulators based on primary pressure, with different nitrogen expansion models.*[5]

To determine the resultant primary system concentration we need to know the initial mass in the primary system. Although, the primary system volume is not strictly constant, and increases due to expansion when heated, the total water mass is around 200 tons. A primary system mass of 202 tons is typically used for dilution and other chemical calculations. This is slightly greater than the volume used in some of the thermodynamic models, such as RELAP which assumes 192 tons, but was chosen for these calculations as it was the more conservative.

Based on the ELAP transient runs on the simulator, the accumulator will only start to inject at around 12 hours, once primary pressure reaches 4.2 MPa. While secondary pressure is lowered over the period of just over an hour, once depressurization has been initiated (after around 30 minutes)

[5] The red background indicates where the full volume of water would be injected, and nitrogen is entering the system. While the green line indicates the most probable water injection based on a constant RCP pressure of 2.2 MPa.

the primary pressure decrease starts to lag. This delay is due to steam flashing in the reactor head, holding the primary pressure above the accumulator pressure. The primary system pressure then gradually reduces as the residual heat decreases and the reactor head cools, stabilizing at 2.2 MPa after about 24 hours. The predicted pressure evolution is presented in Figure 4, above. This duration is anticipated to be shorter in real life, based on the benchmarking of the simulator with the Maanshan SBO event, which indicated that the primary side depressurization in the actual event was faster than what the simulator model predicted, as shown in Appendix H. The present study is therefore likely to have slightly conservative results as the simulator model appears to predict that the accumulator injection to be slower than is anticipated in a real event. The simulator-predicted resultant accumulator injection quantities during the transient analyses, are depicted in Figure 6, above.

Both Table 7 and Figure 11, below, show the associated reactivity insertions based on different nitrogen expansion models, assuming the differential boron worth, discussed previously.

| Pressure | Change in Reactivity due to Boron Injection [BOL] | | | Change in Reactivity due to Boron Injection [BLX] | | | Change in Reactivity due to Boron Injection [MOL] | | | Change in Reactivity due to Boron Injection [EOL] | | |
|---|---|---|---|---|---|---|---|---|---|---|---|---|
| | Adiabatic | Polytropic | Isothermal | Adiabatic | Polytropic | Isothermal | Adiabatic | Polytropic | Isothermal | Adiabatic | Polytropic | Isothermal |
| *[Mpa]* | [pcm] | [pcm] | [pcm] | [pcm] | [pcm] | [pcm] | [pcm] | [pcm] | [pcm] | [pcm] | [pcm] | [pcm] |
| **4.2 MPa** | 0 pcm | 0 pcm | 0 pcm | 0 pcm | 0 pcm | 0 pcm | 0 pcm | 0 pcm | 0 pcm | 0 pcm | 0 pcm | 0 pcm |
| **4.1 MPa** | -13 pcm | -15 pcm | -19 pcm | -22 pcm | -25 pcm | -31 pcm | -40 pcm | -45 pcm | -57 pcm | -63 pcm | -70 pcm | -88 pcm |
| **4.0 MPa** | -27 pcm | -31 pcm | -39 pcm | -45 pcm | -51 pcm | -64 pcm | -82 pcm | -92 pcm | -115 pcm | -127 pcm | -143 pcm | -179 pcm |
| **3.9 MPa** | -42 pcm | -47 pcm | -59 pcm | -69 pcm | -78 pcm | -98 pcm | -125 pcm | -141 pcm | -177 pcm | -195 pcm | -218 pcm | -274 pcm |
| **3.8 MPa** | -57 pcm | -64 pcm | -80 pcm | -94 pcm | -106 pcm | -133 pcm | -170 pcm | -191 pcm | -240 pcm | -264 pcm | -297 pcm | -373 pcm |
| **3.7 MPa** | -72 pcm | -81 pcm | -103 pcm | -120 pcm | -135 pcm | -170 pcm | -217 pcm | -244 pcm | -307 pcm | -337 pcm | -378 pcm | -477 pcm |
| **3.6 MPa** | -89 pcm | -100 pcm | -126 pcm | -147 pcm | -165 pcm | -208 pcm | -265 pcm | -298 pcm | -377 pcm | -412 pcm | -463 pcm | -585 pcm |
| **3.5 MPa** | -105 pcm | -119 pcm | -150 pcm | -175 pcm | -196 pcm | -248 pcm | -316 pcm | -355 pcm | -449 pcm | -490 pcm | -552 pcm | -698 pcm |
| **3.4 MPa** | -123 pcm | -139 pcm | -175 pcm | -204 pcm | -229 pcm | -290 pcm | -368 pcm | -415 pcm | -525 pcm | -572 pcm | -644 pcm | -816 pcm |
| **3.3 MPa** | -141 pcm | -159 pcm | -202 pcm | -234 pcm | -264 pcm | -334 pcm | -423 pcm | -477 pcm | -605 pcm | -657 pcm | -741 pcm | -939 pcm |
| **3.2 MPa** | -160 pcm | -181 pcm | -230 pcm | -265 pcm | -299 pcm | -380 pcm | -480 pcm | -542 pcm | -689 pcm | -746 pcm | -841 pcm | -1 069 pcm |
| **3.1 MPa** | -180 pcm | -204 pcm | -259 pcm | -299 pcm | -337 pcm | -429 pcm | -540 pcm | -610 pcm | -776 pcm | -839 pcm | -947 pcm | -1 205 pcm |
| **3.0 MPa** | -201 pcm | -227 pcm | -290 pcm | -333 pcm | -376 pcm | -480 pcm | -603 pcm | -681 pcm | -869 pcm | -936 pcm | -1 057 pcm | -1 348 pcm |
| **2.9 MPa** | -223 pcm | -252 pcm | -322 pcm | -369 pcm | -418 pcm | -533 pcm | -668 pcm | -756 pcm | -966 pcm | -1 038 pcm | -1 173 pcm | -1 499 pcm |
| **2.8 MPa** | -246 pcm | -279 pcm | -357 pcm | -407 pcm | -461 pcm | -590 pcm | -737 pcm | -834 pcm | -1 068 pcm | -1 145 pcm | -1 295 pcm | -1 658 pcm |
| **2.7 MPa** | -270 pcm | -306 pcm | -393 pcm | -447 pcm | -507 pcm | -650 pcm | -810 pcm | -917 pcm | -1 176 pcm | -1 257 pcm | -1 424 pcm | -1 825 pcm |
| **2.6 MPa** | -296 pcm | -335 pcm | -431 pcm | -489 pcm | -555 pcm | -713 pcm | -886 pcm | -1 004 pcm | -1 290 pcm | -1 375 pcm | -1 559 pcm | -2 002 pcm |
| **2.5 MPa** | -323 pcm | -366 pcm | -471 pcm | -534 pcm | -606 pcm | -779 pcm | -966 pcm | -1 096 pcm | -1 410 pcm | -1 500 pcm | -1 701 pcm | -2 189 pcm |
| **2.4 MPa** | -351 pcm | -398 pcm | -514 pcm | -581 pcm | -659 pcm | -850 pcm | -1 051 pcm | -1 193 pcm | -1 538 pcm | -1 632 pcm | -1 852 pcm | -2 388 pcm |
| **2.3 MPa** | -381 pcm | -433 pcm | -559 pcm | -630 pcm | -716 pcm | -925 pcm | -1 141 pcm | -1 296 pcm | -1 674 pcm | -1 771 pcm | -2 012 pcm | -2 599 pcm |
| **2.2 MPa** | **-413 pcm** | **-469 pcm** | **-607 pcm** | **-683 pcm** | **-777 pcm** | **-1 005 pcm** | **-1 236 pcm** | **-1 406 pcm** | **-1 819 pcm** | **-1 919 pcm** | **-2 182 pcm** | **-2 823 pcm** |
| **2.1 MPa** | -447 pcm | -508 pcm | -659 pcm | -739 pcm | -841 pcm | -1 090 pcm | -1 337 pcm | -1 522 pcm | -1 973 pcm | -2 076 pcm | -2 363 pcm | -3 063 pcm |
| **2.0 MPa** | -483 pcm | -550 pcm | -714 pcm | -798 pcm | -910 pcm | -1 181 pcm | -1 445 pcm | -1 646 pcm | -2 138 pcm | -2 243 pcm | -2 556 pcm | -3 318 pcm |
| **1.9 MPa** | -521 pcm | -594 pcm | -773 pcm | -862 pcm | -983 pcm | -1 278 pcm | -1 560 pcm | -1 779 pcm | -2 314 pcm | -2 422 pcm | -2 762 pcm | -3 592 pcm |
| **1.8 MPa** | -562 pcm | -642 pcm | -836 pcm | -930 pcm | -1 062 pcm | -1 383 pcm | -1 684 pcm | -1 922 pcm | -2 503 pcm | -2 614 pcm | -2 983 pcm | -3 886 pcm |
| **1.7 MPa** | -607 pcm | -693 pcm | -904 pcm | -1 004 pcm | -1 147 pcm | -1 496 pcm | -1 817 pcm | -2 075 pcm | -2 707 pcm | -2 820 pcm | -3 222 pcm | -4 203 pcm |
| **1.6 MPa** | -655 pcm | -748 pcm | -978 pcm | -1 083 pcm | -1 238 pcm | -1 617 pcm | -1 960 pcm | -2 241 pcm | -2 927 pcm | -3 043 pcm | -3 479 pcm | -4 544 pcm |
| **1.5 MPa** | -706 pcm | -808 pcm | -1 057 pcm | -1 169 pcm | -1 337 pcm | -1 749 pcm | -2 115 pcm | -2 420 pcm | -3 165 pcm | -3 284 pcm | -3 757 pcm | -4 914 pcm |
| **1.4 MPa** | -763 pcm | -873 pcm | -1 143 pcm | -1 262 pcm | -1 445 pcm | -1 892 pcm | -2 284 pcm | -2 615 pcm | -3 424 pcm | -3 546 pcm | -4 060 pcm | -5 315 pcm |
| **1.3 MPa** | -825 pcm | -945 pcm | -1 238 pcm | -1 364 pcm | -1 563 pcm | -2 047 pcm | -2 469 pcm | -2 829 pcm | -3 706 pcm | -3 833 pcm | -4 392 pcm | -5 753 pcm |
| **1.2 MPa** | -893 pcm | -1 023 pcm | | -1 477 pcm | -1 693 pcm | | -2 672 pcm | -3 064 pcm | | -4 149 pcm | -4 756 pcm | |
| **1.1 MPa** | -968 pcm | -1 110 pcm | | -1 601 pcm | -1 836 pcm | | -2 897 pcm | -3 323 pcm | | -4 498 pcm | -5 159 pcm | |
| **1.0 MPa** | -1 051 pcm | -1 206 pcm | | -1 739 pcm | -1 995 pcm | | -3 148 pcm | -3 612 pcm | | -4 887 pcm | -5 607 pcm | |
| **0.9 MPa** | -1 146 pcm | | | -1 895 pcm | | | -3 430 pcm | | | -5 325 pcm | | |
| **0.8 MPa** | -1 253 pcm | | | -2 072 pcm | | | -3 751 pcm | | | -5 823 pcm | | |
| **0.7 MPa** | | | | | | | | | | | | |
| **0.6 MPa** | | | | | | | | | | | | |
| **0.5 MPa** | | | | | | | | | | | | |

***Table 7:*** *Reactivity reduction due to accumulator injection.*[6]

Due to the varying differential boron worth, and the initial boron concentration of the primary system during the different stages of the fuel cycle, the reactivity impact of the accumulator injection is highly dependent on where in the fuel cycle the plant is. The initial primary system concentration, for the each of the four stages of the fuel cycle, has been taken as the mean of the twelve cycles considered.

[6] The green line indicates the most probable water injection based on a constant RCP pressure of 2.2 MPa.

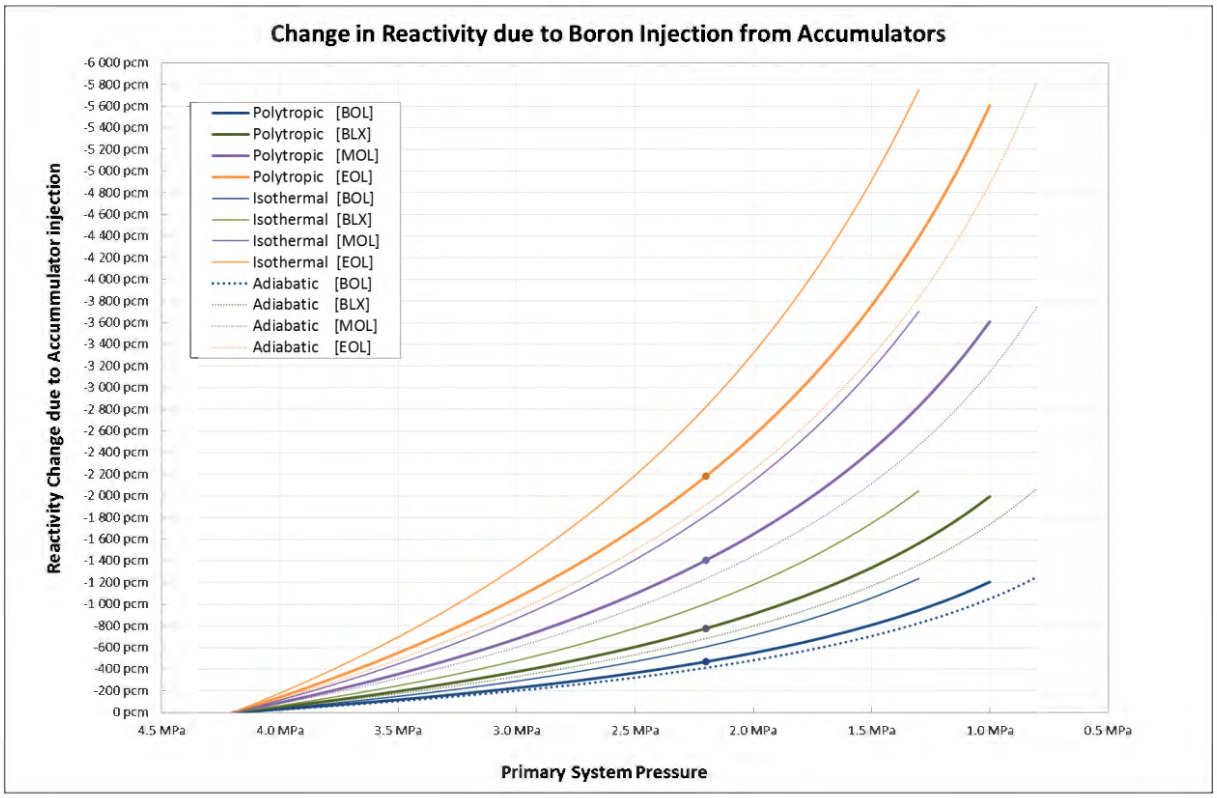


***Figure 11:*** *Reactivity reduction due to accumulator injection*

## *Primary water Inventory*

Figure 12, below, provides some indication of the predicted change in primary system mass due to the accumulator injection. The simulator model predicts a higher accumulator injection than the calculation performed to determine the volume of accumulator injection, confirming that boron injection calculations are probably conservative. The simulator predictions were not considered as the accumulator injection line diameters were significantly larger than those in the actual plant. On further investigation, it was discovered that when the simulator model was initially setup, it was necessary to provide some dampening in the primary system model in order to prevent certain modelling oscillations artifacts within the primary system. To reverse this was non-trivial, and led to concerns that the predicted injected volumes could potentially be significantly affected.

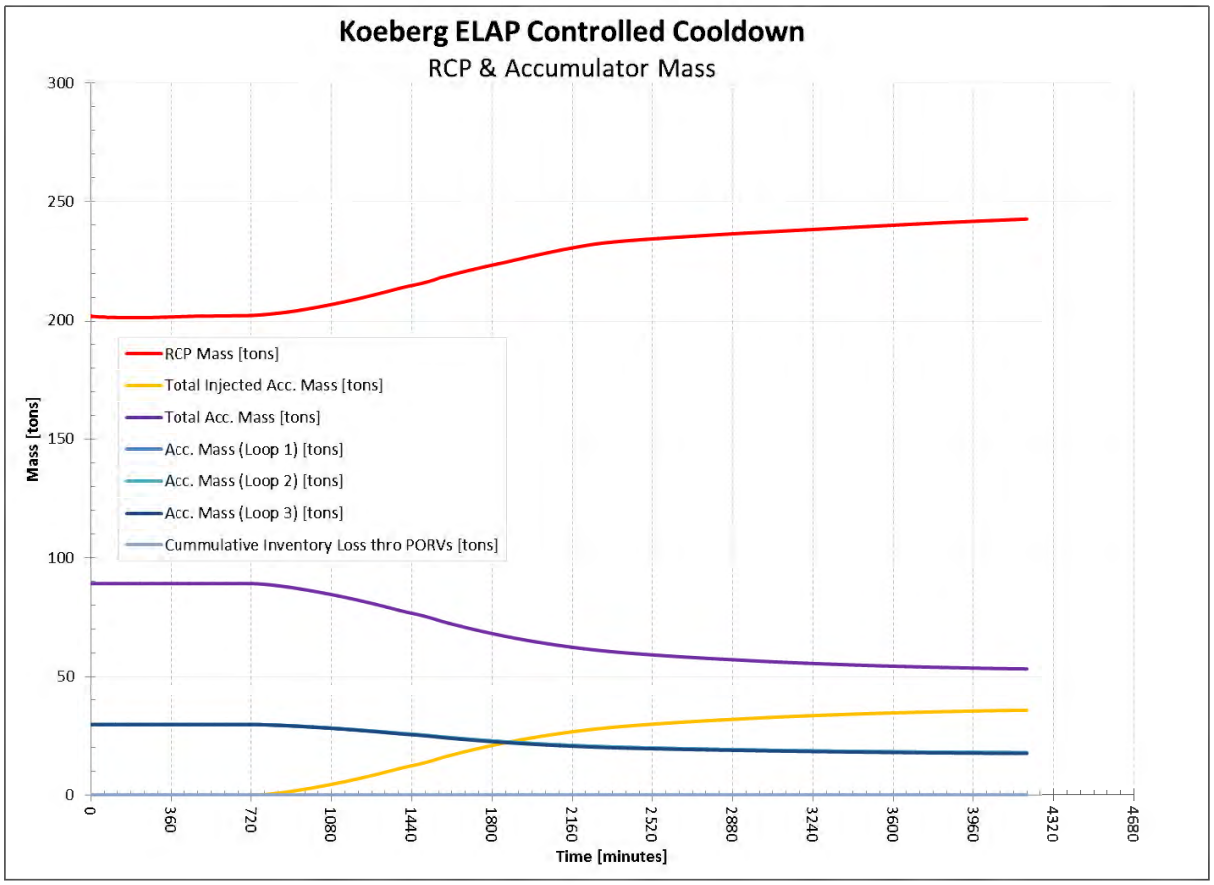


***Figure 12:*** *Primary system mass changes due to accumulator injection*

This provides some confidence that the primary system volume can accommodate at least 40m$^3$ of injected borated water.

## Consolidation of Reactivity Results

Until now all of the reactivity contribution has been calculated separately, and focused on the calculation of reactivity changes as well as the variation from fuel-cycle to fuel-cycle. This section deals with bringing the different contributors together as well as taking in to account the code uncertainties.

For each stage of the fuel cycles it will be determined whether the predicted reactivity meets the proposed acceptance criteria of -1000 pcm, as determined in Section III. However, before this it is necessary to discuss the code uncertainties, before moving on to consolidating the results.

## Neutronics Code Uncertainties

Over and above the different fuel cycle variability, code error and uncertainties need to be accounted for. The SCIENCE code has been qualified to perform safety analysis and was extensively validated but the specific details of the uncertainties are considered proprietary. However CEA has published a number of papers which provide some reasonable estimate of the uncertainties associated the CEA developed APOLLO2 code, on which APOLLO2-F is based.

The code uncertainties of APOLLO-2 have been published in papers given by the CEA (Santamarina, 2004) and Framatome (Girieud, 2001) which provide some estimate of the code uncertainties. The code uncertainties are presented in a format that represents the mean difference between the predicted and actual, or experimental data, with the standard deviation of the spread, of the parameter of interest. If not otherwise specified the uncertainty will be represented first by a figure that represents the bias between the calculated and actual results, followed by the standard deviation of the variation in the results after the '±' symbol.

### *Uncertainty Associated with the Power Co-efficient*

For Uranium-oxide fuels, based on comparison with calculated versus the experimental results, the bias or mean error (i.e. mean difference between the calculated and experimental results), and associated sample deviation (1σ) relating to the Doppler Effect in fuel were +2%±4% (Santamarina, 2004). The mean bias and associated uncertainty with regard to the moderator temperature co-efficient, at around 300$^{o}$C, is - 0.9 ±1.0 pcm/$^{o}$C (Santamarina, 2004).

However, previous attempts, by Framatome, to quantify the uncertainty of the actual power defect were eventually abandoned, as it was not possible to correctly interpret the results as there were too many parameters changing simultaneously, including the measurement inaccuracies. Hence a conservative uncertainty of 20% for code uncertainty of the power defect is adopted in this mini-dissertation.

For some indication of the impact of this large uncertainty on the results: at 97.5% confidence, an additional +280 pcm at BOL (and up to +500 pcm at EOL) should be considered over and above the mean power defect calculated, to confidently account for the associated code error and uncertainty.

### *Uncertainty Associated with Integral Control-Rod Worth Calculations*

Traditional practice at Koeberg is to assume an uncertainty of between 10 and 13% to penalize the shutdown margin to take into account the variation between the measured and predicted control rod worth. This allows the predictions, which are pre-determined before core reload, to demonstrate that the shutdown margin requirement will be met.

A paper outlining the capabilities of the Framatome SCIENCE 3D Nuclear Code (Girieud, 2001) provides some indication of the uncertainties associated with the calculated reactivity worth of the control rods. It is based on a comparison of a set of 62 fuel cycles. These fuel cycles considered were selected as a representative sample of the different types of fuel and fuel management currently used in PWRs, as they use a wide variety of fuel assembly designs with enrichments up to 4.75% (including both uranium oxide and mixed oxide fuel). Across this sample of 62 fuel cycles, the bias (or mean deviation) between the measured and calculated reactivity for control banks was essentially zero. The deviation between calculated values and measured reactivity values was based on the worth of an individual control bank. For 95% of the sample the results were within ±500 pcm, or ±8% exactly. The sample was assumed to have a normal distribution, as it had a clear centre tendency with most results lying between ±300 pcm. So, a standard deviation of ±4% is considered reasonable.

Another method that provides some estimate for any uncertainties between the code calculated and Koeberg's actual plant control-rod worths, is to use the reactor start-up physics test (i.e. Zero Power Core Conformance Tests) to provide an indication of the variation between the measures and predicted worth. However these tests do not measure the total control rod worth, but measures each of the six control bank worths separately and compare them to the predicted control bank worth.

Although the cumulative worth of all the control banks significantly exceeds the sum of the six individual control banks, it does provide some indication of the relative variance between measured and code predictions. Using the start-up physics test of the twelve fuel cycles, to calculate the variance of each of the six control rod banks, it could be concluded that the mean variance was 0.1%, with a standard deviation of 2.5%, as shown in Table 22, in Appendix D. A normal distribution was confirmed using the Chi square normality test, histogram plotting and a Q-Q plot normality test, as shown in Figure 15 in Appendix D. As predicted versus measured variance follows a normal distribution, we can conclude that for the control rod banks, the 95th percentile deviation is 2σ, which is around 5%.

Based on this assessment the more conservative relative standard deviation of 4% is assumed and, therefore, there is a 97.5% confidence that the predicted versus actual integrated control rod worth is less than 8%.

### *Uncertainty Associated with Moderator Temperature Co-efficient*

The mean error (bias) and associated error (standard deviation) with regards to the moderator temperature co-efficient, at around 300$^{o}$C, is -0.9 ±1.0 pcm/$^{o}$C (Santamarina, 2004). Assuming the temperatures decrease during the cooldown from hot shutdown at 286$^{o}$C down to 205$^{o}$C, results in an 80 $^{o}$C drop. The bias can be ignored, but the uncertainty standard deviation will be 80 pcm, over this temperature range. Again, to provide an indication of the effect using the 95$^{th}$ percentile we estimate the error using 2σ, which is ±160 pcm.

### *Uncertainty Associated with Boron Worth*

The average error (bias) and associated error (variance) in the calculation of boron worth, is +3 ±5% (Santamarina, 2004).

## Consolidation of all Significant Reactivity Contributors

The focus of this section is on the calculation of the cumulative change in reactivity due to reactor trip (both control rod insertion and power defect), the primary system cooldown (moderator temperature effects), and accumulator injection (boron insertion). The decay of the uncontrollable neutron poison (xenon) is finally considered before comparing the results to the acceptance criteria.

As part of this consolidation, both the code uncertainties and the variation over different stages of the fuel cycle are considered. As the code uncertainties and the variation of the fuel cycle are independent, the root sum square (RSS) of the constituent uncertainties is applied to determine the overall uncertainties. It is, however, difficult to argue that the combined uncertainties of the four contributors to reactivity are independent. As the degree of correlation between the different reactivity contributors could not be established, they will be treated as totally correlated and, as such, uncertainties will be summed. The first step is to summarize the results for each reactivity component and to determine the uncertainties associated with each component.

A consequence of anomaly in the data collection, discussed earlier, where the Unit 1's boron concentration was variable (based on boron concentration at MOL for each separate cycle), and Unit 2's was maintained constant, resulted in a non-Gaussian distribution of fuel cycle variance. The

standard way of propagating uncertainties was therefore augmented. This was done in order to compensate for the unknown distribution of the variance in the fuel cycles, and the Chebyshev's Inequality was applied for that particular parameter. The only change is the substitution of 3σ to provide a 94%, rather than using the standard Gaussian 2σ to provide a 97.5% percentile to provide a better estimate of the upper bound of the uncertainties of this particular variable. As the focus is on the providing confidence that most of the cycles are adequately covered the analysis of uncertainties focuses on calculation of the 94/97.5$^{th}$ percentiles.

### *Reactivity Reduction from Reactor Trip*

Initially, control rod worth and power defect but be treated separately but as reactivity effects occur simultaneously, the uncertainties may have some degree of correlation. The correlation to do with the fuel cycle variation can be handled by considering the combined results and the variance across the cumulative reactivity changes during the reactor trip. However the code uncertainties need to be treated independently. A conservative additional +200 pcm is included to account for the '*rod wear programme*' (as described earlier) specifically for those fuel cycles for which the control rods are totally withdrawn to only 222 (rather than the 225 steps as assumed in the analysis). For the remainder of the reactivity contributors, the fuel cycle variation and code uncertainties are combined using the root sum square of the uncertainties. It should be noted that, as we are only considering a one-sided distribution there is a 97.5% probability that the parameter will be less that 2σ above the mean.

| Integral Control Rod Worth | Variance/ Uncertainty | BOL | BLX | MOL | EOL |
|---|---|---|---|---|---|
| **Integral Control Rod Worth** | Mean | -7826 pcm | -7852 pcm | -8054 pcm | -8418 pcm |
| *Fuel Cycle Variance* | *σ* | *±372 pcm* | *±354 pcm* | *±366 pcm* | *±369 pcm* |
| *Code Uncertainties* | *σ = ±4%* | *±313 pcm* | *±314 pcm* | *±322 pcm* | *±337 pcm* |
| ***Fuel Cycle and Code Uncertainties*** | $\sigma_{RSS}$ | *±486 pcm* | *±473 pcm* | *±488 pcm* | *±500 pcm* |
| Fuel Cycle and Code Uncertainties | $2\sigma_{RSS}$ | ±972 pcm | ±946 pcm | ±975 pcm | ±999 pcm |
| Rod Wear Program Allowance | ±200 pcm | ±200 pcm | ±200 pcm | ±200 pcm | ±200 pcm |
| **Integral Control Rod Worth** | **97.5th %-tile** | **-6654 pcm** | **-6706 pcm** | **-6879 pcm** | **-7219 pcm** |

***Table 8:*** *Reactivity reduction due to the insertion of all control-rods*

| Power Defect | Variance/ Uncertainty | BOL | BLX | MOL | EOL |
|---|---|---|---|---|---|
| **Power Defect** | Mean | 1371 pcm | 1441 pcm | 1789 pcm | 2515 pcm |
| Fuel Cycle Variance | $\sigma$ | *±46 pcm* | *±44 pcm* | *±55 pcm* | *±53 pcm* |
| Code Uncertainties | σ=20% | *±274 pcm* | *±288 pcm* | *±358 pcm* | *±503 pcm* |
| ***Fuel Cycle and Code Uncertainties*** | $\sigma_{RSS}$ | *±278 pcm* | *±292 pcm* | *±362 pcm* | *±506 pcm* |
| Fuel Cycle and Code Uncertainties | $2\sigma_{RSS}$ | ±556 pcm | ±583 pcm | ±724 pcm | ±1012 pcm |
| **Power Defect** | **97.5th %-tile** | **1927 pcm** | **2024 pcm** | **2513 pcm** | **3527 pcm** |

***Table 9:*** *Reactivity insertion from power defect due to the 100% power reduction*

Combining these two separate reactivity components, (as summarized in Table 8 and Table 9), results in the total reactivity reduction due to the reactor trip, as quantified in Table 10. This shows, that while the mean reactivity inserted immediately after the reactor trip is in the order of -6 000 pcm, we can only take credit for around - 5 000 pcm (and - 4 326 pcm @ EOL) to obtain a 97.5% confidence level of the reactor trip reactivity worth for all the fuel cycle.

| Integral Control Rod Worth & Power Defect | Variance/ Uncertainty | BOL | BLX | MOL | EOL |
|---|---|---|---|---|---|
| **Integral Control Rod Worth & Power Defect** | Mean | -6455 pcm | -6441 pcm | -6265 pcm | -5903 pcm |
| *Fuel Cycle Variance* | $\sigma$ | *±347 pcm* | *±331 pcm* | *±367 pcm* | *±328 pcm* |
| *C/R Worth Code Uncertainty* | $\sigma = \pm 4\%$ | *±313 pcm* | *±314 pcm* | *±322 pcm* | *±337 pcm* |
| *Power Defect Code Uncertainty* | σ=20% | *±274 pcm* | *±288 pcm* | *±358 pcm* | *±503 pcm* |
| **Fuel Cycle and Code Uncertainties** | $\sigma_{RSS}$ | *±542 pcm* | *±540 pcm* | *±605 pcm* | *±688 pcm* |
| Fuel Cycle and Code Uncertainties | $2\sigma_{RSS}$ | ±1084 pcm | ±1079 pcm | ±1211 pcm | ±1377 pcm |
| Rod Wear Program Allowance | ±200 pcm | ±200 pcm | ±200 pcm | ±200 pcm | ±200 pcm |
| **Integral Control Rod Worth & Power Defect** | **97.5th %-tile** | **-5171 pcm** | **-5162 pcm** | **-4854 pcm** | **-4326 pcm** |

**Table 10:** Reactivity change due to control-rods Inserting and power defect

## *Reactivity Insertion from Primary System Cooldown*

Thirty minutes after the reactor trip the cooldown should commence down to a secondary pressure of 1.7 MPa, resulting in an average moderator temperature in the core of initially around 225°C dropping to 215°C as the residual heat decrease. The temperature in the primary cold legs drops down and stabilizes to a little below 210°C. As it was not possible to quantify the uncertainties in the moderator temperature, a conservative average core moderator temperature of 205°C was chosen as the minimum temperature for the cooldown calculation, which is approximately the

saturation temperature at 1.7 MPa. The reactivity results of the cooldown are summarized in Table 11.

| Moderator Temperature Effects | Variance/ Uncertainty | BOL | BLX | MOL | EOL |
|---|---|---|---|---|---|
| **Cooldown Reactivity Insertion** | Mean | 969 pcm | 1240 pcm | 2117 pcm | 3357 pcm |
| *Fuel Cycle Variance* | $\sigma$ | *±76 pcm* | *±72 pcm* | *±93 pcm* | *±13 pcm* |
| *Code Uncertainties* | 1 pcm/°C | *±81 pcm* | *±81 pcm* | *±81 pcm* | *±81 pcm* |
| ***Fuel Cycle and Code Uncertainties*** | $\sigma_{RSS}$ | *±111 pcm* | *±108 pcm* | *±123 pcm* | *±82 pcm* |
| *Fuel Cycle and Code Uncertainties* | $3\sigma_{RSS}$ [Chebyshev's inequality] | ±333 pcm | ±325 pcm | ±370 pcm | ±246 pcm |
| **Cooldown Reactivity Insertion** | **94th %-tile** | **1302 pcm** | **1565 pcm** | **2487 pcm** | **3603 pcm** |

**Table 11:** Reactivity insertion due cooldown from hot-shutdown (286°C) to 205°C

As a reminder, the Chebyshev's Inequality was used as a consequence of anomaly in the data collection, where Unit 1's boron concentration was variable (based on boron concentration at MOL), and Unit 2's was constant. While there is adequate confidence that the data are conservative, there was uncertainty regarding the actual distribution of the data. Therefore it was treated as unknown, and the Chebyshev's Inequality applied, to ensure that the confidence is conservative. Ideally both unit's temperature effects would have been calculated with the same boron concentration, for each of the fuel cycle stages. For Unit 2 it was kept constant but, for the other the boron concentration at the particular fixed burn-up was chosen. While the intention was to redo these runs on Unit 1, the unavailability of the code made this impossible. To illustrate the dominance of the variation of boron concentration, for Unit 2 where a constant boron concentration was adopted for all fuel cycles the spread of results for the cooldown down to 205°C was only ±21 pcm, in contrast to the ±123 pcm for Unit 1 (where the boron concentration was not held constant), for the BOL case.

As the focus is on whether any additional born insertion is needed, the case where no boron is injected is considered initially. However one aspect that has not yet been taken into consideration is the xenon and samarium build up. While the initial intent was to perform a time-dependent analysis, after reviewing the Maanshan event it became apparent that there could be significant delays before the cooldown following the initial reactor trip. While the reactor trip is initiated once grid is lost or degraded, the cooldown is likely to be initiated only once all power is lost. While in some situations this would be simultaneous, it is likely that there could be a significant unquantifiable delay between the two events. The only way in which to deal with this aspect is to use the most limiting case of the time dependent components, specifically xenon decay, and (i.e. the case where xenon has effectively decayed completely). The reactivity changes due to the build-up of samarium gradually reduce the reactivity, but this change is considered beneficial and relativity negligible and is, therefore, not considered any further.

## Reactivity Change due to Xenon Decay

The effects of xenon are substantial, as shown in Figure 13, and need to be considered. The post-trip xenon decay cycle is described in Appendix A.

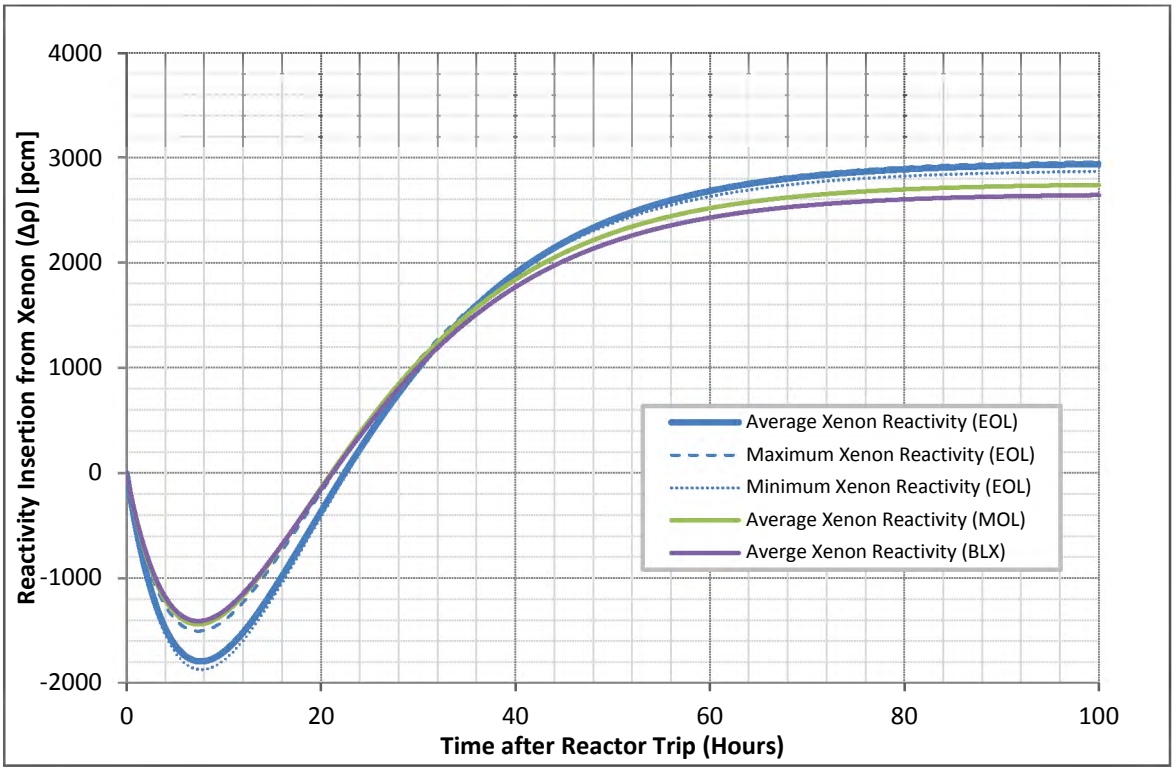


***Figure 13:*** *Relative change in xenon reactivity due to xenon production and depletion*

A review of Koeberg's operating Physics Databooks for fuel cycles 118 to 223 (ESKOM, PDBs) confirmed that the highest calculated reactivity insertion from xenon decay happens at EOL, after a reactor trip from 100% power. Figure 13 shows the reactivity evolution due the change in the Xenon concentration in the core, after a reactor trip from full power, which is the most penalizing case. During the first 22 hours after the reactor trip the xenon initial accumulate reducing the reactivity by as much as -1 750 pcm after 8 hours. However after that the xenon decay exceeds production, and will return to the initial concentration after 22 hours, climbing to a stable value of almost +3 000 pcm, after 100 hours. A review of the fuel cycles indicates that by 100 hours the calculated reactivity insertion, from full power operation at EOL, will be below +3 000 pcm. The xenon reactivity insertion due to xenon depletion at 100 hours range from a minimum of 2 858 pcm to a maximum of 2 958 pcm, with a mean of 2 892 pcm for all the fuel cycles reviewed (cycles x18 to x23).

As the duration of an ELAP transient is not certain, and because the start of the cooldown could be initiated significantly later than the initial reactor trip, a bounding value of 3 000 pcm reactivity insertion due to xenon depletion is used in this study. Therefore, only the peak reactivity insertion of 3 000 pcm is considered in the rest of the study.

## Total Reactivity Change without Boron Injection

As discussed in section III reactivity acceptance criterion is -1 000 pcm, for this ELAP analysis. However the fixed xenon contribution of +3000 pcm, also needs to be considered. Taking both the reactor trip and the subsequent cooldown results, leads to the following picture.

| Δρ Contributor | Parameter | BOL | BLX | MOL | EOL |
|---|---|---|---|---|---|
| **Mean Control Rod Worth & Power Defect** | Mean | -6455 pcm | -6441 pcm | -6265 pcm | -5903 pcm |
| **Mean Cooldown Reactivity Insertion** | Mean | 969 pcm | 1240 pcm | 2117 pcm | 3357 pcm |
| **Neutron Poison Decay (Xenon only)** | Mean | 3000 pcm | 3000 pcm | 3000 pcm | 3000 pcm |
| | | **-2486 pcm** | **-2201 pcm** | **-1148 pcm** | **454 pcm** |

***Table 12:*** *Mean Total Reactivity change in ELAP, with no credit taken for boron Injection*

Table 12 shows that, even without any boron injection, using the average results the reactor should remain sub-critical, up to mid-life, without any additional boron injection, but for the latter half of the cycle will require some boron injection. However, , this picture changes, when the uncertainties are considered, as illustrated in Table 13. While at the beginning of the cycle (BOL and BLX) the results indicate that it is very likely that reactor will remain sub-critical, although not meeting the reactivity acceptance criteria determined in Section III. On the other hand, once mid-life and end-of-life is approached, it is possible that re-critically might be achieved.

| Δρ Contributor | Parameter | BOL | BLX | MOL | EOL |
|---|---|---|---|---|---|
| **Control Rod Worth & Power Defect** | 97.5th %-tile | -5171 pcm | -5162 pcm | -4854 pcm | -4326 pcm |
| **Cooldown Reactivity Insertion** | 94th %-tile | 1302 pcm | 1565 pcm | 2487 pcm | 3603 pcm |
| **Neutron Poison Decay (Xenon only)** | Upper Bound | 3000 pcm | 3000 pcm | 3000 pcm | 3000 pcm |
| | | **-869 pcm** | **-596 pcm** | **633 pcm** | **2277 pcm** |

***Table 13:*** *Enveloping Total Reactivity change in ELAP, with no credit taken for Boron Injection*

However we can see that for the first 50 hours the xenon decay is still low enough that the acceptance criteria would be met for the first half of the fuel cycle, but for the latter part of the cycle the picture is less clear.

## Reactivity Reduction due to Boron Injection from the Accumulator

Now that is clear that the acceptance criteria will not be met without boron injection, let's consider the potential reactivity reduction that can be expected from the accumulators given the depressurization provided by the cooldown. It should be borne in mind the boron injection is expected to occur after the cooldown. Based on a polytropic expansion in the accumulator down to 2.2 MPa provides a conservative total injected volume of 24.6 $m^3$. This will provide a reactivity reduction as indicated in Table 14, for each of the fuel cycle stages. While the uncertainty in the accumulator inject volume is treated by making conservative assumptions specifically regarding the

accumulator nitrogen expansion, the uncertainties regarding the differential boron worth still need to be accounted for. This code uncertainty related to the differential boron worth is represented as the percentage of the mean differential boron worth, to simplify the calculation.

| Accumulator Injection | Variance/ Uncertainty | BOL | BLX | MOL | EOL |
|---|---|---|---|---|---|
| **Boron Injection Reactivity Insertion** | Mean | *-469 pcm* | *-777 pcm* | *-1406 pcm* | *-2182 pcm* |
| *Fuel Cycle Variance* | $\sigma$ = *[4%,3%,2%,1%]* | *±19 pcm* | *±23 pcm* | *±28 pcm* | *±22 pcm* |
| *Code Uncertainties* | $d\rho/dC_b$ = +3%±5% | *±38 pcm* | *±62 pcm* | *±112 pcm* | *±175 pcm* |
| *Fuel Cycle and Code Uncertainties* | $\sigma_{RSS}$ | *±42 pcm* | *±66 pcm* | *±116 pcm* | *±176 pcm* |
| ***Fuel Cycle and Code Uncertainties*** | $2\sigma_{RSS}$ | ±84 pcm | ±133 pcm | ±232 pcm | ±352 pcm |
| **Boron Injection Reactivity Insertion** | **97.5th %-tile** | **-385 pcm** | **-644 pcm** | **-1174 pcm** | **-1830 pcm** |

***Table 14:*** *Reactivity insertion from accumulator injection (Injection volume of 24.6 $m^3$)*

So taking the mean reactivity changes, as shown in Table 15, it would appear that the acceptance criteria would be met over the full cycle.

| Δρ Contributor | Parameter | BOL | BLX | MOL | EOL |
|---|---|---|---|---|---|
| **Average Control Rod Worth & Power Defect** | Mean | -6455 pcm | -6441 pcm | -6265 pcm | -5903 pcm |
| **Average Cooldown Reactivity Insertion** | Mean | 969 pcm | 1240 pcm | 2117 pcm | 3357 pcm |
| **Neutron Poison Decay (Xenon)** | Upper Bound | 3000 pcm | 3000 pcm | 3000 pcm | 3000 pcm |
| **Accumulator Injection** | Mean | -469 pcm | -777 pcm | -1406 pcm | -2182 pcm |
| | | **-2955 pcm** | **-2978 pcm** | **-2554 pcm** | **-1728 pcm** |

**Table 15:** Mean Total Reactivity change in ELAP, including accumulator injection

However taking the code uncertainties and fuel cycle variation into account, see Table 16, the picture again changes. In both cases at the beginning of life (BOL and BLX) the acceptance criteria are met. However, for mid-life the results, and hence for the first half of the fuel cycle, it indicates there is a high confidence that reactor will remain sub-critical, but does not meet the reactivity acceptance criteria of 1 000 pcm. For EOL, it indicates that for some core loads the acceptance criteria are not met in the enveloping case.

| Δρ Contributor | Parameter | BOL | BLX | MOL | EOL |
|---|---|---|---|---|---|
| **Control Rod Worth & Power Defect** | 97.5th %-tile | -5171 pcm | -5162 pcm | -4854 pcm | -4326 pcm |
| **Cooldown Reactivity Insertion** | 94th %-tile | 1302 pcm | 1565 pcm | 2487 pcm | 3603 pcm |
| **Neutron Poison Decay (Xenon)** | Upper Bound | 3000 pcm | 3000 pcm | 3000 pcm | 3000 pcm |
| **Accumulator Injection** | 97.5th %-tile | -385 pcm | -644 pcm | -1174 pcm | -1830 pcm |
| | | **-1254 pcm** | **-1241 pcm** | **-541 pcm** | **447 pcm** |

***Table 16:*** *Enveloping reactivity change in ELAP, including accumulator injection*

## VI. Conclusion

The key objective of this study was to determine whether a typical commercial 3-loop pressurized water reactor, such as Koeberg, will remain sub-critical with a margin of - 1000 pcm, after an extended loss of all AC power until all the xenon (a neutron poison) has decayed away. This is assuming that the primary system cooling is performed in line with the current procedures, and there is the expected injection of boron from the accumulators. The concern is that with the associated cooldown, as the xenon decays away the reactor may become re-critical.

While xenon decay is time dependent from the trip of the reactor, experience has shown that it is likely that a reactor is probably going to be tripped significantly before the actual SBO, as soon as significant degradation of power supplies are evident to the reactor operators. This made performing time analysis difficult and therefore changed to consider the worst case xenon induced reactivity insertion. Four days after the reactor has tripped from full power, this xenon build-up will have essentially all decayed away, effectively creating an additional + 3000 pcm reactivity insertion, which is not controllable. This was consistently shown to remain little lower than + 3000 pcm for all cycles assessed, taking into account the enriched fuel and plutonium build-up at the neutron flux level in a Framatome 900 MW reactor.

Based on the fact that an extended loss of all AC power (ELAP) is a Design Extension Condition (DEC) the reactivity acceptance criterion was chosen to be - 1000 pcm, as explained in Section III. DECs encompass all accidents that are now recognized as part of the plant's safety case, and should be included as part of the plant's design, but were not part of its original design. IAEA and WENRA provide high level guidance on how such analyses should be performed, including the recommendation to apply best estimate analysis.

The other key elements that affect the reactivity are:

- the reactor trip, consisting of the decrease in reactivity from the insertion of all control rods, and the reactivity insertion due to the subsequent drop in power (power defect);
- the moderator temperature effects due to the primary system cooldown, from hot shutdown at 286$^{o}$C down to the low pressure final state, conservatively chosen as 205$^{o}$C;
- the 2 500 ppm borated solution that is injected from the accumulators.

The study assessed four different stages of the fuel cycle, in order to verify that the most penalizing phase of the fuel cycle was not overlooked, as there is significant variation of reactivity of the different reactivity components, over the course of the fuel cycle. These were selected as the four standard stages commonly used on the Koeberg plant and defined in the Physics Databooks namely: 1. BOL: Beginning of Life; 2. BLX: Beginning of Life, once all the core nuclides (specifically neutron poisons) have essentially reached equilibrium; 3. MOL: Middle of Life; and 4. EOL: End of Life.

Not surprisingly the most significant contribution to the reactivity reduction comes from the reactor trip. The minimum reactivity reduction for the last twelve fuel cycles, due to reactor trip (including uncertainties), from both the control rods insertion and power defect, ranges from - 5 171 pcm, at start of the fuel cycle, to - 4 326 pcm at the end of the fuel cycle. The cooldown from hot shutdown for the final cooldown state leads to a positive reactivity insertion ranging from about + 1 300 pcm at BOL, to around + 3 600 pcm at EOL, when including uncertainties. Therefore at the end of the cooldown, ignoring any benefit from the accumulators as well as the effects of the decay of xenon, the reactivity will drop from around - 4 800 pcm at BOL, and to around - 1 600 pcm at EOL. As neither xenon decay or samarium insert positive reactivity for the first 22 hours post reactor trip, even without crediting the accumulator injection, the reactor will meet the acceptance criterion of - 1 000 pcm, and will remain sub-critical for the first 22 hours after the reactor trip. Thus, in a shorter duration ELAP (including a more traditional SBO) there is no criticality concern.

Looking beyond 22 hours, after the initial reactor trip, the xenon decay will at this stage insert more reactivity than at the initial pre-reactor trip conditions. If we consider the best estimate (mean) results for the different stages of the fuel cycle, all stages still meet the acceptance criteria, as shown in Table 17.

| Δρ Contributor | Parameter | BOL | BLX | MOL | EOL |
|---|---|---|---|---|---|
| **Average Control Rod Worth & Power Defect** | Mean | -6455 pcm | -6441 pcm | -6265 pcm | -5903 pcm |
| **Average Cooldown Reactivity Insertion** | Mean | 969 pcm | 1240 pcm | 2117 pcm | 3357 pcm |
| **Neutron Poison Decay (Xenon)** | Upper Bound | 3000 pcm | 3000 pcm | 3000 pcm | 3000 pcm |
| **Accumulator Injection** | Mean | -469 pcm | -777 pcm | -1406 pcm | -2182 pcm |
| | | **-2955 pcm** | **-2978 pcm** | **-2554 pcm** | **-1728 pcm** |

***Table 17:*** *Mean total reactivity change in ELAP, including accumulator injection*

However, when the variation in fuel cycles and code uncertainties are considered (Table 18), using a penalizing case which represents approximately 97.5% of cases, this is only true at the beginning of the fuel cycle. While at mid-life (MOL) the acceptance criteria of -1 000 pcm is not achieved, the results still indicate a high level of confidence that re-criticality will not happen. However, in the latter half of the cycle, in the cases taking the uncertainties into account, return to criticality is indicated.

| Δρ Contributor | Parameter | BOL | BLX | MOL | EOL |
|---|---|---|---|---|---|
| **Control Rod Worth & Power Defect** | 97.5th %-tile | -5171 pcm | -5162 pcm | -4854 pcm | -4326 pcm |
| **Cooldown Reactivity Insertion** | 94th %-tile | 1302 pcm | 1565 pcm | 2487 pcm | 3603 pcm |
| **Neutron Poison Decay (Xenon)** | Upper Bound | 3000 pcm | 3000 pcm | 3000 pcm | 3000 pcm |
| **Accumulator Injection** | 97.5th %-tile | -385 pcm | -644 pcm | -1174 pcm | -1830 pcm |
| | | **-1254 pcm** | **-1241 pcm** | **-541 pcm** | **447 pcm** |

***Table 18:*** *Mean total reactivity change in ELAP, including accumulator injection*

In summary, for the first 22 hours, the acceptance criterion is met for the entire fuel cycle. However after 22 hours, the acceptance criterion is only met at the beginning of fuel cycle (BOL and BLX), when both the fuel cycle variation and code uncertainties are considered. However, at mid-life (MOL), and hence for the first half of the fuel cycle, the results indicate there is a reasonable degree of confidence that reactor will remain sub-critical, but the reactivity acceptance criteria of - 1 000 pcm is not met. It could not be demonstrated with a high degree of confidence that sub-criticality will be maintained at EOL as it does not meet the acceptance criteria and, in some cases, could result re-criticality. In order to meet the reactivity acceptance criteria over the full cycle an addition reactivity reduction of approximately - 1 500 pcm, is necessary later in the cycle.

## Potential Solutions

The first conclusion that can be made is that EOL is the limiting case, and providing a solution for that stage of the fuel cycle should solve the issue for the full cycle. However, in looking at a solution, it should be confirmed that the acceptance criterion (of -1 000 pcm) is also met for MOL. From the results, we can conclude that, to meet the acceptance criteria, the reactivity needs to be decreased by an additional 1 500 pcm. This could potentially be achieved in one of two ways: either by injecting additional borated water or by increasing the primary system water temperature. However, it should be highlighted that with only 24.6 $m^3$ of accumulator water injected, there is potentially still over 60 $m^3$ of inventory in the accumulators that could be available to be injected.

The first and simplest option is that once criticality becomes a concern, the operator could reduce cooling and let the primary temperature increase to 250$^{o}$C, which would reduce the reactivity by around 1500 pcm. Another alternative is to attempt to inject some of the additional accumulator volume. In order to achieve the additional 1 500 pcm required, only around 22 $m^3$ of the remaining volume in the accumulators is required. This could be achieved by further reducing the primary pressure down to 1.5 MPa, which would require the secondary pressure to be decreased to around 1 MPa. This, of course, raises the risk of nitrogen injection, which would have to be assessed. It should be highlighted that this assumes a polytropic expansion and, after a significant period of time the isothermal expansion is probably more realistic. This would lessen the necessary pressure reduction required, down to 1.8 MPa.

The major concern here is the current instrumentation uncertainty. This is because the aim is to maximize the accumulator injected volume, while confidently ensuring that no nitrogen is injected into the primary system. The existing primary pressure sensors are designed to measure the pressure at full power and, at the much lower pressures that are relevant to this study, the uncertainties are large. The accumulators do not have suitable instrumentation, and so the primary pressure is determined by inference from the secondary side pressure, which also incurs large uncertainties. The measured or inferred primary pressure uncertainty could be resolved by either installing improved primary or accumulator pressure measurement for these lower pressures. Another alternative would be to provide a means of venting the nitrogen from the accumulator, using a 'reversed' relief valve, which, when a certain low-pressure signal is met, bleeds the accumulator of the residual nitrogen, preventing it from being injected into the primary system, thus allowing the primary pressure to be further reduced.

## Areas for Further Study

During the course of this dissertation, a few issues were uncovered, which could not be resolved in the scope of this mini-dissertation, opening them up to areas of further study. A list of these potential areas of further study and investigation is provided below.

1. The simulator is not an engineering tool, so re-running the transient analysis in a thermohydraulic code such as RELAP, would be an area that could be further pursued to validate the result of this study. Ultimately, once the Koeberg's RELAP model is capable and qualified to perform ELAP transient analysis it would be a more ideal platform for this time-dependent transient analysis. However, given the amount of time required, it now falls outside the scope of this mini-dissertation.
2. For this particular transient, a specific area of interest is the cooldown rate of the reactor head as existing models do not model it with great accuracy. The Maanshan SBO event provides a good benchmarking case, but it could be dependent on whether the plant has what, is referred to as a *'hot'* or '*cold' reactor head*. This relates to the amount of internal flow of coolant diverted to the reactor head during normal operation, which is different for the two types of reactor heads. Further work could be done to refine the modelling of the reactor head cooling, to obtain more confidence in this modelling.

3. Another area of further study could be to investigate ways of improving the accuracy of the available plant instrumentation, to limit the risk of nitrogen injection, while maximizing the volume of accumulator injection.
4. The twelve core 4.4% enriched fuel cycles selected for this study are the best representation of the current and future anticipated fuel loads. In the future, after power uprating, Koeberg may move to 4.6% enrichment. While large discrepancies are not anticipated, this is a potential area for future study, when more details become available.
5. With the planned steam generator replacement, the accident analysis is now performed with a hypothetical enveloping core design. This is referred to as the SGR reference core. An area of further study could be to evaluate whether the reference core will ensure sub-criticality.
6. Further work could be done to extend the assessment to confirm that it envelopes stretch-out.

## VII. Acknowledgements

I would like to thank and acknowledge:

- Emeritus Professor David Aschman for his guidance, and patience, and constantly reminding me to keep the focus in mind, and not to overdo some aspects.

- Dr Steph Steyn for his assistance in navigating the murky world of practical versus theoretical reactivity analysis.

- John Gomes for his time, practical education, guidance and reviews, in the world of reactivity analysis, and for being the saviour from the erratic wrath of the neutronics code.

- Grant Murphy needs a special mention for his assistance with the simulator, modelling support and setting-up both the ELAP and the Maanshan SBO scenario's on the Koeberg simulator. More specifically for the necessary simulator re-modelling required for the long duration ELAP thermohydraulic model, taking the Koeberg simulator, where no other analysis has taken it before. He was invaluable in identifying, and deactivating these problematic system models which prevented simulator from running for this extended duration required, and in setting up the standardized programmed routines to be able to repeatedly perform the ELAP transient on the simulator.

- Dr. Emmanuel Lamprecht for providing constant advice, encouragement, reviews, and interest, adding chemical confidence and being the constant sounding board necessary to maintain my sanity.

## VIII. References


(Bennet, 1989) Bennet & Thomson, *The Elements of Nuclear Power*, Longman, Third Edition, 1989.

(Dominion, 2015) Virginia Electric and Power Company (Dominion Power), *North Anna Power Station Units 1 and 2, Compliance Letter and Final Integrated Plan In Response to the March 12, 2012 Commission Order Modifying Licenses With Regard to Requirements for Mitigating Strategies for Beyond-Design-Basis External Events (Order Number EA-12-049),* May 2015.

(ESKOM, 2017) ESKOM, KWB-ECA-0.0, *Koeberg Optimal Recovery Procedure: Loss of all AC Power*, Rev 12, 2017.

(ESKOM, 2019) ESKOM, *Koeberg Safety Analysis Report – Part II Chapter 12*, Rev 5b, 2019.

(ESKOM, PDBs) ESKOM, *Koeberg Physics Databook: Fuel Cycles x18-x23**, KWB-OP-PDB-001/2, 2007-2017*.
*[*This reference covers all revisions of the Physics Databooks which cover the 12 fuel cycles of interest.]*

(GPC, 1999) General Physics Corporation, *PWR Generic Fundamentals – Reactor Theory*, 1999.

(Ghasemi, 2012) Ghasemi A., Zahediasl S., *Normality Tests for Statistical Analysis: A Guide for Non-Statisticians*, Int. J. Endocrinol Metab. 2012; 10(2):486-9. DOI.

(Girieud, 2001) P. Girieud, L Daudin, C. Garat, P. Marotte, S. Tarle, *SCIENCE Version 2: The Most Recent Capabilities of the Framatome 3D Nuclear Code Package*, Framatome, 2001.

(IAEA, 1998) IAEA, *Control assembly materials for water reactors: Experience, performance and perspectives, Proceedings of a Technical Committee*, IAEA-TECDOC-1132, 1998.

(IAEA, 2015a) IAEA, *The Fukushima Daiichi Accident: Technical Volume 1, Description and Context of the Accident*, 2015.

(IAEA, 2015b) IAEA, *Design Provisions for Withstanding Station Blackout at Nuclear Power Plants*, IAEA-TECDOC-1770, 2015.

(IAEA, 2016) IAEA, *Safety of Nuclear Power Plants: Design*, Safety Standard SSR-2/1, Rev 1, 2016.

(IAEA, 2019) IAEA, *Deterministic Safety Analysis for Nuclear Power Plants*, Safety Guide SSG-2, Rev. 1, 2019.

(IRSN, 2007) IRSN*, IRSN's Viewpoint on the Safety and Radiation Protection of French Nuclear Power Plants in 2007*, DSR Report No. 271, 2007.

(Lamarsh, 2001) Lamarsh J.R., Baratta A.J., *Introduction to Nuclear Engineering*, Third Edition, Prentice-Hall, Inc, 2001.

(NAoNT, 2014) National Academy for Nuclear Training, *Reactivity Coefficients - Student Guide*, 2014.

(Peretyazhko, 2003) Peretyazhko. I. S., Zagorsk Y. V., *Calculation of Isochores and Density Of Boric Acid Solutions,* Acta Mineralogica-Petrographica, Abstract Series 2, Szeged, 2003.

(Razili, 2011) Razali N.M., Wah Y.B., *Power comparisons of Shapiro-Wilk, Kolmogorov-Smirnov, Lilliefors and Anderson-Darling tests,* Journal of Statistical Modeling and Analytics, Vol.2 No. I, 21-33, 2011.

(Rhodes, 2012) Rhodes M., *The Making of the Atomic Bomb 25th Anniversary Edition*, Simon & Schuster, 2012.

(Santamarina, 2004) Santamarina A., Collignon C., Garat C., *French Calculation Schemes for Light Water Reactor Analysis*, PHYSOR 2004: The Physics of Fuel Cycles and Advanced Nuclear Systems: Global Developments, Chicago, April 2004, American Nuclear Society.

(T-AEC, 2001) Taiwan Atomic Energy Council, *The Station Blackout Incident of the Maanshan NPP unit 1*, April 2001.

(US-AEC, 1962) US-AEC, *Additional Analysis of the SL-1 Excursion*, In: COMMISSION, U. S. A. E. (ed.). Idaho Falls, Idaho, USA.

(US-NRC/West) US-NRC, *Westinghouse Technology Systems Manual Section*, Section 2.1, Rev 1208.

(US-NRC, 1999) US-NRC, *Safety Evaluation by the Office Of Nuclear Reactor Regulation : SCIENCE*, Topical Report BAW-10228P, Oct 1999.

(US-NRC, 2011) US-NRC, 0523 - R504P - *Westinghouse Advanced Technology*, <www.nrc.gov/docs/ML1121/ML11216A051.pdf>, viewed 5 December 2018.

(US-NRC, 2013) US-NRC, *TRACE Simulation of SBO Accident and Mitigation Strategy in Maanshan PWR*, NUREG/IA-0430, 2013.

(US-NRC, 2017) US-NRC, 10 CFR 50 Appendix A, *General Design Criteria for Nuclear Power Plants,* <www.nrc.gov/reading-rm/doc-collections/cfr/part050/part050-appa.html>, viewed 3 March 2021.

(Venner, 2003) Venner J., Haley R.M., Bowden, R. L., *K-Effective as a Measure of Criticality Safety*, Japan Atomic Energy Research Institute conference, 2003.

(Wämundson, 2016) Wämundson M., *Operational Events in Off-Site Power System: Nuclear Power Plant Experiences and Mitigating Actions*, 6 ENERGIFORSK Report 2016:323, 2016.

# Appendix A: Reactivity Concepts

In this appendix the key reactivity related concepts are introduced, here with their relevance to a PWR, as well as providing some indication of the typical ranges for PWRs. The following reactivity concepts are discussed:

- Reactivity;
- Excess Reactivity;
- Reactivity Co-efficient;
- Control Rod Worth;
- Moderator Temperature Co-efficient;
- Fuel Temperature Co-efficient;
- Void Content;
- Power Co-efficient and Power Defect;
- Uncontrollable Neutron Poisons

## *Reactivity*

Reactivity (ρ) is a measure of the fractional change in neutron population in a nuclear core, between neutron generations (NAoNT, 2014). If the neutron population is decreasing the reactor has a negative reactivity, and is said to be *sub-criticality* In contrast, an increasing neutron population means the reactor has a positive reactivity, and is said to be *super-critical*. When the reactor maintains a constant neutron population its reactivity is zero, and the reactor is referred to as *critical*.

To maintain a constant power a reactor must be critical, but to start a reactor it will be made slightly supercritical in a controlled fashion, to gradually increase the neutron population. However, if shutdown, or after a transient or accident reactors are designed to be sub-critical, and must be maintained sub-critical.

The neutron population in a PWR, and hence reactivity, is affected by fuel temperature, moderator temperature, moderator density, and neutron poisons. Neutron poisons consists of both controllable and uncontrollable neutron poison. Uncontrollable neutron poisons are daughter products of the fission reactions which have high neutron cross-sections, such as $^{135}$Xe and $^{149}$Sm, and are not under the direct control of the reactor operator. In contrast, controllable poisons are neutron absorbers that are included in the plant design, for the operator to control, such as the boron in the moderator and the control rods.

## *Excess Reactivity*

To maintain criticality throughout core life, additional or excess positive reactivity must be provided during periodic reactor refueling. This is achieved by replacing depleted fuel with fresh fuel during the core reloads. This is required to compensate for the power and temperature increases to normal power operation levels, the build-up of fission product poisons (such as $^{135}$Xe and $^{149}$Sm), fuel ($^{235}$U)burn-up during the fuel cycle, and the increased neutron resonance capture due to the build-up of $^{240}$Pu.

This initial positive excess reactivity is counteracted through the addition of negative reactivity such as control rods, soluble boron, and fixed burnable neutron poisons. In the existing fleet of PWR, the most common method of controlling the excessive reactivity is through soluble boron, and burnable poisons. This allows the control rods to be essentially withdrawn from the reactor during power operation.

The initial fuel composition (including the insertion of burnable poisons), changes in the fuel composition and adjustments to the boron concentration in the moderator over the operating cycle, significantly affect the reactivity response of the reactor over the cycle.

## Reactivity Coefficients

The reactivity of the reactor is a function of numerous parameters, which are

- Reactor Scram – Control Rod Worth
- Fuel Temperature Coefficient
- Power Defect
- Moderator Temperature Coefficient
- Void Co-efficient
- Controllable Neutron Poisons
  - Boron
  - Control Rods
- Uncontrollable Neutron Poisons
  - Xenon
  - Samarium
  - Other Fission Products

In order to ensure that the reactivity-related assumptions in deterministic design base accidents are met the shutdown margin of the proposed reload pattern is predicted by means of computer codes. These predictions are made before each core reload using neutronics codes such as SCIENCE or BEACON, which are used at Koeberg. The shutdown margin takes into account the control rod worth and power defect. These predictions are then validated during the start-up physics test, which assesses the deviation from the predicted control bank worth versus the actual, measured worth. Before each reload, the shutdown margin is predicted. In simple terms this is the cumulative reactivity change that will occur due to the control rod insertion, including the power defect. Power defect takes into account the cumulative effects of change fuel temperature, moderator temperature and void changes, as the reactor core goes from a particular power level to hot shutdown, or zero power.

The following key elements are required to determine the immediate insertion of negative reactivity due to the control rod insertion:

- The initial fuel load configuration;
- The reactor power level at the time of shutdown or trip;
- The duration that the reactors has been at-power (burn-up & boron concentration);
- The position of the control rods during operation;
- Variation between the predicted and measured control rod worth.

The calculation of shutdown margin is performed in a very conservative way to ensure that the design basis analysis remains valid. The typical design basis shutdown margin acceptance criteria is 2 300 pcm. This is calculated for the most limiting DBA which is a Steam-line Break occurring at the end of the fuel cycle. The calculation of the shutdown margin is typically done by the fuel vendors, and conservatively takes into account the most conservative permissible control rod operating positions, defined by control rod insertion limits, and the *rod wear programme*.

Since both SBO and ELAP are not design basis accidents, but rather *design extension conditions*, best estimate assumption are permitted (IAEA, 2019). This permits a relaxation of the acceptance criteria and the removal of some of the conservatisms in the calculation. A high degree of confidence of not returning to criticality is still desired. Therefore, as a general rule, a 97.5% percentile will be adopted for the two key uncertainties, namely the uncertainties of the codes and the variability of

the different fuel loads, as well as changes in the reactor core and moderator concentration, over different fuel cycles.

While for the DBA studies it was concluded that the most penalizing reactivity case would be at the end of life, this is not immediately obvious for the ELAP scenario. While control rod worth (-ρ) increases, the power defect (+ρ) also increase as the fuel cycle progresses. With the boron concentration decreasing over the cycle, it also results in any accumulator injection having more negative reactivity worth, but results in the moderator temperature coefficient increasing which leads to any cooldown having a greater reactivity insertion toward end-of-life.

After considering the above-mentioned competing effects it was decided that the reactivity assessment would be done for four distinct stages of the fuel cycle, up to the start of stretch-out (when primary system boron concentration is fully diluted and the core power drops as the core excess reactivity is inadequate to maintain full power).

## Control Rod Worth

The control rods consist of neutron absorbing materials, and are used to reduce the core reactivity to render the reactor sub-critical when they are inserted. Control rod assemblies are referred to as rod cluster control assemblies (RCCA) in the PWR industry. Neutron absorber materials commonly used in control rods, in the nuclear power industry, include silver, iridium, cadmium, gadolinium, hafnium, boron carbide, and borosilicate glass.

Koeberg and the Framatome 900 MW fleet utilize control rod assemblies that consist of a silver, iridium and cadmium alloy (called AIC), encased in 316L stainless steel (IAEA, 1998).

There are two main measures of control rod worth. The first is the *differential control rod worth* which represents the change in reactivity by inserting a control rod in by one step. This changes as the control rod is inserted because the neutron absorption becomes more effective as the control rod travel through the centre of the core (where the neutron flux is normally greatest). The second measure is the *integral control rod worth* which represents the reactivity change due to the control rod being fully inserted. The latter measure is relevant to this dissertation.

The control rods are the primary method of reducing the reactivity of the core in order to ensure sub-criticality following an abnormal transient. However, the reactivity worth of the control rods varies not only from cycle-to-cycle, but also over the duration of a fuel cycle. These cycle-to-cycle variations are due to different fuel enrichment, the variation of burnable poison, and differing fuel assembly reload patterns. Control rod worth also changes during each cycle due to the gradual changes in the fuel composition and burnable poison burn-ups as well the gradual dilution of boron in the moderator.

## Moderator Temperature Co-efficient

The reactivity change due to the changes in the moderator temperature is referred to as the *moderator temperature co-efficient* (MTC). Reactors can have both positive and negative MTCs of varying magnitudes, which is primarily a function of the reactors moderator-fuel ratio, its moderator density, and the moderator boron concentration. Commercial PWRs generally have a negative moderator co-efficient as they are designed with an under-moderated moderator-to-fuel ratio. However, with cores now being designed with longer fuel cycles, the MTC maybe positive during the early stage of the cycle due to the high initial boron concentration.

The benefit of a negative MTC is that during a power excursion, the moderator temperature will increase providing a rapid negative reactivity excursion. However, when a reactor is cooled, it will

have the opposite effect and insert positive reactivity. In an ELAP, it is desirable to reduce the primary system pressure, to maintain primary inventory by reducing the flow through any primary leak paths. In order to reduce the pressure it is necessary to reduce the coolant/moderator temperature. This temperature reduction is one of the primary causes of positive reactivity insertion in a typical ELAP scenario.

A property of water is that at higher temperatures the density change per degree Celsius is larger. The larger density change at higher moderator temperature leads to a greater change in the moderator-to-fuel ratio which results in a larger MTC at higher temperatures. This means that the MTC changes as the moderator temperature increase.

The moderator of a PWR is not pure water. Commercial PWRs use a low concentration boric acid solution as the moderator to control the excess reactivity during the fuel cycle. It is used to compensate for fission product poisons as well as for reactivity adjustment (in order to trim the control rods to be fully withdrawn at full power operation). As the fuel cycle proceeds the moderator is gradually diluted as the excess reactivity of the core reduces. At the low boron concentration in the primary system, the density effect of the moderator can be treated as if it is water (Peretyazhko, 2003).

The presence of the boron in the moderator significantly affects the MTC. With a borated solution, a temperature decrease causes three distinct competing effects:

1. The boron concentration increases, causing a decrease in of the thermal utilization factor resulting in a negative reactivity insertion;
2. An increase in the moderator density increases the water density causing the thermal utilization factor to decrease slightly, resulting in a negative reactivity insertion. This negative reactivity insertion is due to the greater density of water and boron atoms available for absorption reactions in the reactor core.
3. The resonance escape probability increases due to more moderator molecules being available in the core, reducing the neutron path length, making resonance capture less likely.

For higher boron concentrations, typical at the beginning of a cycle, MTC tends to be less negative. However as the boron concentration approaches zero, typically at the end of a fuel cycle, the MTC will be at its most negative. A typical MTC for a commercial reactor is around -20 pcm/$^{o}$C. The MTC becomes more negative over core life, primarily due to the decreasing boron concentration becoming more negative to approximately - 60 pcm/$^{o}$C at the end-of-life, when the boron concentration is very low.

It should be noted that, beyond the point-of-adding heat (i.e. when the reactivity in the core starts increasing the coolant temperature) the effects of MTC, fuel temperature co-efficient (FTC) and voiding are combined into a common reactivity measure referred to as *power defect* which is easier to measure on a commercial reactor. Power defect is measured as pcm/%power.

## Fuel Temperature Co-efficient

The *fuel temperature co-efficient*, also known as the Doppler co-efficient of reactivity, is the reactivity change that accompanies changes in fuel temperature. It arises as the resonance cross sections of the fuel changes with a change in the fuel temperature. It is primarily related to the resonance cross section broadening of certain fuel materials, primarily non-fissile $^{238}$U and $^{240}$Pu. As the fuel temperature increases, the width of the resonance energy capture peak broaden which results in a greater portion of the neutrons being captured by non-fissile fuel material, thus reducing the core reactivity. The fuel temperature co-efficient is always negative, and it effects is the first

almost instantaneous response to any reactivity change, due to the rapid change in heat production and hence fuel temperature.

The fuel temperature co-efficient is more negative toward end of the fuel cycle than it is at beginning of the fuel cycle. Three important factors affect the Doppler power co-efficient over the core lifetime. The first is the build-up of $^{240}Pu$ which has relativity high neutron capture cross-section, making the Doppler power co-efficient more negative. The second is as a result of the production fission product gases, such as xenon and krypton, which reduce the fuel clad-gap thermal conductivity co-efficient of the original helium, which was initially used to pressurize the fuel rods during manufacturing. This results in the Doppler co-efficient becoming more negative during core life. However, the fuel-clad gap reduction is the overriding effect, out-weighing the combined effect of the other two causes.

During the fuel cycle the fuel pellets swell due to the production of fission gases. The pellet expansion, clad creep and distortion of the zircalloy fuel cladding (due to external pressure) reduces the fuel-clad gap, causing direct contact between the fuel pellets and the cladding. This improves the overall thermal fuel-to-moderator conductivity, resulting in the Doppler-only power co-efficient becoming less negative over the fuel cycle. At beginning of the fuel cycle the fuel temperature rises to approximately 540 $^{o}$C at full power, but at end of the cycle it reduces to approximately 425 $^{o}$C.

As a result of all three of these effects, the Doppler-only power co-efficient will become less negative over core life, resulting in the BOL values being more negative than the EOL values.

## Void Content

The moderator void co-efficient is the change in neutron multiplication as a result of the presence of voids in the moderator. This is a significant reactivity contributor in BWRs, but in a PWR there is only a small void content in the core, due to nucleate boiling at full power. In a PWR, the void coefficient, due to local or random boiling, is less than half a percent, which is not very significant.

Typically, the void coefficient is approximately - 250 pcm/%-void, during normal operating temperatures (at the EOL). The negative void co-efficient at operating temperature becomes more negative with fuel burn-up. With void only occupying about 0.5% of the total moderator/coolant volume in PWR at full power, like the pressure co-efficient, the total reactivity inserted by the void fraction is very small. The void collapse coincident with power reduction makes a small reactivity contribution.

## Power Co-efficient and Power Defect

Power defect is the change in reactivity due to the power increase. It is the cumulative reactivity change due to the changes in fuel temperature (fuel temperature co-efficient), void content (void co-efficient) and moderator temperature (moderator temperature co-efficient) from the point of adding heat to operating power level, measured as a percentage of rated power. It is used as a surrogate measure of fuel temperature, and voiding which cannot be measured in the reactor. This is one of the reactivity parameters that are considered in this study.

## Boron Worth

The primary way of countering the excess reactivity present in the core after the initial reloading of light water reactors is with soluble boron. The boron concentration in the coolant is gradually diluted over the fuel cycle (from around 2 000 ppm, down to as low 10 ppm) as the core's excess reactivity gradually depletes. Adjustments to the concentration of the boron in the primary system,

is referred to as *chemical shimming*. The introduction of boron is to provide an additional neutron poison by increasing the macroscopic cross section for neutron absorption of the coolant/moderator through-out the core.

Both the passive and active safety injection systems introduce higher concentration of boron, typically around 2 500 ppm. This is in order to provide additional shutdown margin, and to limit the core re-criticality in rapid cooldown accidents, such as steam line breaks.

In order to establish the change in reactivity due to boron concentration changes it is necessary to introduce the concept of *differential boron worth*, which is the incremental change of reactivity caused by incremental change in boron concentration in the coolant. In PWRs this is typically expressed in units of pcm/ppm, and is typically between - 6 pcm/ppm and - 10 pcm/ppm, dependent on boron concentration and moderator temperature.

Lower boron concentrations result in a higher differential (most negative) boron-worth, due to competition. At lower concentrations the boron atoms in the moderator are not competing with the number of boron atoms at higher concentration, so their individual worth is higher. Another important consideration is the changes in boron worth due to moderator temperature. At lower temperatures the reactor core will contain a larger mass of water, and hence a larger mass of boron in the core, for a particular concentration of boron. This leads to greater neutron absorption, and therefore a higher differential boron worth.

## Uncontrollable Neutron Poisons

During the fission process, fission products are generated that absorb neutrons. Some of these fission products, or subsequent decay isotopes, have significant neutron cross-sections that can have a significant impact on the reactivity of the reactor. In the operation of any nuclear reactor, the reactivity associated with xenon and samarium in the core is important. The most significant of these isotopes are xenon-135 ($^{135}$Xe) and samarium-149 ($^{149}$Sm), which must be considered in the reactivity calculation. The typical operating reactivity associated with equilibrium concentrations of these two isotopes, is - 3 000 pcm due to the equilibrium for xenon and - 1 000 pcm for samarium. Therefore, at power the core typically requires an additional 4 000 pcm reactivity insertion to maintain power.

### *Xenon*

On 26$^{th}$ September 1944, during the start-up of the first Pile at Hanford (Pile B), xenon made an unexpected entrance into the reactivity game. While the reactor was successfully brought to criticality, after a few hours the reactor unexpectedly started to lose power and eventually went sub-critical. After initially baffling the scientists and engineers it was noticed that the reactivity change was similar to the exponential decay of a particular radioactive isotope. The guilty party was Iodine-135 ($^{135}$I), which was decaying into $^{135}$Xe (Rhodes, 2012).

This particular fission product isotope, $^{135}$Xe, has an extremely large neutron capture cross section, and its build-up prevented the reactor from remaining criticality. Fortunately, certain Du Pont engineers had insisted that the piles be built with extra fuel channels, to cater for unforeseen complications. These additional fuel channels were utilized to give the reactor the necessary excess reactivity to compensate for the xenon buildup, allowing the reaction to be sustainable. Utilizing these additional channels provided the reactor with the additional excess reactivity required to overcome the xenon build-up.

While other neutron poisons such as samarium, are also produced during the nuclear reactor operation, $^{135}$Xe is the most significant uncontrollable neutron poison. $^{135}$Xe has an extremely large neutron capture cross section (2.6 million barns). During reactor power operation, the isotope $^{135}$Xe is formed as a fission product. Both tellurium and iodine are created as daughter products in

significant quantities (~6%) during $^{235}U$ fission reactions. Tellurium-135 quickly decays (with a half-life of 19.2 seconds) to iodine, but iodine decays to xenon with a longer half-life of 6.6 hours, but is shorter than $^{135}Xe$ half-life of 9.1 hours. The $^{135}Xe$ isotope depletes in two ways. It can capture a thermal neutron, forming $^{136}Xe$, which is stable and has a very small capture cross section, or it can decay to $^{135}Cs$.

The radioactive decay chain of $^{135}Te$ is as follows:

$$^{135}_{52}\mathrm{Te} \xrightarrow[19.2\ \mathrm{sec}]{\beta^-} {}^{135}_{53}\mathrm{I} \xrightarrow[6.6\ \mathrm{hrs}]{\beta^-} {}^{135}_{54}\mathrm{Xe} \xrightarrow[9.1\ \mathrm{hrs}]{\beta^-} {}^{135}_{55}\mathrm{Cs}$$

When the reactor is first brought to power, the concentration of $^{135}Xe$ (atoms/cm$^3$) slowly builds up to an equilibrium value. This is due primarily to the relatively long half-lives of $^{135}I$ (6.6 hours) and $^{135}Xe$ (9.1 hours). After start-up the $^{135}Xe$ concentration builds-up in the core, and after approximately 48 hours (dependent on the neutron flux, which is a function of reactor power) reaches an equilibrium level. After this the condition is reached where the production rate of $^{135}Xe$ is equal to the removal rate of $^{135}Xe$ by neutron capture plus the loss of $^{135}Xe$ through radioactive decay. Because of the high thermal neutron cross section of $^{135}Xe$, as the concentration of the isotope increases, the macroscopic absorption cross section of the core also increases.

Once the $^{235}U$ reaction is stopped, the production of xenon directly from fission and removal by burnout almost ceases. The remaining process which produces and consumes any of the relevant fission products is the radioactive decay of iodine to produce xenon, and radioactive decay of the xenon which removes it. This leads to an initial spike in xenon concentration, which further poisons the core. This increases until the decay rate of xenon overcomes its production rate, mainly through the reduced concentration of iodine, with a xenon concentration peak occurring around 8 or 9 hours after shutdown. There is a general rule of thumb for PWRs (GPC, 1999) for the time (in hours) that the xenon peak will occur after the reactor shutdown, or trip, is the square root of the percentage reactor power before the shutdown. After around 22 hours, the $^{135}Xe$ concentration decreases back to the initial full power operation concentration. Thereafter, a relative net positive reactivity insertion occurs, that needs to be taken into account, and possibly compensated for. Ultimately, after about three days, almost all of the $^{135}Xe$ will have decayed away.

After a reactor trip, the point of interest is the relative reactivity insertion generated by the long-term depletion of the $^{135}Xe$ isotope. It is known that, after 4 days almost all the $^{135}Xe$ will have decayed away. It is important to establish the reactivity insertion required in order to offset all the xenon induced reactivity effects at the at power equilibrium xenon concentration.

When a reactor is at power the reactor will need to produce additional reactivity to compensate for the xenon buildup (Bennet, 1989). Once the reactor has reached xenon equilibrium (constant xenon concentration) the maximum equilibrium reactivity for a nuclear power reactor with a typical thermal neutron flux of $\phi_{th} = 10^{14}$ neutrons/cm$^2$ (Koeberg's thermal flux $\phi_{th}$ ranges from 3.6 to 4.2x10$^{13}$ neutrons/cm$^2$) reaches a limiting equilibrium reactivity insertion of:

$$\rho_{Xe}^{Max} = \frac{f\eta(\gamma_I + \gamma_{Xe})}{\upsilon}$$

To illustrate, a natural uranium reactor has $\eta = 1.32$, $\upsilon = 2.42$ and a cumulative iodine and xenon fission yield ($\Upsilon_I + \Upsilon_{Xe}$) of 0.064. Assuming $f = 0.9$ the maximum reactivity insertion will be around - 3100 pcm (Bennet, 1989). For a typical PWR at full power, the reactivity insertion associated with the equilibrium $^{135}Xe$ level is around - 2 700 pcm. This will be less at lower power levels, with the induced reactivity insertion from the equilibrium xenon concentration for a PWR at 50% power,

being around - 2 100 pcm (GPC, 1999). It should be noted that these are generic reactivity insertion estimates which can be affected by the size of the reactor core.

In reality, the xenon induced reactivity insertion is in fact a little higher than - 3000 pcm, with the enriched fuel and plutonium build-up at the neutron flux level in a Framatome 900 MW reactor. Four days after a reactor has tripped from full power, this xenon will have essentially decayed away, effectively creating an additional + 3000 pcm reactivity insertion, which is not controllable.

### *Samarium*

Samarium-149 ($^{149}$Sm) is the other neutron poison considered significant enough to track, which is created in the fission cycle. It is a stable isotope and has a neutron capture cross-section of around $4.2x10^4$ barns. It is generated through beta decay, involving the decay of both neodymium ($^{149}$Nd) and promethium ($^{149}$Pm) isotopes. $^{149}$Nd beta decays to $^{149}$Pm with a short half-life of 1.7 hours. Then $^{149}$Pm beta decays to $^{149}$Sm, with a relatively longer half-life of 53 hours.

These fission products occur in about 2.1% of $^{235}$U fissions, and their equilibrium concentrations in any reactor produce - 650 pcm of reactivity. As $^{149}$Sm is a stable isotope, its equilibrium concentration is independent of the power level (neutron flux). However, after a reactor shutdown the $^{149}$Sm concentration builds up to an asymptotic value that is dependent on the promethium equilibrium concentration, which in turn is power dependent. The rate at which the $^{149}$Sm concentration reaches this new equilibrium is related to the $^{149}$Pm decay rate (which has a half-life of 53-hours).

Due to the build-up of samarium, a reactor trip (or shutdown) from full power, eventually reduces the reactivity (after 400 hours) by a further - 250 pcm at BOL, and - 500 pcm at EOL (ESKOM, PDBs).

# Appendix B: Development of Accident Analysis in PWRs

The PWR was originally designed in the United States by Westinghouse. This design was guided by the US-NRC general design criteria for nuclear power plants, as legislated in the code of federal regulations 10 CFR 50, Appendix A (US-NRC, 2017).

## *General Design Criteria for PWRs*

These regulations included general design criteria (GDC) such as the single failure criterion, used in the design of the nuclear island and its safety systems. The general design rules were developed in order to ensure that the design of the then-new technology was robust, with some degree of consistency. The GDC drew on and used the existing electrical, material, and pressure vessel design codes of the time, as well as incorporating insight from early incident on the original experimental reactors. One such accident that resulted in a significant criticality accident, that influenced the GDC, was the SL-1 accident. This accident occurred on a military experimental reactor (US-AEC, 1962), and is discussed in detail below.

However, subsequent to the development of the GDC which has formed the backbone of PWR design over the past decades some limitations of these design rules have been highlighted. However, it has often taken a significant accident in the nuclear industry to create the necessary consensus to adopt additional tools and methodologies to address these deficiencies. Below is a brief overview of those major nuclear accidents that have led in some way to the evolution of nuclear safety in the PWR industry, with a specific focus on those developments that impact on ELAP and reactivity events.

## *SL-1 Accident*

SL-1 was a US army experimental reactor situated in Idaho, USA. In 1961, the SL-1 reactor experienced a criticality accident which caused a steam explosion, while the operators were attempting to reconnect the control drive mechanism after a shutdown. The central control rod assembly is believed to have been lifted excessively, which resulted in the reactor inadvertently going critical and causing a steam explosion. As a result the control rod was ejected and impaled one of the reactor operators on the roof of the facility. After the reactivity excursion that resulted in three fatalities, it was recommended that all reactivity analyses is conducted assuming that the highest worth control rod assembly is not inserted (US-AEC, 1962). This recommendation has subsequently been incorporated into the general design criteria in 10 CFR 50, appendix A. This is reflected in the requirements for all design base analysis by the US-NRC, specifically general design criteria 23, and has become the norm for all PWR design base analysis.

Subsequent to the development of the GDC in 10-CFR-50 Appendix A, other commercial nuclear power plant accidents have occurred, leading to nuclear regulators including the US-NRC, IAEA and the South African NNR, to supplement the GDCs with additional rules, as well as tools such as PSA. This evolution has often been in response to certain major nuclear accidents which are described below.

## *Three Mile Incident*

The Three Mile Island (TMI) accident was the first major nuclear accident on a PWR reactor. Following the loss of both main and auxiliary feed-water, a misdiagnosed pressurizer relief valve that was stuck open, led to core damage when the operators turned off both trains of safety injection, in the mistaken belief that a high pressurize level indicated that the reactor core was still covered. The containment building limited the radioactive releases to the public. In the nuclear industry it was a significant accident as it involved the failure and inoperability of multiple safety systems, which had not been considered in the original design basis. This highlighted deficiencies in the original design basis rules, such as single failure criteria, and the inadequacy of state-based accident procedures.

The key insights that the nuclear industry internalized as a result of the TMI accident was that, while the original design criteria were more arduous than those used in most other industries, they still did not guarantee that an accident could not happen. Specifically, it cast doubt on the single failure assumption that all the plants' accident mitigation systems were designed to meet. A few months earlier the first probabilistic risk assessment (PSA) for US commercial nuclear reactors, known as *Wash 1400*, was released. By performing a detailed estimation of the frequency of nuclear accidents, it correctly predicted that a nuclear accident of some type was imminent, in spite of elaborate design basis requirements intended to eliminate this. PSA specifically dealt with the likelihood of multiple failures occurring, a consideration that is generally excluded in design basis analysis. The important insight internalized by the industry was that multiple failures were in fact possible, and that the conservative design rules applied to nuclear reactor could not guarantee that a nuclear accident would not occur.

## Chernobyl Accident

After the infamous Chernobyl accident in 1986, it was widely publicized that the RBMK reactor design was significantly different from the Western commercial reactor designs, and that little insight could be drawn from the event for the BWRs and PWRs, except to re-emphasize the importance of designing and adhering to safe operating procedures. However, the accident did make the nuclear industry beyond Russia focus its attention towards rigorously identifying potential reactivity accidents that had not been considered before. These assessments did identify a few additional ways leading to inadvertent dilution that could cause significant reactivity excursions on PWRs. This led to a design upgrade to PWRs in order to eliminate the risk of dilution incidents.

## Fukushima Accident

On Friday, 11 March 2011, Japan was struck by the Great East Japan Earthquake with a magnitude of 9.0 $M_w$. Its epicentre was 130 km offshore from the city of Sendai on the east coast of Honshu Island. The earthquake initiated a series of large tsunami waves, which inundated the east coast of Japan. The earthquake affected eleven operational nuclear reactors at four nuclear power plants. All of the affected units scrammed automatically, as designed, when the earthquake hit. Subsequent inspection showed that there was no significant damage to any of the units resulting from the earthquake. The main nuclear concern was centred on the Fukushima Daiichi plant, specifically, Units 1 to 3, which were at power before the earthquake struck. The plant was initially struck by the beyond-design-basis earthquake, followed by a series of tsunami waves, the highest reaching a height of 15 m.

At 2:46 pm, the earthquake caused a seismic automatic reactor scram on Units 1 to 3, and the control rods on all three operational reactors inserted successfully. The other units were in outage. The earthquake resulted in measured horizontal peak ground accelerations as high as 0.56 g, and vertical peak ground accelerations up to 0.31 g. Although the seismic accelerations exceeded the seismic design basis of the plant, the plant did not experience significant seismic damage to any of its main structures. As a result of the earthquake, the off-site electrical power supplies to all units were lost, but initially the emergency diesel generators all started up automatically. The off-site supplies were lost due to earthquake induced damage to the transmission lines and electrical equipment in the switchyard.

Forty minutes later, the first tsunami wave arrived at the Fukushima Daiichi plant. It submerged a breakwater that was 5.7 m above sea level, destroying the seawater pumps near the water intakes. One of the subsequent waves, estimated to be as high as 14 m, inundated the turbine buildings, with up to 5 m of water, completely submerging the entrances to the facilities, and inundating the basement levels. The flooding level of the tsunami was beyond the design basis of the Fukushima Daiichi plant. The diesel generators, the electrical switchgear, and the batteries were inundated, as

they were located in the basements of the turbine buildings. The site remained flooded for approximately 30 minutes, resulting in the inundation of many buildings with compartments below terrace level. All of the onsite diesel generators on Unit 1 to Unit 4 were lost due to the flooding. Although the water-cooled diesel generators at Unit 5 and Unit 6, situated on a higher terrace were not flooded, they were also rendered inoperable due to the loss of their seawater cooling pumps. With the exception of a single air cooled diesel generator on Unit 6, which eventually supplied both Unit 5 and Unit 6 with AC power, all of the on-site emergency diesel generators (EDGs) were lost. This resulted in an extended loss of all AC power (ELAP), until off-site power was restored 11 days later. All of the medium-voltage switchgear was damaged by the tsunami, on units 1 to 5. Even if the diesel generators had been operable, it still would not have been possible to supply power to the necessary equipment as most of the low-voltage switchgear was also damaged by seawater. By 22 March 2011, the AC electricity supply from an external source was connected to all units. However, radiation levels inside the plant were so high that normal access was impossible until June 2011.

Until this event the nuclear industry had assumed that it was possible to recover safety system within a day. This assumption is reflected in most PSA which only model most accidents up to 24 hours, implicitly assuming that an event beyond 24 hours can be recovered by the emergency team. As a consequence of the Fukushima accident, nuclear plants and supporting emergency organization have been upgraded to cater for both prolonged accidents and multi-unit events. The concept of Design Extension Conditions (DEC) was introduced to cater with beyond design base accidents.

## Appendix C: SBO or Near SBO Events that have occurred at NPPs

The primary source for these SBO events is the IAEA (IAEA, 2015).

| Year | Plant | Rx Type | Cause |
|---|---|---|---|
| **1986** | Kori-4 *(Republic of Korea)* | PWR | SBO caused by a typhoon. |
| **1990** | Vogtle-1 *(USA)* | PWR 4-loop | Offsite power was lost from switchyard work during a refuelling outage, and the only operable EDG failed to start. |
| **1993** | Narora 1 *(India)* | HWR | Ejected turbine blade caused a fire and hydrogen explosion. Due to fire, cables started burning and there was complete loss of power supply in the unit including loss of class I & II supplies. The extended SBO lasted for approximately seventeen hours. |
| **1993** | Kola-1 & 2 *(Russia)* | VVER-440/230 | LOOP induced by high winds with the subsequent loss of EDGs lead to an SBO. Hurricane strength winds (40 m/s) damaged the surrounding the high voltage transmission lines, leading unstable (voltage & frequency) grid to a grid collapse. Voltage transients in the NPP unit auxiliary power line resulted in trips of the turbine generators and other main equipment and reactor scrams. An attempt to supply power to both Units 1 and 2's equipment using the emergency diesel generators (EDGs) was unsuccessful due to design deficiencies in in the automatic control of the EDGs, and the lack of uninterruptible power supplies for the vital 380 V loads. (Wämundson, 2016) |
| **2001** | Maanshan-1 *(Taiwan)* | PWR | The unit lost its offsite power supply due to salt-laden sea mist, leading to grid instability and eventually grid failure. On unit 1 both EDGs failed to start, one due to a bus grounding fault, and the other due to a loss of power to its exciter as well as the onsite diesel. The SBO lasted for just over 2 hours. |
| **2006** | Forsmark -1 *(Sweden)* | BWR | Switchyard work resulted in overvoltage and a degraded electrical safety systems performance that nearly resulted in a SBO event. A short-circuit on the national electric grid (400 kV) first caused loss of the main offsite power supply. The power plant's two Turbo-generators then generated a significant overvoltage on the internal network, putting two UPS's out of service, making it impossible to use two diesel generator sets that would have provided a backup supply for the safety equipment of two trains out of four. Other failures also led to the failure of house load operation and switching over to the second auxiliary offsite line (70 kV). Fortunately, the over-voltage did not take the remaining two UPS's of the other two safety trains out of service, and the corresponding two diesel generator sets managed to automatically supply the safety equipment of two out of four of the trains. The incident thus demonstrated a common mode failure on the emergency power supply (diesel generator sets) of the safety equipment in addition to an electrical disturbance on the national grid, that had not been taken into account in the design. |
| **2007** | Dampierre-3 *(France)* | PWR | Unit 3 lost the power supplies to the train A safety equipment, and then subsequently lost power supplied from the grid. The failure of an overcurrent protection relay on the LHA emergency switchboard made it impossible to connect the emergency diesel generator set to the LHA switchboard. Only the Train B safety equipment could be supplied via the LHB switchboard. In accordance with the applicable emergency response procedures, the operators started reducing reactor power (initially to 60% of nominal power) with the goal of shutting the reactor down. During the shutdown when the turbine was tripped, another fault on the closing switch for coupling the turbo-generator set to the grid aggravated the situation (opening of the line circuit breaker) causing loss of the plant power supply via the external "main" line. Furthermore, in accordance with a new operating procedure, the operator load-shed certain electrical panels to economize the associated backup batteries, thus making it impossible for the power plant to be re-supplied via the "auxiliary" external line provided for this type of situation. The loss of off-site power supply led to an automatic reactor scram and the automatic starting of the Train B emergency diesel generator. The reactor was thus able to be taken to the shutdown status planned for in such a situation by using train B safety equipment. The plant operator restored the offsite power supplies the following day, enabling the reactor to be shutdown. |

| Year | Plant | Rx Type | Cause |
|---|---|---|---|
| **2011** | Fukushima Daiichi *(Japan)* | BWR | Following a major earthquake of magnitude 9.0 $M_w$, a 15-metre tsunami disabled the power supply and cooling of three Fukushima Daiichi reactors, causing an extended SBO. |
| **2012** | Byron (USA) | PWR | Failure of an insulator resulted in open phase conditions on the off-site power source. The failure was not detected by the onsite degraded voltage relays and, as a result, the EDGs did not start. *The degraded voltage conditions resulted in inability to use offsite and onsite AC power sources.* |
| **2012** | Kori 1 (Republic of Korea) | PWR | An error in generator protective relay testing resulted in the loss of offsite power to shutdown cooling. Consecutive failure of the EDG to start resulted in SBO event. Off-site power was restored 12 minutes after the SBO condition began. |

***Table 19:*** *SBO or near SBO events that have occurred at commercial nuclear power plants*

## Appendix D: Integrated Control Rod Worth

| Fuel Cycle | Fuel Manufacturer | Burn-up (MWd/MTU) | | | |
|---|---|---|---|---|---|
| | | BOL | BLX | MOL | EOL |
| | | 0 | 150 | 8000 | 16142 |
| KB118 [A] | AREVA | -7 541 pcm | -7 580 pcm | -7 763 pcm | -8 134 pcm |
| KB119 [A] | AREVA | -7 500 pcm | -7 539 pcm | -7 703 pcm | -8 072 pcm |
| KB120 [W] | Westinghouse | -8 573 pcm | -8 566 pcm | -8 752 pcm | -9 087 pcm |
| KB121 [W] | Westinghouse | -8 462 pcm | -8 457 pcm | -8 675 pcm | -8 966 pcm |
| KB122 [W] | Westinghouse | -7 684 pcm | -7 682 pcm | -8 118 pcm | -8 710 pcm |
| KB123 [W] | Westinghouse | -8 181 pcm | -8 188 pcm | -8 430 pcm | -8 824 pcm |
| KB218 [A] | AREVA | -7 620 pcm | -7 654 pcm | -7 822 pcm | -8 176 pcm |
| KB219 [A] | AREVA | -7 508 pcm | -7 557 pcm | -7 755 pcm | -8 112 pcm |
| KB220 [A] | AREVA | -7 746 pcm | -7 781 pcm | -7 917 pcm | -8 247 pcm |
| KB221 [A] | AREVA | -7 582 pcm | -7 624 pcm | -7 814 pcm | -8 149 pcm |
| KB222 [A] | AREVA | -7 723 pcm | -7 765 pcm | -7 935 pcm | -8 274 pcm |
| KB223 [A] | AREVA | -7 793 pcm | -7 830 pcm | -7 959 pcm | -8 264 pcm |
| **4.4% Enrichment Cycles for Both Units** | **Maximum C/Rod Worth** | -8 573 pcm | -8 566 pcm | -8 752 pcm | -9 087 pcm |
| | **5th Percentile** | -8 512 pcm | -8 506 pcm | -8 710 pcm | -9 020 pcm |
| | **95th Percentile** | -7 504 pcm | -7 549 pcm | -7 732 pcm | -8 094 pcm |
| | **Minimum C/Rod Worth** | **-7 500 pcm** | **-7 539 pcm** | **-7 703 pcm** | **-8 072 pcm** |
| | **Average C/Rod Worth** | -7 826 pcm | -7 852 pcm | -8 054 pcm | -8 418 pcm |
| | *Standard Deviation* | *372 pcm* | *354 pcm* | *366 pcm* | *369 pcm* |
| **Unit 1 4.4% Enrichment Cycles** | **Maximum Rod Worth** | -8 573 pcm | -8 566 pcm | -8 752 pcm | -9 087 pcm |
| | **5th Percentile** | -8 545 pcm | -8 539 pcm | -8 733 pcm | -9 057 pcm |
| | **95th Percentile** | -7 510 pcm | -7 549 pcm | -7 718 pcm | -8 087 pcm |
| | **Minimum Rod Worth** | **-7 500 pcm** | **-7 539 pcm** | **-7 703 pcm** | **-8 072 pcm** |
| | **Average Rod Worth** | -7 990 pcm | -8 002 pcm | -8 240 pcm | -8 632 pcm |
| | *Standard Deviation* | *476 pcm* | *459 pcm* | *452 pcm* | *430 pcm* |
| **Unit 2 4.4% Enrichment Cycles** | **Maximum Rod Worth** | -7 793 pcm | -7 830 pcm | -7 959 pcm | -8 274 pcm |
| | **5th Percentile** | -7 781 pcm | -7 817 pcm | -7 953 pcm | -8 272 pcm |
| | **95th Percentile** | -7 526 pcm | -7 574 pcm | -7 770 pcm | -8 122 pcm |
| | **Minimum Rod Worth** | **-7 508 pcm** | **-7 557 pcm** | **-7 755 pcm** | **-8 112 pcm** |
| | **Average Rod Worth** | -7 662 pcm | -7 702 pcm | -7 867 pcm | -8 204 pcm |
| | *Standard Deviation* | *110 pcm* | *106 pcm* | *81 pcm* | *67 pcm* |

***Table 19:*** *Integrated control-rod insertion worth (all 48 assemblies inserted)*

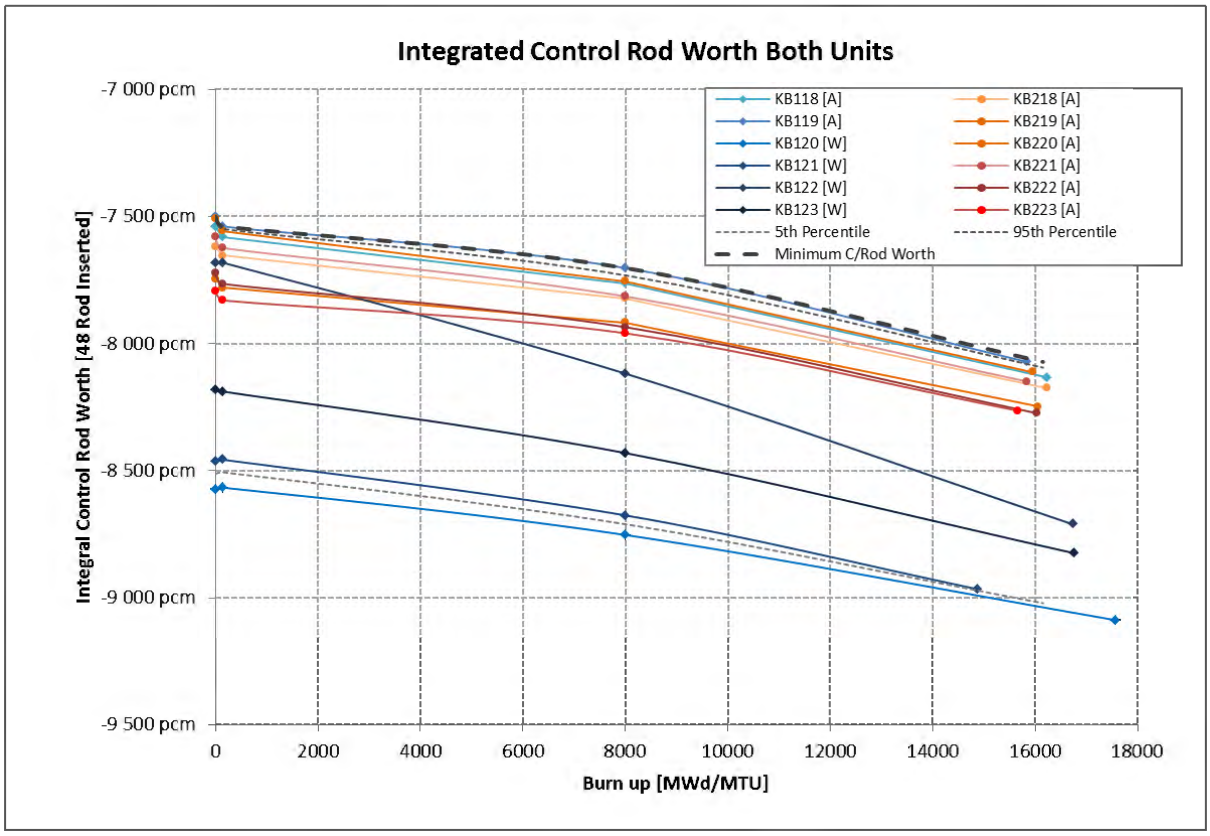


***Figure 14:*** *Integral control-rod worth with all 48 assemblies inserted for all cycles considered*

| Fuel Cycle | Fuel Manufacturer | Control Rod Bank Worth - BOL/HZP - Measured | | | | | |
|---|---|---|---|---|---|---|---|
| | | D | SA | SB | A | B | C |
| KB117 [A] | AREVA | 1 101 pcm | 1 038 pcm | 814 pcm | 474 pcm | 1 037 pcm | 855 pcm |
| KB118 [A] | AREVA | 947 pcm | 1 019 pcm | 774 pcm | 491 pcm | 1 090 pcm | 995 pcm |
| KB119 [A] | AREVA | 993 pcm | 1 077 pcm | 902 pcm | 484 pcm | 1 112 pcm | 793 pcm |
| KB120 [W] | Westinghouse | 1 008 pcm | 1 227 pcm | 1 124 pcm | 388 pcm | 856 pcm | 939 pcm |
| KB121 [W] | Westinghouse | 1 032 pcm | 1 210 pcm | 1 143 pcm | 247 pcm | 818 pcm | 1 003 pcm |
| KB122 [W] | Westinghouse | 1 099 pcm | 1 209 pcm | 958 pcm | 226 pcm | 835 pcm | 1 114 pcm |
| KB123 [W] | Westinghouse | 1 066 pcm | 1 015 pcm | 988 pcm | 436 pcm | 892 pcm | 984 pcm |
| KB217 [A] | AREVA | 823 pcm | 1 223 pcm | 897 pcm | 421 pcm | 780 pcm | 1 011 pcm |
| KB218 [A] | AREVA | 865 pcm | 1 063 pcm | 730 pcm | 473 pcm | 1 047 pcm | 923 pcm |
| KB219 [A] | AREVA | 992 pcm | 1 075 pcm | 790 pcm | 492 pcm | 1 081 pcm | 811 pcm |
| KB220 [A] | AREVA | 791 pcm | 1 311 pcm | 840 pcm | 507 pcm | 1 086 pcm | 765 pcm |
| KB221 [A] | AREVA | 980 pcm | 1 127 pcm | 731 pcm | 514 pcm | 1 084 pcm | 863 pcm |
| KB222 [A] | AREVA | 1 041 pcm | 1 104 pcm | 737 pcm | 515 pcm | 1 153 pcm | 831 pcm |
| KB223 [A] | AREVA | 1 091 pcm | 1 031 pcm | 807 pcm | 472 pcm | 1 057 pcm | 871 pcm |
| | | | | | | | |
| **Minimum Bank Worth** | | 791 pcm | 1 015 pcm | 730 pcm | 226 pcm | 780 pcm | 765 pcm |
| **5th Percentile** | | 812 pcm | 1 018 pcm | 731 pcm | 240 pcm | 805 pcm | 783 pcm |
| **95th Percentile** | | 1 100 pcm | 1 256 pcm | 1 131 pcm | 514 pcm | 1 126 pcm | 1 047 pcm |
| **Maximum Bank Worth** | | **1 101 pcm** | **1 311 pcm** | **1 143 pcm** | **515 pcm** | **1 153 pcm** | **1 114 pcm** |
| **Average Bank Worth** | | 988 pcm | 1 124 pcm | 874 pcm | 439 pcm | 995 pcm | 911 pcm |

***Table 20:*** *Hot Physics Test measured control bank worth*

| Fuel Cycle | Fuel Manufacturer | Control Rod Bank Worth - BOL/HZP - Delta (Measured - Predicted)/Predicted | | | | | | |
|---|---|---|---|---|---|---|---|---|
| | | D | SA | SB | A | B | C | Delta for All Banks |
| KB117 [A] | AREVA | 10 pcm | 11 pcm | 2 pcm | 19 pcm | 4 pcm | 41 pcm | 87 pcm |
| KB118 [A] | AREVA | 32 pcm | 45 pcm | -2 pcm | 36 pcm | 72 pcm | 48 pcm | 231 pcm |
| KB119 [A] | AREVA | 14 pcm | -4 pcm | -2 pcm | 25 pcm | 35 pcm | 14 pcm | 82 pcm |
| KB120 [W] | Westinghouse | -33 pcm | 47 pcm | 31 pcm | 1 pcm | -6 pcm | 14 pcm | 54 pcm |
| KB121 [W] | Westinghouse | -49 pcm | 30 pcm | -20 pcm | 16 pcm | -11 pcm | -18 pcm | -52 pcm |
| KB122 [W] | Westinghouse | 27 pcm | 72 pcm | 43 pcm | -10 pcm | -8 pcm | 52 pcm | 176 pcm |
| KB123 [W] | Westinghouse | -27 pcm | 0 pcm | -2 pcm | 4 pcm | -26 pcm | 9 pcm | -42 pcm |
| KB217 [A] | AREVA | 8 pcm | 20 pcm | -1 pcm | 17 pcm | 21 pcm | 30 pcm | 95 pcm |
| KB218 [A] | AREVA | -14 pcm | -10 pcm | -22 pcm | -13 pcm | -3 pcm | 15 pcm | -47 pcm |
| KB219 [A] | AREVA | -5 pcm | -1 pcm | -6 pcm | 21 pcm | -2 pcm | 15 pcm | 22 pcm |
| KB220 [A] | AREVA | -60 pcm | -42 pcm | -65 pcm | -19 pcm | -27 pcm | -46 pcm | -259 pcm |
| KB221 [A] | AREVA | -24 pcm | -34 pcm | -43 pcm | -8 pcm | -39 pcm | 0 pcm | -148 pcm |
| KB222 [A] | AREVA | -10 pcm | -41 pcm | -18 pcm | 3 pcm | -41 pcm | -6 pcm | -113 pcm |
| KB223 [A] | AREVA | -15 pcm | -36 pcm | -35 pcm | 0 pcm | -31 pcm | -11 pcm | -128 pcm |
| | | | | | | | | |
| **Max. Bank Over-prediction** | | -60 pcm | -42 pcm | -65 pcm | -19 pcm | -41 pcm | -46 pcm | -65 pcm |
| **95th Percentile** | | -53 pcm | -41 pcm | -51 pcm | -15 pcm | -40 pcm | -28 pcm | -43 pcm |
| **5th Percentile** | | 29 pcm | 56 pcm | 35 pcm | 29 pcm | 48 pcm | 49 pcm | 47 pcm |
| **Max. Bank Under-prediction** | | 32 pcm | 72 pcm | 43 pcm | 36 pcm | 72 pcm | 52 pcm | 72 pcm |
| **Mean Bank Difference** | | -10 pcm | 4 pcm | -10 pcm | 7 pcm | -4 pcm | 11 pcm | -2 pcm |
| Standard Deviation | | 27 pcm | 36 pcm | 28 pcm | 16 pcm | 31 pcm | 27 pcm | 138 pcm |

***Table 21:*** *Predicted versus Hot Physics Test measured control bank worth results*

| Fuel Cycle | Fuel Manufacturer | Control Rod Bank Worth - BOL/HZP - %Delta (Measured - Predicted)/Predicted | | | | | | |
|---|---|---|---|---|---|---|---|---|
| | | D | SA | SB | A | B | C | All Banks |
| KB117 [A] | AREVA | 0.92% | 1.07% | 0.25% | 4.18% | 0.39% | 5.04% | 1.7% |
| KB118 [A] | AREVA | 3.50% | 4.62% | -0.26% | 7.91% | 7.07% | 5.07% | 4.5% |
| KB119 [A] | AREVA | 1.43% | -0.37% | -0.22% | 5.45% | 3.25% | 1.80% | 1.6% |
| KB120 [W] | Westinghouse | -3.17% | 3.98% | 2.84% | 0.26% | -0.70% | 1.51% | 1.0% |
| KB121 [W] | Westinghouse | -4.53% | 2.54% | -1.72% | 6.93% | -1.33% | -1.76% | -0.9% |
| KB122 [W] | Westinghouse | 2.52% | 6.33% | 4.70% | -4.24% | -0.95% | 4.90% | 3.3% |
| KB123 [W] | Westinghouse | -2.47% | 0.00% | -0.20% | 0.93% | -2.83% | 0.92% | -0.8% |
| KB217 [A] | AREVA | 0.98% | 1.66% | -0.11% | 4.21% | 2.77% | 3.06% | 1.9% |
| KB218 [A] | AREVA | -1.59% | -0.93% | -2.93% | -2.67% | -0.29% | 1.65% | -0.9% |
| KB219 [A] | AREVA | -0.50% | -0.09% | -0.75% | 4.46% | -0.18% | 1.88% | 0.4% |
| KB220 [A] | AREVA | -7.05% | -3.10% | -7.18% | -3.61% | -2.43% | -5.67% | -4.7% |
| KB221 [A] | AREVA | -2.39% | -2.93% | -5.56% | -1.53% | -3.47% | 0.00% | -2.7% |
| KB222 [A] | AREVA | -0.95% | -3.58% | -2.38% | 0.59% | -3.43% | -0.72% | -2.1% |
| KB223 [A] | AREVA | -1.36% | -3.37% | -4.16% | 0.00% | -2.85% | -1.25% | -2.3% |
| **Max. Bank Over-prediction** | | -7.1% | -3.6% | -7.2% | -4.2% | -3.5% | -5.7% | -7.2% |
| **95th Percentile** | | -5.4% | -3.4% | -6.1% | -3.8% | -3.4% | -3.1% | **-4.5%** |
| **5th Percentile** | | 2.9% | 5.2% | 3.5% | 7.3% | 4.6% | 5.0% | 5.4% |
| **Max. Bank Under-prediction** | | 3.5% | 6.3% | 4.7% | 7.9% | 7.1% | 5.1% | 7.9% |
| **Mean Bank Difference** | | -1.0% | 0.4% | -1.3% | 1.6% | -0.4% | 1.2% | **0.1%** |
| Standard Deviation | | 2.8% | 3.1% | 3.1% | 3.9% | 3.0% | 3.0% | **2.5%** |

***Table 22:*** *Predicted versus Hot Physics Test measured control bank worth relative results*

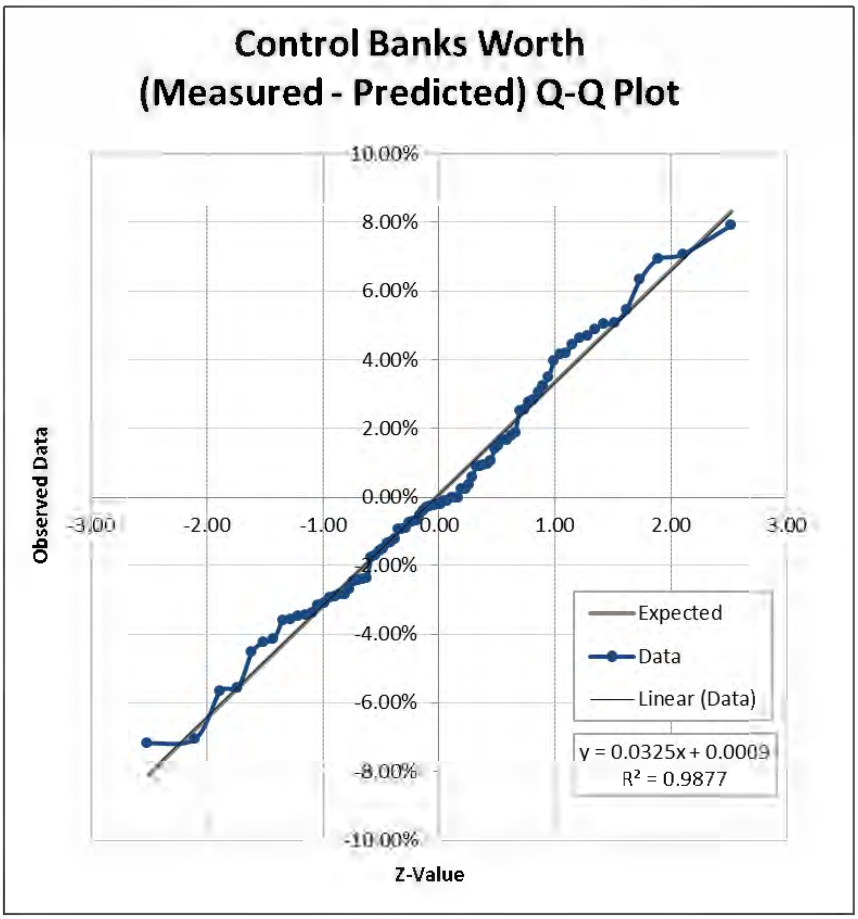


***Figure 15:*** *Predicted versus Hot Physics Test measured control bank worth Chi-squared normality test*

## Appendix E: Power Defect

| Fuel Cycle | Fuel Manufacturer | Burn-up (MWd/MTU) | | | |
|---|---|---|---|---|---|
| | | BOL | BLX | MOL | EOL |
| | | 0 | 150 | 8000 | 16142 |
| KB118 [A] | AREVA | 1 356 pcm | 1 385 pcm | 1 771 pcm | 2 477 pcm |
| KB119 [A] | AREVA | 1 371 pcm | 1 415 pcm | 1 814 pcm | 2 527 pcm |
| KB120 [W] | Westinghouse | 1 358 pcm | 1 401 pcm | 1 693 pcm | 2 574 pcm |
| KB121 [W] | Westinghouse | 1 488 pcm | 1 519 pcm | 1 929 pcm | 2 552 pcm |
| KB122 [W] | Westinghouse | 1 412 pcm | 1 451 pcm | 1 796 pcm | 2 613 pcm |
| KB123 [W] | Westinghouse | 1 410 pcm | 1 455 pcm | 1 755 pcm | 2 579 pcm |
| KB218 [A] | AREVA | 1 332 pcm | 1 369 pcm | 1 756 pcm | 2 463 pcm |
| KB219 [A] | AREVA | 1 337 pcm | 1 381 pcm | 1 791 pcm | 2 486 pcm |
| KB220 [A] | AREVA | 1 339 pcm | 1 380 pcm | 1 778 pcm | 2 468 pcm |
| KB221 [A] | AREVA | 1 339 pcm | 1 386 pcm | 1 785 pcm | 2 460 pcm |
| KB222 [A] | AREVA | 1 336 pcm | 1 381 pcm | 1 782 pcm | 2 480 pcm |
| KB223 [A] | AREVA | 1 373 pcm | 1 413 pcm | 1 820 pcm | 2 500 pcm |
| **Minimum Power Defect** | | **1 332 pcm** | **1 369 pcm** | **1 693 pcm** | **2 460 pcm** |
| **5th Percentile** | | 1 334 pcm | 1 375 pcm | 1 727 pcm | 2 462 pcm |
| **95th Percentile** | | 1 446 pcm | 1 483 pcm | 1 869 pcm | 2 594 pcm |
| **Maximum Power Defect** | | 1 488 pcm | 1 519 pcm | 1 929 pcm | 2 613 pcm |
| **Average Power Defect** | | 1 371 pcm | 1 411 pcm | 1 789 pcm | 2 515 pcm |
| *Standard Deviation* | | *46 pcm* | *44 pcm* | *55 pcm* | *53 pcm* |

***Table 23:*** *Calculated power defect for all fuel cycles*

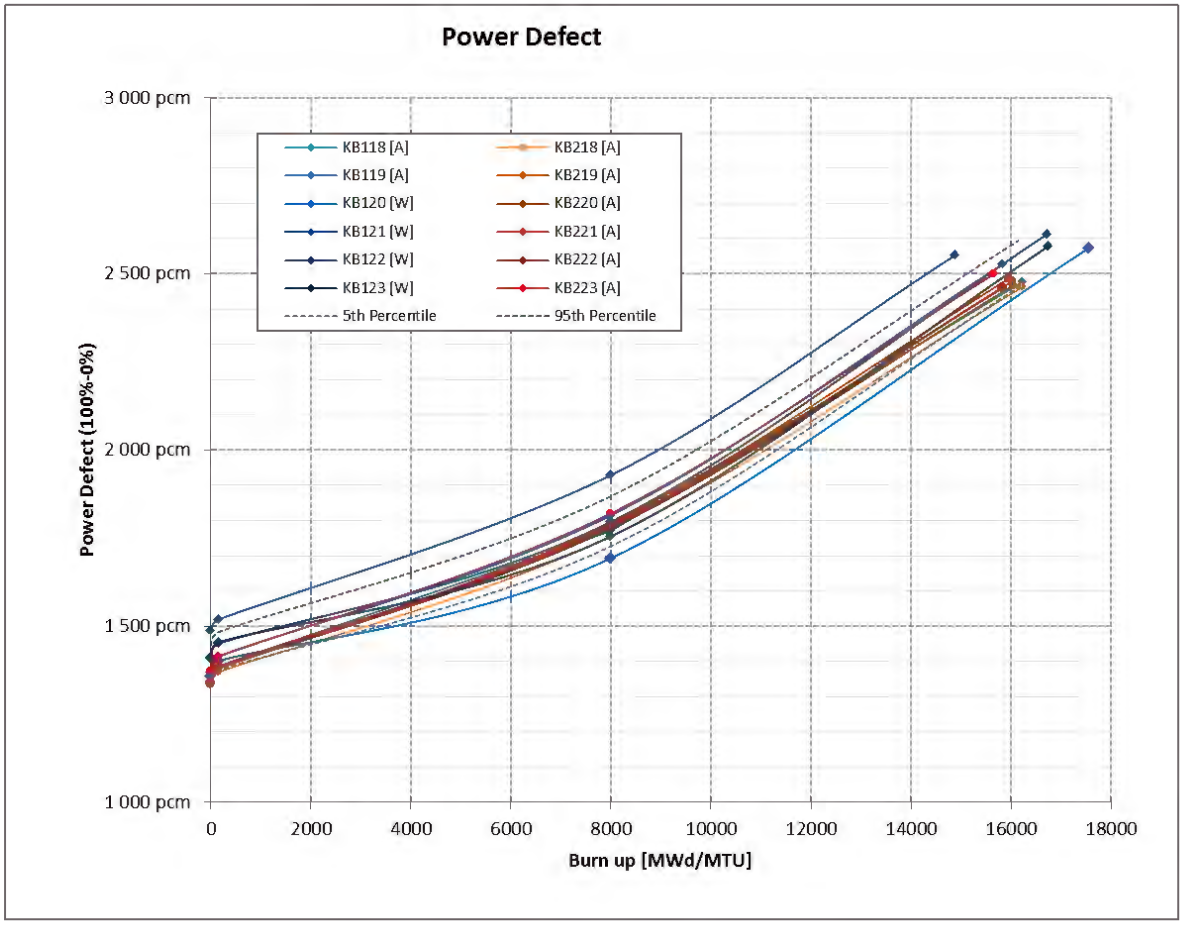


***Figure 16:*** *Power defect for all the fuel cycles considered*

## Appendix F: Reactivity Reduction due to Reactor Trip

| Fuel Cycle | Fuel Manufacturer | Burn-up [MWd/MTU] | | | |
|---|---|---|---|---|---|
| | | BOL | BLX | 8000 | EOL |
| | | 0 | 150 | 8000 | 16142 |
| KB118 [A] | AREVA | -6 184 pcm | -6 195 pcm | -5 992 pcm | -5 657 pcm |
| KB119 [A] | AREVA | -6 129 pcm | -6 124 pcm | -5 888 pcm | -5 544 pcm |
| KB120 [W] | Westinghouse | -7 214 pcm | -7 165 pcm | -7 060 pcm | -6 513 pcm |
| KB121 [W] | Westinghouse | -6 975 pcm | -6 938 pcm | -6 746 pcm | -6 414 pcm |
| KB122 [W] | Westinghouse | -6 272 pcm | -6 232 pcm | -6 322 pcm | -6 097 pcm |
| KB123 [W] | Westinghouse | -6 771 pcm | -6 734 pcm | -6 676 pcm | -6 245 pcm |
| KB218 [A] | AREVA | -6 288 pcm | -6 285 pcm | -6 066 pcm | -5 713 pcm |
| KB219 [A] | AREVA | -6 171 pcm | -6 176 pcm | -5 964 pcm | -5 627 pcm |
| KB220 [A] | AREVA | -6 407 pcm | -6 401 pcm | -6 139 pcm | -5 780 pcm |
| KB221 [A] | AREVA | -6 243 pcm | -6 238 pcm | -6 030 pcm | -5 689 pcm |
| KB222 [A] | AREVA | -6 388 pcm | -6 384 pcm | -6 154 pcm | -5 794 pcm |
| KB223 [A] | AREVA | -6 420 pcm | -6 417 pcm | -6 139 pcm | -5 764 pcm |
| **Avg Reactivity Insertion** | | -6 455 pcm | -6 441 pcm | -6 265 pcm | -5 903 pcm |
| **Max Reactivity Insertion** | | -7 214 pcm | -7 165 pcm | -7 060 pcm | -6 513 pcm |
| **Min Reactivity Insertion** | | **-6 129 pcm** | **-6 124 pcm** | **-5 888 pcm** | **-5 544 pcm** |
| **5th %-tile** | | -7 083 pcm | -7 040 pcm | -6 887 pcm | -6 458 pcm |
| **95th %-tile** | | -6 152 pcm | -6 153 pcm | -5 930 pcm | -5 590 pcm |
| *Standard Deviation* | | *347 pcm* | *331 pcm* | *367 pcm* | *328 pcm* |

***Table 24:*** *Calculated reactivity reduction after reactor trip*

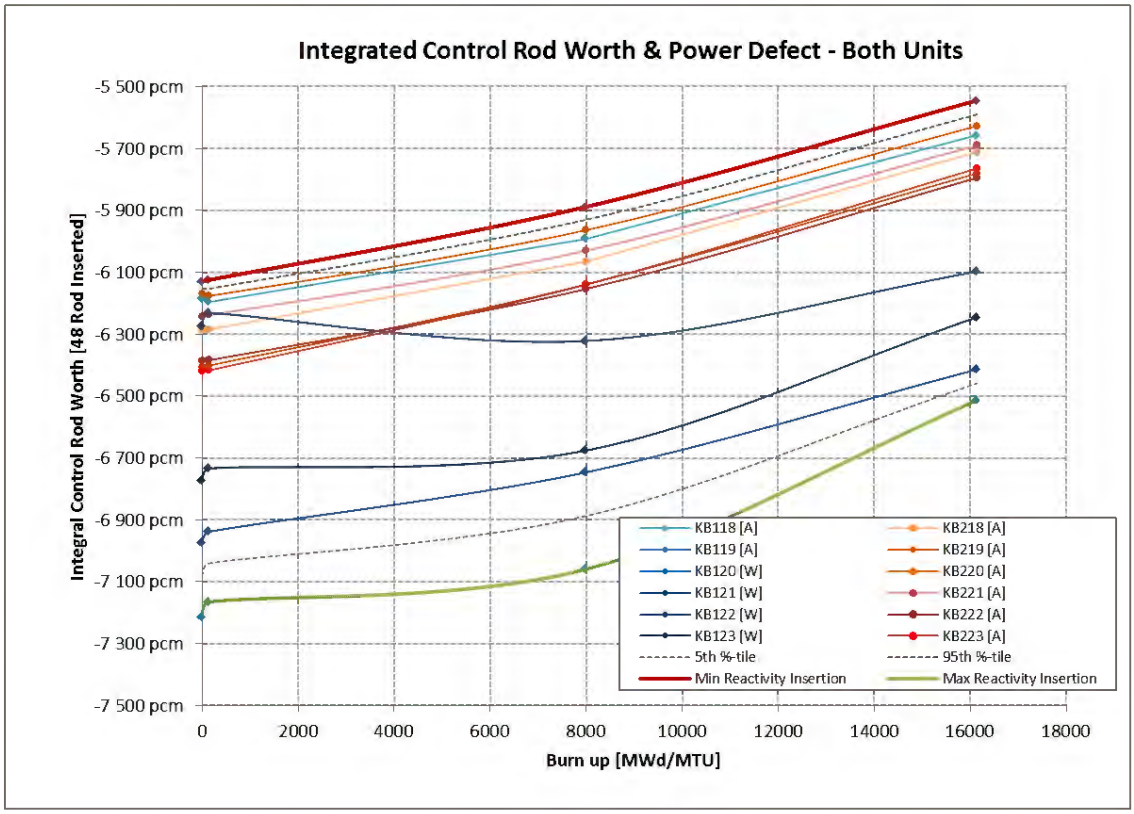


***Figure 17:*** *Reactivity Reduction due to both control-rod insertion and power defect for all the fuel cycles considered*

## **Appendix G1:** Reactivity Change during Cooldown from Hot Shutdown (286°C) down to RRA Conditions (155°C), at BOL, with All Rods Inserted

**Reactivity Change due to Moderator Temperature Reduction (@ BOL, from HZP, All Rods Inserted, $C_B$ =~1851 ppm)**

Appendix G: Reactivity Change during Cooldown from Hot Shutdown down to RRA Conditions

| Cycle | Moderator Temperature | 155.0 °C | 165.0 °C | 175.0 °C | 185.0 °C | 195.0 °C | 205.0 °C | 215.0 °C | 225.0 °C | 235.0 °C | 245.0 °C | 255.0 °C | 265.0 °C | 275.0 °C | 285.0 °C | AFI 286°C |
|---|---|---|---|---|---|---|---|---|---|---|---|---|---|---|---|---|
| KB118 [A] | $C_B$ = 1916 ppm | 1 016 pcm | 996 pcm | 974 pcm | 949 pcm | 917 pcm | 879 pcm | 832 pcm | 775 pcm | 702 pcm | 611 pcm | 496 pcm | 352 pcm | 199 pcm | 19 pcm | 0 pcm |
| KB119 [A] | $C_B$ = 1888 ppm | 982 pcm | 967 pcm | 947 pcm | 924 pcm | 896 pcm | 860 pcm | 817 pcm | 762 pcm | 692 pcm | 603 pcm | 491 pcm | 348 pcm | 198 pcm | 19 pcm | 0 pcm |
| KB120 [W] | $C_B$ = 1806 ppm | 1 289 pcm | 1 246 pcm | 1 201 pcm | 1 152 pcm | 1 097 pcm | 1 036 pcm | 966 pcm | 886 pcm | 792 pcm | 682 pcm | 550 pcm | 392 pcm | 220 pcm | 22 pcm | 0 pcm |
| KB121 [W] | $C_B$ = 1710 ppm | 1 312 pcm | 1 274 pcm | 1 233 pcm | 1 187 pcm | 1 136 pcm | 1 076 pcm | 1 008 pcm | 928 pcm | 833 pcm | 720 pcm | 583 pcm | 415 pcm | 234 pcm | 23 pcm | 0 pcm |
| KB122 [W] | $C_B$ = 1814 ppm | 1 013 pcm | 995 pcm | 972 pcm | 947 pcm | 916 pcm | 877 pcm | 830 pcm | 771 pcm | 700 pcm | 610 pcm | 497 pcm | 355 pcm | 202 pcm | 19 pcm | 0 pcm |
| KB123 [W] | $C_B$ = 1721 ppm | 1 373 pcm | 1 327 pcm | 1 278 pcm | 1 226 pcm | 1 167 pcm | 1 100 pcm | 1 025 pcm | 940 pcm | 839 pcm | 722 pcm | 583 pcm | 416 pcm | 234 pcm | 23 pcm | 0 pcm |
| KB218 [A] | $C_B$ = 1851 ppm | 1 142 pcm | 1 114 pcm | 1 084 pcm | 1 049 pcm | 1 009 pcm | 962 pcm | 905 pcm | 837 pcm | 756 pcm | 654 pcm | 530 pcm | 375 pcm | 212 pcm | 21 pcm | 0 pcm |
| KB219 [A] | $C_B$ = 1851 ppm | 1 138 pcm | 1 113 pcm | 1 083 pcm | 1 050 pcm | 1 010 pcm | 964 pcm | 908 pcm | 841 pcm | 759 pcm | 658 pcm | 534 pcm | 379 pcm | 214 pcm | 21 pcm | 0 pcm |
| KB220 [A] | $C_B$ = 1851 ppm | 1 107 pcm | 1 083 pcm | 1 055 pcm | 1 023 pcm | 985 pcm | 942 pcm | 888 pcm | 824 pcm | 744 pcm | 646 pcm | 523 pcm | 370 pcm | 209 pcm | 20 pcm | 0 pcm |
| KB221 [A] | $C_B$ = 1851 ppm | 1 180 pcm | 1 152 pcm | 1 119 pcm | 1 082 pcm | 1 039 pcm | 990 pcm | 931 pcm | 860 pcm | 775 pcm | 671 pcm | 543 pcm | 384 pcm | 217 pcm | 20 pcm | 0 pcm |
| KB222 [A] | $C_B$ = 1851 ppm | 1 135 pcm | 1 108 pcm | 1 079 pcm | 1 045 pcm | 1 005 pcm | 959 pcm | 904 pcm | 836 pcm | 754 pcm | 654 pcm | 530 pcm | 375 pcm | 212 pcm | 20 pcm | 0 pcm |
| KB223 [A] | $C_B$ = 1851 ppm | 1 170 pcm | 1 143 pcm | 1 111 pcm | 1 074 pcm | 1 032 pcm | 983 pcm | 925 pcm | 855 pcm | 771 pcm | 667 pcm | 541 pcm | 383 pcm | 216 pcm | 22 pcm | 0 pcm |
| **Unit 1** | Mean | 1 164 pcm | 1 134 pcm | 1 101 pcm | 1 064 pcm | 1 021 pcm | 971 pcm | 913 pcm | 844 pcm | 760 pcm | 658 pcm | 533 pcm | 379 pcm | 215 pcm | 21 pcm | 0 pcm |
| | 5th %tile | 990 pcm | 974 pcm | 953 pcm | 930 pcm | 901 pcm | 864 pcm | 820 pcm | 764 pcm | 694 pcm | 604 pcm | 492 pcm | 349 pcm | 198 pcm | 19 pcm | 0 pcm |
| | 95th %tile | 1 358 pcm | 1 314 pcm | 1 267 pcm | 1 216 pcm | 1 159 pcm | 1 094 pcm | 1 021 pcm | 937 pcm | 838 pcm | 722 pcm | 583 pcm | 415 pcm | 234 pcm | 23 pcm | 0 pcm |
| **Unit 2** | Mean | 1 145 pcm | 1 119 pcm | 1 088 pcm | 1 054 pcm | 1 013 pcm | 967 pcm | 910 pcm | 842 pcm | 760 pcm | 658 pcm | 534 pcm | 378 pcm | 213 pcm | 21 pcm | 0 pcm |
| | 5th %tile | 1 114 pcm | 1 089 pcm | 1 061 pcm | 1 028 pcm | 990 pcm | 946 pcm | 892 pcm | 827 pcm | 746 pcm | 648 pcm | 525 pcm | 371 pcm | 210 pcm | 20 pcm | 0 pcm |
| | 95th %tile | 1 178 pcm | 1 149 pcm | 1 117 pcm | 1 080 pcm | 1 037 pcm | 988 pcm | 930 pcm | 859 pcm | 774 pcm | 670 pcm | 542 pcm | 384 pcm | 216 pcm | 21 pcm | 0 pcm |
| **Both Units** | Mean (BOL) | 1 155 pcm | 1 126 pcm | 1 095 pcm | 1 059 pcm | 1 017 pcm | **969 pcm** | 912 pcm | 843 pcm | 760 pcm | 658 pcm | 533 pcm | 379 pcm | 214 pcm | 21 pcm | 0 pcm |
| | 5th %tile (BOL) | 999 pcm | 982 pcm | 961 pcm | 937 pcm | 907 pcm | 869 pcm | 824 pcm | 767 pcm | 696 pcm | 606 pcm | 494 pcm | 350 pcm | 199 pcm | 19 pcm | 0 pcm |
| | 95th %tile (BOL) | 1 340 pcm | 1 298 pcm | 1 253 pcm | 1 205 pcm | 1 150 pcm | **1 087 pcm** | 1 016 pcm | 933 pcm | 836 pcm | 721 pcm | 583 pcm | 415 pcm | 234 pcm | 23 pcm | 0 pcm |
| | Standard Deviation | 122 pcm | 113 pcm | 104 pcm | 95 pcm | 85 pcm | **76 pcm** | 66 pcm | 57 pcm | 48 pcm | 39 pcm | 30 pcm | 22 pcm | 12 pcm | 1 pcm | 0 pcm |

**Reactivity due to Moderator Temperature Reduction (@ BOL, from HZP, All Rods Inserted, $C_B$ =~1851 ppm)**

| Cycle | Moderator Temperature | 155.0 °C | 165.0 °C | 175.0 °C | 185.0 °C | 195.0 °C | 205.0 °C | 215.0 °C | 225.0 °C | 235.0 °C | 245.0 °C | 255.0 °C | 265.0 °C | 275.0 °C | 285.0 °C | AFI 286°C |
|---|---|---|---|---|---|---|---|---|---|---|---|---|---|---|---|---|
| KB118 [A] | $C_B$ = 1916 ppm | -5 168 pcm | -5 188 pcm | -5 210 pcm | -5 235 pcm | -5 268 pcm | -5 305 pcm | -5 352 pcm | -5 410 pcm | -5 482 pcm | -5 573 pcm | -5 688 pcm | -5 832 pcm | -5 985 pcm | -6 165 pcm | -6 184 pcm |
| KB119 [A] | $C_B$ = 1888 ppm | -5 147 pcm | -5 162 pcm | -5 182 pcm | -5 204 pcm | -5 233 pcm | -5 269 pcm | -5 312 pcm | -5 367 pcm | -5 437 pcm | -5 526 pcm | -5 638 pcm | -5 781 pcm | -5 931 pcm | -6 110 pcm | -6 129 pcm |
| KB120 [W] | $C_B$ = 1806 ppm | -5 927 pcm | -5 969 pcm | -6 014 pcm | -6 064 pcm | -6 119 pcm | -6 180 pcm | -6 250 pcm | -6 330 pcm | -6 424 pcm | -6 534 pcm | -6 666 pcm | -6 824 pcm | -6 995 pcm | -7 194 pcm | -7 216 pcm |
| KB121 [W] | $C_B$ = 1710 ppm | -5 662 pcm | -5 700 pcm | -5 742 pcm | -5 788 pcm | -5 839 pcm | -5 899 pcm | -5 967 pcm | -6 047 pcm | -6 141 pcm | -6 255 pcm | -6 392 pcm | -6 560 pcm | -6 741 pcm | -6 952 pcm | -6 975 pcm |
| KB122 [W] | $C_B$ = 1814 ppm | -5 259 pcm | -5 278 pcm | -5 300 pcm | -5 325 pcm | -5 356 pcm | -5 395 pcm | -5 442 pcm | -5 501 pcm | -5 572 pcm | -5 662 pcm | -5 775 pcm | -5 918 pcm | -6 070 pcm | -6 253 pcm | -6 272 pcm |
| KB123 [W] | $C_B$ = 1721 ppm | -5 399 pcm | -5 444 pcm | -5 493 pcm | -5 545 pcm | -5 604 pcm | -5 671 pcm | -5 746 pcm | -5 831 pcm | -5 932 pcm | -6 049 pcm | -6 189 pcm | -6 356 pcm | -6 537 pcm | -6 749 pcm | -6 771 pcm |
| KB218 [A] | $C_B$ = 1851 ppm | -4 666 pcm | -4 693 pcm | -4 724 pcm | -4 759 pcm | -4 799 pcm | -4 846 pcm | -4 903 pcm | -4 970 pcm | -5 052 pcm | -5 154 pcm | -5 278 pcm | -5 433 pcm | -5 596 pcm | -5 787 pcm | -5 808 pcm |
| KB219 [A] | $C_B$ = 1851 ppm | -4 741 pcm | -4 766 pcm | -4 795 pcm | -4 828 pcm | -4 868 pcm | -4 914 pcm | -4 970 pcm | -5 038 pcm | -5 119 pcm | -5 220 pcm | -5 344 pcm | -5 500 pcm | -5 665 pcm | -5 857 pcm | -5 878 pcm |
| KB220 [A] | $C_B$ = 1851 ppm | -5 027 pcm | -5 051 pcm | -5 078 pcm | -5 110 pcm | -5 148 pcm | -5 191 pcm | -5 245 pcm | -5 310 pcm | -5 390 pcm | -5 487 pcm | -5 610 pcm | -5 763 pcm | -5 924 pcm | -6 113 pcm | -6 133 pcm |
| KB221 [A] | $C_B$ = 1851 ppm | -4 880 pcm | -4 909 pcm | -4 942 pcm | -4 978 pcm | -5 021 pcm | -5 071 pcm | -5 129 pcm | -5 200 pcm | -5 285 pcm | -5 390 pcm | -5 518 pcm | -5 676 pcm | -5 844 pcm | -6 040 pcm | -6 060 pcm |
| KB222 [A] | $C_B$ = 1851 ppm | -4 806 pcm | -4 833 pcm | -4 862 pcm | -4 897 pcm | -4 936 pcm | -4 982 pcm | -5 038 pcm | -5 105 pcm | -5 187 pcm | -5 288 pcm | -5 411 pcm | -5 567 pcm | -5 729 pcm | -5 921 pcm | -5 941 pcm |
| KB223 [A] | $C_B$ = 1851 ppm | -5 250 pcm | -5 278 pcm | -5 310 pcm | -5 346 pcm | -5 389 pcm | -5 437 pcm | -5 495 pcm | -5 565 pcm | -5 649 pcm | -5 753 pcm | -5 879 pcm | -6 038 pcm | -6 204 pcm | -6 399 pcm | -6 420 pcm |
| | Mean | -5 161 pcm | -5 189 pcm | -5 221 pcm | -5 257 pcm | -5 298 pcm | -5 347 pcm | -5 404 pcm | -5 473 pcm | -5 556 pcm | -5 658 pcm | -5 782 pcm | -5 937 pcm | -6 102 pcm | -6 295 pcm | -6 316 pcm |
| | 5th %tile | -5 781 pcm | -5 821 pcm | -5 864 pcm | -5 912 pcm | -5 965 pcm | -6 025 pcm | -6 094 pcm | -6 174 pcm | -6 268 pcm | -6 381 pcm | -6 515 pcm | -6 679 pcm | -6 855 pcm | -7 061 pcm | -7 083 pcm |
| | 95th %tile | -4 707 pcm | -4 733 pcm | -4 763 pcm | -4 797 pcm | -4 837 pcm | -4 883 pcm | -4 940 pcm | -5 007 pcm | -5 089 pcm | -5 190 pcm | -5 314 pcm | -5 470 pcm | -5 634 pcm | -5 825 pcm | -5 847 pcm |

## **Appendix G2:** Reactivity during Cooldown from Hot Shutdown (286°C) down to RRA Conditions (155°C), at BLX, with All Rods Inserted

**Reactivity Change due to Temperature Reduction (@ BLX, from HZP, All Rods Inserted, $C_B$ = 1441 ppm)**

| Cycle | Moderator Temperature | 155.0 °C | 165.0 °C | 175.0 °C | 185.0 °C | 195.0 °C | 205.0 °C | 215.0 °C | 225.0 °C | 235.0 °C | 245.0 °C | 255.0 °C | 265.0 °C | 275.0 °C | 285.0 °C | 286°C |
|---|---|---|---|---|---|---|---|---|---|---|---|---|---|---|---|---|
| KB118 [A] | Cb = 1527 ppm | 1 435 pcm | 1 385 pcm | 1 331 pcm | 1 272 pcm | 1 207 pcm | 1 136 pcm | 1 056 pcm | 966 pcm | 860 pcm | 739 pcm | 597 pcm | 427 pcm | 241 pcm | 24 pcm | 0 pcm |
| KB119 [A] | Cb = 1497 ppm | 1 415 pcm | 1 367 pcm | 1 316 pcm | 1 259 pcm | 1 197 pcm | 1 127 pcm | 1 048 pcm | 959 pcm | 856 pcm | 736 pcm | 595 pcm | 426 pcm | 239 pcm | 24 pcm | 0 pcm |
| KB120 [W] | Cb = 1418 ppm | 1 695 pcm | 1 623 pcm | 1 547 pcm | 1 466 pcm | 1 380 pcm | 1 286 pcm | 1 183 pcm | 1 071 pcm | 946 pcm | 806 pcm | 647 pcm | 465 pcm | 261 pcm | 26 pcm | 0 pcm |
| KB121 [W] | Cb = 1328 ppm | 1 727 pcm | 1 660 pcm | 1 586 pcm | 1 509 pcm | 1 425 pcm | 1 333 pcm | 1 231 pcm | 1 119 pcm | 992 pcm | 849 pcm | 683 pcm | 491 pcm | 276 pcm | 27 pcm | 0 pcm |
| KB122 [W] | Cb = 1424 ppm | 1 451 pcm | 1 400 pcm | 1 346 pcm | 1 285 pcm | 1 220 pcm | 1 148 pcm | 1 066 pcm | 974 pcm | 867 pcm | 745 pcm | 603 pcm | 434 pcm | 244 pcm | 24 pcm | 0 pcm |
| KB123 [W] | Cb = 1336 ppm | 1 786 pcm | 1 710 pcm | 1 630 pcm | 1 545 pcm | 1 453 pcm | 1 354 pcm | 1 246 pcm | 1 128 pcm | 997 pcm | 849 pcm | 681 pcm | 490 pcm | 275 pcm | 27 pcm | 0 pcm |
| KB218 [A] | Cb = 1441 ppm | 1 599 pcm | 1 539 pcm | 1 473 pcm | 1 404 pcm | 1 328 pcm | 1 245 pcm | 1 152 pcm | 1 048 pcm | 931 pcm | 797 pcm | 640 pcm | 458 pcm | 257 pcm | 26 pcm | 0 pcm |
| KB219 [A] | Cb = 1441 ppm | 1 604 pcm | 1 544 pcm | 1 480 pcm | 1 410 pcm | 1 335 pcm | 1 251 pcm | 1 159 pcm | 1 055 pcm | 938 pcm | 802 pcm | 646 pcm | 462 pcm | 260 pcm | 25 pcm | 0 pcm |
| KB220 [A] | Cb = 1441 ppm | 1 572 pcm | 1 513 pcm | 1 450 pcm | 1 384 pcm | 1 310 pcm | 1 229 pcm | 1 139 pcm | 1 038 pcm | 923 pcm | 791 pcm | 637 pcm | 455 pcm | 256 pcm | 25 pcm | 0 pcm |
| KB221 [A] | Cb = 1441 ppm | 1 641 pcm | 1 577 pcm | 1 511 pcm | 1 438 pcm | 1 359 pcm | 1 274 pcm | 1 178 pcm | 1 072 pcm | 951 pcm | 813 pcm | 654 pcm | 467 pcm | 262 pcm | 25 pcm | 0 pcm |
| KB222 [A] | Cb = 1441 ppm | 1 599 pcm | 1 539 pcm | 1 474 pcm | 1 404 pcm | 1 329 pcm | 1 246 pcm | 1 153 pcm | 1 050 pcm | 932 pcm | 798 pcm | 642 pcm | 459 pcm | 258 pcm | 26 pcm | 0 pcm |
| KB223 [A] | Cb = 1441 ppm | 1 600 pcm | 1 540 pcm | 1 476 pcm | 1 406 pcm | 1 331 pcm | 1 248 pcm | 1 155 pcm | 1 052 pcm | 934 pcm | 799 pcm | 644 pcm | 460 pcm | 259 pcm | 25 pcm | 0 pcm |
| **Unit 1** | Mean | 1 585 pcm | 1 524 pcm | 1 459 pcm | 1 389 pcm | 1 314 pcm | 1 230 pcm | 1 139 pcm | 1 036 pcm | 920 pcm | 787 pcm | 634 pcm | 455 pcm | 256 pcm | 25 pcm | 0 pcm |
| | 5th %tile | 1 420 pcm | 1 372 pcm | 1 320 pcm | 1 262 pcm | 1 200 pcm | 1 129 pcm | 1 050 pcm | 960 pcm | 857 pcm | 737 pcm | 595 pcm | 426 pcm | 240 pcm | 24 pcm | 0 pcm |
| | 95th %tile | 1 771 pcm | 1 697 pcm | 1 619 pcm | 1 536 pcm | 1 446 pcm | 1 349 pcm | 1 243 pcm | 1 126 pcm | 996 pcm | 849 pcm | 683 pcm | 490 pcm | 276 pcm | 27 pcm | 0 pcm |
| **Unit 2** | Mean | 1 602 pcm | 1 542 pcm | 1 477 pcm | 1 408 pcm | 1 332 pcm | 1 249 pcm | 1 156 pcm | 1 052 pcm | 935 pcm | 800 pcm | 644 pcm | 460 pcm | 259 pcm | 25 pcm | 0 pcm |
| | 5th %tile | 1 579 pcm | 1 519 pcm | 1 456 pcm | 1 389 pcm | 1 315 pcm | 1 233 pcm | 1 142 pcm | 1 041 pcm | 925 pcm | 792 pcm | 638 pcm | 456 pcm | 256 pcm | 25 pcm | 0 pcm |
| | 95th %tile | 1 631 pcm | 1 569 pcm | 1 503 pcm | 1 431 pcm | 1 353 pcm | 1 268 pcm | 1 174 pcm | 1 068 pcm | 948 pcm | 810 pcm | 652 pcm | 466 pcm | 261 pcm | 26 pcm | 0 pcm |
| **Both Units** | Mean (BLX) | 1 594 pcm | 1 533 pcm | 1 468 pcm | 1 398 pcm | 1 323 pcm | **1 240 pcm** | 1 147 pcm | 1 044 pcm | 927 pcm | 794 pcm | 639 pcm | 458 pcm | 257 pcm | 25 pcm | 0 pcm |
| | 5th %tile (BLX) | 1 426 pcm | 1 377 pcm | 1 324 pcm | 1 266 pcm | 1 203 pcm | 1 132 pcm | 1 053 pcm | 962 pcm | 858 pcm | 738 pcm | 596 pcm | 427 pcm | 240 pcm | 24 pcm | 0 pcm |
| | 95th %tile (BLX) | 1 753 pcm | 1 682 pcm | 1 606 pcm | 1 525 pcm | 1 438 pcm | **1 342 pcm** | 1 238 pcm | 1 123 pcm | 994 pcm | 849 pcm | 682 pcm | 490 pcm | 275 pcm | 27 pcm | 0 pcm |
| | Standard Deviation | 115 pcm | 107 pcm | 98 pcm | 90 pcm | 81 pcm | **72 pcm** | 63 pcm | 55 pcm | 46 pcm | 37 pcm | 29 pcm | 21 pcm | 12 pcm | 1 pcm | 0 pcm |

**Reactivity due to Temperature Reduction (as Calculated by SCIENCE @BLX, from HZP, All Rods Inserted, $C_B$ = 1441 ppm)**

| Cycle | Moderator Temperature | 155.0 °C | 165.0 °C | 175.0 °C | 185.0 °C | 195.0 °C | 205.0 °C | 215.0 °C | 225.0 °C | 235.0 °C | 245.0 °C | 255.0 °C | 265.0 °C | 275.0 °C | 285.0 °C | AFI 286°C |
|---|---|---|---|---|---|---|---|---|---|---|---|---|---|---|---|---|
| KB118 [A] | Cb = 1527 ppm | -4 761 pcm | -4 812 pcm | -4 866 pcm | -4 924 pcm | -4 989 pcm | -5 061 pcm | -5 140 pcm | -5 231 pcm | -5 336 pcm | -5 457 pcm | -5 600 pcm | -5 770 pcm | -5 956 pcm | -6 173 pcm | -6 197 pcm |
| KB119 [A] | Cb = 1497 ppm | -4 710 pcm | -4 757 pcm | -4 809 pcm | -4 866 pcm | -4 927 pcm | -4 998 pcm | -5 076 pcm | -5 166 pcm | -5 269 pcm | -5 389 pcm | -5 530 pcm | -5 698 pcm | -5 885 pcm | -6 101 pcm | -6 124 pcm |
| KB120 [W] | Cb = 1418 ppm | -5 471 pcm | -5 543 pcm | -5 619 pcm | -5 700 pcm | -5 787 pcm | -5 881 pcm | -5 983 pcm | -6 095 pcm | -6 220 pcm | -6 360 pcm | -6 519 pcm | -6 701 pcm | -6 905 pcm | -7 140 pcm | -7 166 pcm |
| KB121 [W] | Cb = 1328 ppm | -5 212 pcm | -5 280 pcm | -5 353 pcm | -5 431 pcm | -5 514 pcm | -5 607 pcm | -5 708 pcm | -5 820 pcm | -5 947 pcm | -6 091 pcm | -6 256 pcm | -6 449 pcm | -6 663 pcm | -6 912 pcm | -6 939 pcm |
| KB122 [W] | Cb = 1424 ppm | -4 780 pcm | -4 832 pcm | -4 886 pcm | -4 946 pcm | -5 011 pcm | -5 084 pcm | -5 166 pcm | -5 258 pcm | -5 364 pcm | -5 486 pcm | -5 629 pcm | -5 798 pcm | -5 987 pcm | -6 208 pcm | -6 232 pcm |
| KB123 [W] | Cb = 1336 ppm | -4 949 pcm | -5 025 pcm | -5 105 pcm | -5 190 pcm | -5 282 pcm | -5 381 pcm | -5 489 pcm | -5 607 pcm | -5 738 pcm | -5 886 pcm | -6 054 pcm | -6 245 pcm | -6 460 pcm | -6 708 pcm | -6 735 pcm |
| KB218 [A] | Cb = 1441 ppm | -4 079 pcm | -4 140 pcm | -4 205 pcm | -4 274 pcm | -4 350 pcm | -4 433 pcm | -4 526 pcm | -4 630 pcm | -4 747 pcm | -4 881 pcm | -5 038 pcm | -5 220 pcm | -5 421 pcm | -5 652 pcm | -5 678 pcm |
| KB219 [A] | Cb = 1441 ppm | -4 146 pcm | -4 206 pcm | -4 270 pcm | -4 339 pcm | -4 415 pcm | -4 499 pcm | -4 590 pcm | -4 695 pcm | -4 812 pcm | -4 947 pcm | -5 104 pcm | -5 288 pcm | -5 490 pcm | -5 725 pcm | -5 750 pcm |
| KB220 [A] | Cb = 1441 ppm | -4 422 pcm | -4 481 pcm | -4 543 pcm | -4 610 pcm | -4 684 pcm | -4 765 pcm | -4 855 pcm | -4 956 pcm | -5 071 pcm | -5 203 pcm | -5 357 pcm | -5 539 pcm | -5 738 pcm | -5 969 pcm | -5 994 pcm |
| KB221 [A] | Cb = 1441 ppm | -4 289 pcm | -4 353 pcm | -4 419 pcm | -4 492 pcm | -4 571 pcm | -4 656 pcm | -4 752 pcm | -4 858 pcm | -4 979 pcm | -5 117 pcm | -5 276 pcm | -5 463 pcm | -5 668 pcm | -5 905 pcm | -5 930 pcm |
| KB222 [A] | Cb = 1441 ppm | -4 219 pcm | -4 279 pcm | -4 344 pcm | -4 414 pcm | -4 489 pcm | -4 572 pcm | -4 665 pcm | -4 768 pcm | -4 886 pcm | -5 020 pcm | -5 176 pcm | -5 359 pcm | -5 560 pcm | -5 792 pcm | -5 818 pcm |
| KB223 [A] | Cb = 1441 ppm | -4 810 pcm | -4 870 pcm | -4 934 pcm | -5 005 pcm | -5 080 pcm | -5 162 pcm | -5 255 pcm | -5 359 pcm | -5 476 pcm | -5 611 pcm | -5 766 pcm | -5 950 pcm | -6 151 pcm | -6 385 pcm | -6 410 pcm |
| | Mean | -4 654 pcm | -4 715 pcm | -4 779 pcm | -4 849 pcm | -4 925 pcm | -5 008 pcm | -5 100 pcm | -5 203 pcm | -5 320 pcm | -5 454 pcm | -5 609 pcm | -5 790 pcm | -5 990 pcm | -6 223 pcm | -6 248 pcm |
| | 5th %tile | -5 329 pcm | -5 398 pcm | -5 473 pcm | -5 552 pcm | -5 637 pcm | -5 730 pcm | -5 832 pcm | -5 944 pcm | -6 070 pcm | -6 212 pcm | -6 375 pcm | -6 562 pcm | -6 772 pcm | -7 014 pcm | -7 041 pcm |
| | 95th %tile | -4 116 pcm | -4 176 pcm | -4 241 pcm | -4 310 pcm | -4 386 pcm | -4 469 pcm | -4 561 pcm | -4 665 pcm | -4 783 pcm | -4 917 pcm | -5 074 pcm | -5 257 pcm | -5 459 pcm | -5 692 pcm | -5 717 pcm |

## **Appendix G3:** Reactivity during Cooldown from Hot Shutdown (286°C) down to RRA Conditions (155°C), at MOL, with All Rods Inserted

**Reactivity Change due to Temperature Reduction (@ MOL, from HZP, ARI, $C_B$ = 721 ppm)**

| Cycle | Moderator Temperature | 155.0 °C | 165.0 °C | 175.0 °C | 185.0 °C | 195.0 °C | 205.0 °C | 215.0 °C | 225.0 °C | 235.0 °C | 245.0 °C | 255.0 °C | 265.0 °C | 275.0 °C | 285.0 °C | AFI 286°C |
|---|---|---|---|---|---|---|---|---|---|---|---|---|---|---|---|---|
| KB118 [A] | CB = 744 ppm | 2 813 pcm | 2 689 pcm | 2 557 pcm | 2 416 pcm | 2 265 pcm | 2 101 pcm | 1 925 pcm | 1 733 pcm | 1 523 pcm | 1 290 pcm | 1 031 pcm | 741 pcm | 414 pcm | 40 pcm | 0 pcm |
| KB119 [A] | CB = 719 ppm | 2 820 pcm | 2 697 pcm | 2 566 pcm | 2 425 pcm | 2 274 pcm | 2 111 pcm | 1 934 pcm | 1 741 pcm | 1 530 pcm | 1 297 pcm | 1 037 pcm | 746 pcm | 417 pcm | 40 pcm | 0 pcm |
| KB120 [W] | CB = 801 ppm | 2 597 pcm | 2 480 pcm | 2 357 pcm | 2 227 pcm | 2 087 pcm | 1 937 pcm | 1 774 pcm | 1 598 pcm | 1 404 pcm | 1 190 pcm | 952 pcm | 686 pcm | 384 pcm | 37 pcm | 0 pcm |
| KB121 [W] | CB = 592 ppm | 3 141 pcm | 2 996 pcm | 2 843 pcm | 2 679 pcm | 2 506 pcm | 2 320 pcm | 2 120 pcm | 1 903 pcm | 1 667 pcm | 1 409 pcm | 1 124 pcm | 809 pcm | 452 pcm | 44 pcm | 0 pcm |
| KB122 [W] | CB = 759 ppm | 2 666 pcm | 2 551 pcm | 2 429 pcm | 2 298 pcm | 2 157 pcm | 2 005 pcm | 1 840 pcm | 1 658 pcm | 1 458 pcm | 1 238 pcm | 991 pcm | 713 pcm | 400 pcm | 40 pcm | 0 pcm |
| KB123 [W] | CB = 718 ppm | 2 771 pcm | 2 647 pcm | 2 515 pcm | 2 374 pcm | 2 224 pcm | 2 062 pcm | 1 888 pcm | 1 698 pcm | 1 491 pcm | 1 263 pcm | 1 010 pcm | 727 pcm | 406 pcm | 40 pcm | 0 pcm |
| KB218 [A] | CB = 721 ppm | 2 860 pcm | 2 733 pcm | 2 596 pcm | 2 452 pcm | 2 298 pcm | 2 131 pcm | 1 950 pcm | 1 754 pcm | 1 540 pcm | 1 305 pcm | 1 041 pcm | 749 pcm | 418 pcm | 39 pcm | 0 pcm |
| KB219 [A] | CB = 721 ppm | 2 886 pcm | 2 758 pcm | 2 622 pcm | 2 476 pcm | 2 320 pcm | 2 152 pcm | 1 970 pcm | 1 773 pcm | 1 557 pcm | 1 317 pcm | 1 053 pcm | 757 pcm | 423 pcm | 40 pcm | 0 pcm |
| KB220 [A] | CB = 721 ppm | 2 866 pcm | 2 739 pcm | 2 604 pcm | 2 459 pcm | 2 305 pcm | 2 138 pcm | 1 958 pcm | 1 762 pcm | 1 548 pcm | 1 311 pcm | 1 048 pcm | 752 pcm | 420 pcm | 41 pcm | 0 pcm |
| KB221 [A] | CB = 721 ppm | 2 896 pcm | 2 765 pcm | 2 629 pcm | 2 482 pcm | 2 324 pcm | 2 156 pcm | 1 973 pcm | 1 775 pcm | 1 558 pcm | 1 319 pcm | 1 054 pcm | 757 pcm | 423 pcm | 41 pcm | 0 pcm |
| KB222 [A] | CB = 721 ppm | 2 865 pcm | 2 737 pcm | 2 601 pcm | 2 457 pcm | 2 302 pcm | 2 135 pcm | 1 954 pcm | 1 758 pcm | 1 543 pcm | 1 307 pcm | 1 044 pcm | 750 pcm | 419 pcm | 39 pcm | 0 pcm |
| KB223 [A] | CB = 721 ppm | 2 894 pcm | 2 766 pcm | 2 628 pcm | 2 483 pcm | 2 327 pcm | 2 159 pcm | 1 976 pcm | 1 778 pcm | 1 562 pcm | 1 322 pcm | 1 057 pcm | 759 pcm | 424 pcm | 41 pcm | 0 pcm |
| Unit 1 | Mean | 2 801 pcm | 2 677 pcm | 2 544 pcm | 2 403 pcm | 2 252 pcm | 2 089 pcm | 1 913 pcm | 1 722 pcm | 1 512 pcm | 1 281 pcm | 1 024 pcm | 737 pcm | 412 pcm | 40 pcm | 0 pcm |
| | 5th %tile | 2 614 pcm | 2 498 pcm | 2 375 pcm | 2 245 pcm | 2 105 pcm | 1 954 pcm | 1 791 pcm | 1 613 pcm | 1 417 pcm | 1 202 pcm | 962 pcm | 692 pcm | 388 pcm | 37 pcm | 0 pcm |
| | 95th %tile | 3 061 pcm | 2 921 pcm | 2 773 pcm | 2 616 pcm | 2 448 pcm | 2 268 pcm | 2 073 pcm | 1 862 pcm | 1 633 pcm | 1 381 pcm | 1 102 pcm | 793 pcm | 443 pcm | 43 pcm | 0 pcm |
| Unit 2 | Mean | 2 878 pcm | 2 750 pcm | 2 613 pcm | 2 468 pcm | 2 313 pcm | 2 145 pcm | 1 964 pcm | 1 767 pcm | 1 551 pcm | 1 314 pcm | 1 049 pcm | 754 pcm | 421 pcm | 40 pcm | 0 pcm |
| | 5th %tile | 2 862 pcm | 2 734 pcm | 2 598 pcm | 2 453 pcm | 2 299 pcm | 2 132 pcm | 1 951 pcm | 1 755 pcm | 1 541 pcm | 1 305 pcm | 1 042 pcm | 749 pcm | 418 pcm | 39 pcm | 0 pcm |
| | 95th %tile | 2 895 pcm | 2 766 pcm | 2 628 pcm | 2 483 pcm | 2 326 pcm | 2 158 pcm | 1 975 pcm | 1 777 pcm | 1 561 pcm | 1 322 pcm | 1 056 pcm | 759 pcm | 423 pcm | 41 pcm | 0 pcm |
| Both Units | Mean (MOL) | 2 840 pcm | 2 713 pcm | 2 579 pcm | 2 436 pcm | 2 283 pcm | **2 117 pcm** | 1 939 pcm | 1 744 pcm | 1 532 pcm | 1 297 pcm | 1 037 pcm | 745 pcm | 416 pcm | 40 pcm | 0 pcm |
| | 5th %tile (MOL) | 2 635 pcm | 2 519 pcm | 2 397 pcm | 2 266 pcm | 2 126 pcm | 1 975 pcm | 1 810 pcm | 1 631 pcm | 1 434 pcm | 1 216 pcm | 974 pcm | 701 pcm | 393 pcm | 38 pcm | 0 pcm |
| | 95th %tile (MOL) | 3 006 pcm | 2 869 pcm | 2 725 pcm | 2 572 pcm | 2 408 pcm | **2 231 pcm** | 2 041 pcm | 1 834 pcm | 1 609 pcm | 1 361 pcm | 1 087 pcm | 782 pcm | 436 pcm | 42 pcm | 0 pcm |
| | Standard Deviation | 133 pcm | 126 pcm | 118 pcm | 110 pcm | 102 pcm | **93 pcm** | 84 pcm | 74 pcm | 64 pcm | 53 pcm | 41 pcm | 29 pcm | 16 pcm | 2 pcm | 0 pcm |

**Reactivity due to Temperature Reduction (@ MOL, from HZP, ARI, CB = 721 ppm)**

| Cycle | Moderator Temperature | 155.0 °C | 165.0 °C | 175.0 °C | 185.0 °C | 195.0 °C | 205.0 °C | 215.0 °C | 225.0 °C | 235.0 °C | 245.0 °C | 255.0 °C | 265.0 °C | 275.0 °C | 285.0 °C | AFI 286°C |
|---|---|---|---|---|---|---|---|---|---|---|---|---|---|---|---|---|
| KB118 [A] | CB = 744 ppm | -3 180 pcm | -3 304 pcm | -3 436 pcm | -3 576 pcm | -3 728 pcm | -3 892 pcm | -4 068 pcm | -4 260 pcm | -4 470 pcm | -4 703 pcm | -4 962 pcm | -5 252 pcm | -5 579 pcm | -5 952 pcm | -5 993 pcm |
| KB119 [A] | CB = 719 ppm | -3 069 pcm | -3 193 pcm | -3 324 pcm | -3 465 pcm | -3 615 pcm | -3 779 pcm | -3 956 pcm | -4 148 pcm | -4 359 pcm | -4 593 pcm | -4 853 pcm | -5 144 pcm | -5 473 pcm | -5 849 pcm | -5 890 pcm |
| KB120 [W] | CB = 801 ppm | -4 463 pcm | -4 580 pcm | -4 702 pcm | -4 833 pcm | -4 973 pcm | -5 123 pcm | -5 285 pcm | -5 462 pcm | -5 656 pcm | -5 869 pcm | -6 108 pcm | -6 374 pcm | -6 676 pcm | -7 023 pcm | -7 060 pcm |
| KB121 [W] | CB = 592 ppm | -3 607 pcm | -3 752 pcm | -3 905 pcm | -4 068 pcm | -4 242 pcm | -4 428 pcm | -4 628 pcm | -4 845 pcm | -5 081 pcm | -5 339 pcm | -5 623 pcm | -5 939 pcm | -6 296 pcm | -6 703 pcm | -6 748 pcm |
| KB122 [W] | CB = 759 ppm | -3 657 pcm | -3 772 pcm | -3 894 pcm | -4 025 pcm | -4 166 pcm | -4 318 pcm | -4 483 pcm | -4 665 pcm | -4 865 pcm | -5 085 pcm | -5 332 pcm | -5 610 pcm | -5 923 pcm | -6 283 pcm | -6 323 pcm |
| KB123 [W] | CB = 718 ppm | -3 906 pcm | -4 030 pcm | -4 162 pcm | -4 302 pcm | -4 453 pcm | -4 615 pcm | -4 789 pcm | -4 979 pcm | -5 186 pcm | -5 414 pcm | -5 667 pcm | -5 950 pcm | -6 271 pcm | -6 637 pcm | -6 677 pcm |
| KB218 [A] | CB = 721 ppm | -3 027 pcm | -3 154 pcm | -3 291 pcm | -3 435 pcm | -3 589 pcm | -3 756 pcm | -3 937 pcm | -4 133 pcm | -4 347 pcm | -4 583 pcm | -4 846 pcm | -5 138 pcm | -5 470 pcm | -5 848 pcm | -5 887 pcm |
| KB219 [A] | CB = 721 ppm | -3 079 pcm | -3 207 pcm | -3 343 pcm | -3 489 pcm | -3 645 pcm | -3 813 pcm | -3 994 pcm | -4 192 pcm | -4 408 pcm | -4 647 pcm | -4 912 pcm | -5 208 pcm | -5 542 pcm | -5 924 pcm | -5 965 pcm |
| KB220 [A] | CB = 721 ppm | -3 238 pcm | -3 365 pcm | -3 499 pcm | -3 644 pcm | -3 798 pcm | -3 965 pcm | -4 145 pcm | -4 341 pcm | -4 555 pcm | -4 792 pcm | -5 055 pcm | -5 351 pcm | -5 683 pcm | -6 063 pcm | -6 103 pcm |
| KB221 [A] | CB = 721 ppm | -3 232 pcm | -3 362 pcm | -3 499 pcm | -3 646 pcm | -3 803 pcm | -3 972 pcm | -4 155 pcm | -4 353 pcm | -4 570 pcm | -4 809 pcm | -5 074 pcm | -5 371 pcm | -5 705 pcm | -6 087 pcm | -6 128 pcm |
| KB222 [A] | CB = 721 ppm | -3 169 pcm | -3 297 pcm | -3 433 pcm | -3 578 pcm | -3 732 pcm | -3 899 pcm | -4 080 pcm | -4 276 pcm | -4 491 pcm | -4 727 pcm | -4 990 pcm | -5 284 pcm | -5 616 pcm | -5 995 pcm | -6 034 pcm |
| KB223 [A] | CB = 721 ppm | -3 321 pcm | -3 449 pcm | -3 586 pcm | -3 731 pcm | -3 887 pcm | -4 056 pcm | -4 238 pcm | -4 436 pcm | -4 653 pcm | -4 892 pcm | -5 158 pcm | -5 455 pcm | -5 791 pcm | -6 174 pcm | -6 215 pcm |
| | Mean | -3 412 pcm | -3 539 pcm | -3 673 pcm | -3 816 pcm | -3 969 pcm | -4 135 pcm | -4 313 pcm | -4 507 pcm | -4 720 pcm | -4 954 pcm | -5 215 pcm | -5 506 pcm | -5 835 pcm | -6 212 pcm | -6 252 pcm |
| | 5th %tile | -4 156 pcm | -4 277 pcm | -4 405 pcm | -4 541 pcm | -4 687 pcm | -4 843 pcm | -5 012 pcm | -5 196 pcm | -5 397 pcm | -5 619 pcm | -5 865 pcm | -6 141 pcm | -6 467 pcm | -6 847 pcm | -6 888 pcm |
| | 95th %tile | -3 050 pcm | -3 176 pcm | -3 309 pcm | -3 452 pcm | -3 604 pcm | -3 768 pcm | -3 947 pcm | -4 141 pcm | -4 354 pcm | -4 588 pcm | -4 850 pcm | -5 141 pcm | -5 471 pcm | -5 849 pcm | -5 889 pcm |

## **Appendix G4:** Reactivity during Cooldown from Hot Shutdown (286°C) down to RRA Conditions (155°C), at EOL, with All Rods Inserted

**Reactivity Change due to Temperature Reduction (@ EOL, from HZP, ARI, $C_B$ = 10 ppm)**

| Cycle | Moderator Temperature | 155.0 °C | 165.0 °C | 175.0 °C | 185.0 °C | 195.0 °C | 205.0 °C | 215.0 °C | 225.0 °C | 235.0 °C | 245.0 °C | 255.0 °C | 265.0 °C | 275.0 °C | 285.0 °C | AFI 286°C |
|---|---|---|---|---|---|---|---|---|---|---|---|---|---|---|---|---|
| KB118 [A] | CB = 10 ppm | 4 634 pcm | 4 405 pcm | 4 165 pcm | 3 911 pcm | 3 640 pcm | 3 352 pcm | 3 045 pcm | 2 718 pcm | 2 365 pcm | 1 986 pcm | 1 577 pcm | 1 133 pcm | 630 pcm | 60 pcm | 0 pcm |
| KB119 [A] | CB = 10 ppm | 4 610 pcm | 4 384 pcm | 4 146 pcm | 3 894 pcm | 3 625 pcm | 3 340 pcm | 3 034 pcm | 2 708 pcm | 2 358 pcm | 1 981 pcm | 1 573 pcm | 1 130 pcm | 628 pcm | 60 pcm | 0 pcm |
| KB120 [W] | CB = 15 ppm | 4 651 pcm | 4 422 pcm | 4 178 pcm | 3 921 pcm | 3 649 pcm | 3 359 pcm | 3 049 pcm | 2 721 pcm | 2 367 pcm | 1 987 pcm | 1 577 pcm | 1 134 pcm | 630 pcm | 61 pcm | 0 pcm |
| KB121 [W] | CB = 15 ppm | 4 707 pcm | 4 473 pcm | 4 226 pcm | 3 964 pcm | 3 687 pcm | 3 393 pcm | 3 080 pcm | 2 747 pcm | 2 389 pcm | 2 005 pcm | 1 592 pcm | 1 143 pcm | 636 pcm | 61 pcm | 0 pcm |
| KB122 [W] | CB = 15 ppm | 4 631 pcm | 4 403 pcm | 4 163 pcm | 3 908 pcm | 3 636 pcm | 3 349 pcm | 3 042 pcm | 2 714 pcm | 2 362 pcm | 1 984 pcm | 1 575 pcm | 1 132 pcm | 629 pcm | 61 pcm | 0 pcm |
| KB123 [W] | CB = 15 ppm | 4 647 pcm | 4 417 pcm | 4 175 pcm | 3 918 pcm | 3 646 pcm | 3 357 pcm | 3 049 pcm | 2 719 pcm | 2 366 pcm | 1 987 pcm | 1 577 pcm | 1 132 pcm | 630 pcm | 60 pcm | 0 pcm |
| KB218 [A] | CB = 10 ppm | 4 630 pcm | 4 403 pcm | 4 163 pcm | 3 908 pcm | 3 638 pcm | 3 350 pcm | 3 043 pcm | 2 715 pcm | 2 363 pcm | 1 985 pcm | 1 575 pcm | 1 131 pcm | 629 pcm | 59 pcm | 0 pcm |
| KB219 [A] | CB = 10 ppm | 4 652 pcm | 4 425 pcm | 4 183 pcm | 3 927 pcm | 3 656 pcm | 3 366 pcm | 3 057 pcm | 2 728 pcm | 2 374 pcm | 1 994 pcm | 1 583 pcm | 1 137 pcm | 632 pcm | 60 pcm | 0 pcm |
| KB220 [A] | CB = 10 ppm | 4 641 pcm | 4 413 pcm | 4 173 pcm | 3 919 pcm | 3 647 pcm | 3 360 pcm | 3 052 pcm | 2 723 pcm | 2 370 pcm | 1 991 pcm | 1 581 pcm | 1 135 pcm | 631 pcm | 60 pcm | 0 pcm |
| KB221 [A] | CB = 10 ppm | 4 647 pcm | 4 418 pcm | 4 177 pcm | 3 921 pcm | 3 649 pcm | 3 360 pcm | 3 052 pcm | 2 723 pcm | 2 370 pcm | 1 990 pcm | 1 580 pcm | 1 134 pcm | 630 pcm | 60 pcm | 0 pcm |
| KB222 [A] | CB = 10 ppm | 4 628 pcm | 4 401 pcm | 4 160 pcm | 3 905 pcm | 3 635 pcm | 3 348 pcm | 3 041 pcm | 2 713 pcm | 2 362 pcm | 1 983 pcm | 1 574 pcm | 1 131 pcm | 628 pcm | 59 pcm | 0 pcm |
| KB223 [A] | CB = 10 ppm | 4 634 pcm | 4 407 pcm | 4 166 pcm | 3 912 pcm | 3 641 pcm | 3 353 pcm | 3 046 pcm | 2 718 pcm | 2 366 pcm | 1 987 pcm | 1 578 pcm | 1 132 pcm | 630 pcm | 60 pcm | 0 pcm |
| **Unit 1** | Mean | 4 647 pcm | 4 417 pcm | 4 175 pcm | 3 919 pcm | 3 647 pcm | 3 358 pcm | 3 050 pcm | 2 721 pcm | 2 368 pcm | 1 988 pcm | 1 578 pcm | 1 134 pcm | 631 pcm | 61 pcm | 0 pcm |
| | 5th %tile | 4 615 pcm | 4 389 pcm | 4 150 pcm | 3 897 pcm | 3 628 pcm | 3 342 pcm | 3 036 pcm | 2 709 pcm | 2 359 pcm | 1 981 pcm | 1 573 pcm | 1 130 pcm | 628 pcm | 60 pcm | 0 pcm |
| | 95th %tile | 4 693 pcm | 4 460 pcm | 4 214 pcm | 3 953 pcm | 3 678 pcm | 3 385 pcm | 3 072 pcm | 2 740 pcm | 2 383 pcm | 2 001 pcm | 1 588 pcm | 1 140 pcm | 635 pcm | 61 pcm | 0 pcm |
| **Unit 2** | Mean | 4 639 pcm | 4 411 pcm | 4 170 pcm | 3 915 pcm | 3 644 pcm | 3 356 pcm | 3 049 pcm | 2 720 pcm | 2 368 pcm | 1 988 pcm | 1 578 pcm | 1 133 pcm | 630 pcm | 60 pcm | 0 pcm |
| | 5th %tile | 4 629 pcm | 4 401 pcm | 4 161 pcm | 3 906 pcm | 3 636 pcm | 3 349 pcm | 3 042 pcm | 2 714 pcm | 2 362 pcm | 1 983 pcm | 1 575 pcm | 1 131 pcm | 628 pcm | 59 pcm | 0 pcm |
| | 95th %tile | 4 651 pcm | 4 423 pcm | 4 182 pcm | 3 926 pcm | 3 654 pcm | 3 364 pcm | 3 056 pcm | 2 727 pcm | 2 373 pcm | 1 993 pcm | 1 582 pcm | 1 136 pcm | 632 pcm | 60 pcm | 0 pcm |
| **Both Units** | Mean (EOL) | 4 643 pcm | 4 414 pcm | 4 173 pcm | 3 917 pcm | 3 646 pcm | **3 357 pcm** | 3 049 pcm | 2 721 pcm | 2 368 pcm | 1 988 pcm | 1 578 pcm | 1 134 pcm | 630 pcm | 60 pcm | 0 pcm |
| | 5th %tile (EOL) | 4 620 pcm | 4 393 pcm | 4 154 pcm | 3 900 pcm | 3 631 pcm | 3 345 pcm | 3 038 pcm | 2 711 pcm | 2 360 pcm | 1 982 pcm | 1 574 pcm | 1 130 pcm | 628 pcm | 59 pcm | 0 pcm |
| | 95th %tile (EOL) | 4 677 pcm | 4 446 pcm | 4 202 pcm | 3 944 pcm | 3 670 pcm | **3 378 pcm** | 3 068 pcm | 2 737 pcm | 2 381 pcm | 1 999 pcm | 1 587 pcm | 1 139 pcm | 634 pcm | 61 pcm | 0 pcm |
| | Standard Deviation | 24 pcm | 21 pcm | 19 pcm | 17 pcm | 15 pcm | **13 pcm** | 11 pcm | 10 pcm | 8 pcm | 7 pcm | 5 pcm | 3 pcm | 2 pcm | 1 pcm | 0 pcm |

**Reactivity due to Temperature Reduction (as Calculated by SCIENCE @EOL, ARI, $C_B$ = 10 ppm)**

| Cycle | Moderator Temperature | 155.0 °C | 165.0 °C | 175.0 °C | 185.0 °C | 195.0 °C | 205.0 °C | 215.0 °C | 225.0 °C | 235.0 °C | 245.0 °C | 255.0 °C | 265.0 °C | 275.0 °C | 285.0 °C | AFI 286°C |
|---|---|---|---|---|---|---|---|---|---|---|---|---|---|---|---|---|
| KB118 [A] | CB = 10 ppm | -1 024 pcm | -1 252 pcm | -1 493 pcm | -1 747 pcm | -2 018 pcm | -2 306 pcm | -2 613 pcm | -2 940 pcm | -3 293 pcm | -3 672 pcm | -4 081 pcm | -4 525 pcm | -5 028 pcm | -5 598 pcm | -5 658 pcm |
| KB119 [A] | CB = 10 ppm | -936 pcm | -1 161 pcm | -1 399 pcm | -1 652 pcm | -1 920 pcm | -2 206 pcm | -2 512 pcm | -2 837 pcm | -3 187 pcm | -3 565 pcm | -3 973 pcm | -4 416 pcm | -4 917 pcm | -5 485 pcm | -5 545 pcm |
| KB120 [W] | CB = 15 ppm | -1 863 pcm | -2 093 pcm | -2 336 pcm | -2 594 pcm | -2 866 pcm | -3 156 pcm | -3 465 pcm | -3 794 pcm | -4 147 pcm | -4 527 pcm | -4 937 pcm | -5 381 pcm | -5 884 pcm | -6 453 pcm | -6 514 pcm |
| KB121 [W] | CB = 15 ppm | -1 708 pcm | -1 942 pcm | -2 189 pcm | -2 451 pcm | -2 727 pcm | -3 022 pcm | -3 335 pcm | -3 668 pcm | -4 026 pcm | -4 409 pcm | -4 823 pcm | -5 272 pcm | -5 779 pcm | -6 354 pcm | -6 415 pcm |
| KB122 [W] | CB = 15 ppm | -1 467 pcm | -1 695 pcm | -1 936 pcm | -2 191 pcm | -2 462 pcm | -2 750 pcm | -3 057 pcm | -3 385 pcm | -3 737 pcm | -4 115 pcm | -4 524 pcm | -4 967 pcm | -5 470 pcm | -6 038 pcm | -6 099 pcm |
| KB123 [W] | CB = 15 ppm | -1 599 pcm | -1 829 pcm | -2 071 pcm | -2 328 pcm | -2 600 pcm | -2 889 pcm | -3 197 pcm | -3 527 pcm | -3 880 pcm | -4 259 pcm | -4 669 pcm | -5 114 pcm | -5 617 pcm | -6 186 pcm | -6 246 pcm |
| KB218 [A] | CB = 10 ppm | -1 083 pcm | -1 310 pcm | -1 550 pcm | -1 805 pcm | -2 075 pcm | -2 363 pcm | -2 669 pcm | -2 997 pcm | -3 350 pcm | -3 728 pcm | -4 137 pcm | -4 582 pcm | -5 084 pcm | -5 654 pcm | -5 713 pcm |
| KB219 [A] | CB = 10 ppm | -975 pcm | -1 203 pcm | -1 445 pcm | -1 700 pcm | -1 972 pcm | -2 262 pcm | -2 570 pcm | -2 900 pcm | -3 254 pcm | -3 633 pcm | -4 045 pcm | -4 491 pcm | -4 996 pcm | -5 568 pcm | -5 628 pcm |
| KB220 [A] | CB = 10 ppm | -1 140 pcm | -1 367 pcm | -1 607 pcm | -1 862 pcm | -2 134 pcm | -2 421 pcm | -2 728 pcm | -3 058 pcm | -3 410 pcm | -3 790 pcm | -4 200 pcm | -4 646 pcm | -5 150 pcm | -5 721 pcm | -5 781 pcm |
| KB221 [A] | CB = 10 ppm | -1 001 pcm | -1 230 pcm | -1 471 pcm | -1 727 pcm | -1 999 pcm | -2 288 pcm | -2 596 pcm | -2 925 pcm | -3 278 pcm | -3 658 pcm | -4 068 pcm | -4 514 pcm | -5 018 pcm | -5 588 pcm | -5 648 pcm |
| KB222 [A] | CB = 10 ppm | -1 123 pcm | -1 351 pcm | -1 592 pcm | -1 846 pcm | -2 117 pcm | -2 403 pcm | -2 711 pcm | -3 039 pcm | -3 390 pcm | -3 769 pcm | -4 178 pcm | -4 621 pcm | -5 124 pcm | -5 693 pcm | -5 752 pcm |
| KB223 [A] | CB = 10 ppm | -1 089 pcm | -1 316 pcm | -1 557 pcm | -1 811 pcm | -2 081 pcm | -2 370 pcm | -2 677 pcm | -3 005 pcm | -3 357 pcm | -3 736 pcm | -4 145 pcm | -4 590 pcm | -5 093 pcm | -5 662 pcm | -5 723 pcm |
| | Mean | -1 251 pcm | -1 479 pcm | -1 721 pcm | -1 976 pcm | -2 248 pcm | -2 536 pcm | -2 844 pcm | -3 173 pcm | -3 526 pcm | -3 905 pcm | -4 315 pcm | -4 760 pcm | -5 263 pcm | -5 833 pcm | -5 893 pcm |
| | 5th %tile | -1 778 pcm | -2 010 pcm | -2 255 pcm | -2 515 pcm | -2 790 pcm | -3 082 pcm | -3 393 pcm | -3 724 pcm | -4 080 pcm | -4 462 pcm | -4 874 pcm | -5 321 pcm | -5 826 pcm | -6 398 pcm | -6 460 pcm |
| | 95th %tile | -958 pcm | -1 184 pcm | -1 424 pcm | -1 679 pcm | -1 949 pcm | -2 237 pcm | -2 544 pcm | -2 872 pcm | -3 224 pcm | -3 602 pcm | -4 013 pcm | -4 457 pcm | -4 960 pcm | -5 531 pcm | -5 591 pcm |

## Appendix H: Koeberg Simulator Benchmarking of Maanshan Event

Koeberg employs two plant simulators which are used for operator training. The simulators are MAPS-L3 simulators which are primarily designed to train the reactor operators and were not configured with engineering analysis in mind. In order to ensure that the simulator provided an adequate model to represent the cooldown and depressurization in an ELAP transient, the Maanshan event provided an ideal benchmarking opportunity for an SBO, or at least for the initial stages of an ELAP.

Historically there has already been a station black-out (SBO) event which occurred on a PWR reactor with a very similar design to that of Koeberg. In 2001, Maanshan Unit 1 experienced a SBO for approximately two hours (T-AEC, 2001). On the 17$^{th}$ March 2001, the plant experienced a loss of all of the main off-site lines power due to salt-laden sea mist, leading to grid instability. The units were tripped and the power supply was initially swapped over to the alternative back-up off-site power supply. However in the early morning of the following day (at 00:45 am) all off-site power was lost. The emergency electrical trains automatically swapped over to the redundant emergency diesel generators (EDGs), but on Unit 1, both EDGs failed to start: one due to a bus grounding fault, and the other due to a loss of power to its exciter. This led to a loss of all AC power to the Unit 1 essential power supplies, plunging the unit into a station blackout for just over two hours. The SBO event finished once the swing diesel was lined up to one of the essential power supplies (by 02:54 am) which effectively terminated the SBO transient.

An ELAP is essentially a prolonged or SBO. This particular event provides a good benchmark for the initial thermo-hydraulic response of a PWR reactor, in particular Koeberg, due to their design similarities, during the initial phase of an ELAP event. Both Maanshan units, in Taiwan, are Westinghouse PWRs both with a very similar design and thermal capacity rating to the two Koeberg units. The thermal power rating of the Maanshan units (2950 $MW_t$) is similar to the thermal power rating to the Koeberg units (2775 $MW_t$). While Koeberg is a Framatome 3-loop CPY PWR design, the nuclear island design for the Maanshan units is based on the Westinghouse 3-loop PWR (model 54F) technology. Although the Westinghouse emergency core cooling systems are not the same as those on the Framatome CPY plants, because they are unpowered during this particular transient, any difference in the active emergency core cooling systems (ECCS) is irrelevant. Only the two safeguard systems that don't require electrical supplies were available, namely the turbine driven feed water pump, and the accumulators, which are essentially the same for both designs.

The bench-marking is primarily focuses on the two thermodynamic parameters that are required as input for the reactivity analysis, specifically primary pressure and moderator core temperature. The primary pressure dictates the quantity of accumulator boron injection, and the drop in moderator temperature to determine the reactivity insertion.

The mitigation of the Maanshan SBO was achieved by the cooling of the core through steam generator (SG) steam dump to atmosphere, and providing feed-water to the SGs which was achieved with the auxiliary feed-water turbine pump. The turbine pump started to feed the steam generators 10 minutes after the SBO. Primary system cooldown was initiated after 45 minutes by opening the SG steam dump to atmosphere on one of the SGs, at a cooldown rate of 80 $^{o}$C/hour, until the SG pressure of 1.2 MPa was reached (US-NRC, 2013). This response was similar to guidance provided in the Koeberg accident procedure at the time, although this procedure has been subsequently revised at Koeberg, to account for improved nitrogen expansion modelling in the accumulators. The cooldown and depressurization was terminated once the secondary pressure in the SG reached 1.2 MPa. This is to prevent any inadvertent risk of nitrogen injection from the accumulators into the primary system, which could arrest the natural circulation in the primary system.

One important issue to consider is the 20 hour delay from the original reactor trip, which was initiated when the loss of offsite power occurred. The SBO and hence the associated cooldown will often only commence once all power was lost, in this event 20 hours later. The cooldown was initially initiated on one SG, and then on the other two. The secondary side cooldown profile was approximated, and the primary resultant pressure compared with the available data from the actual event. The simulation resulted in good correlation with the primary pressure transient up to and including the formation of the steam bubble in the reactor head. Thereafter the simulator primary side depressurization was slower than the actual event, indicating that the reactor head thermal losses maybe a little inaccurate. However, the simulator's predicted primary pressure reduction rate was reduced, which will result in a delay in the accumulator injection and hence conservative from a reactivity perspective.

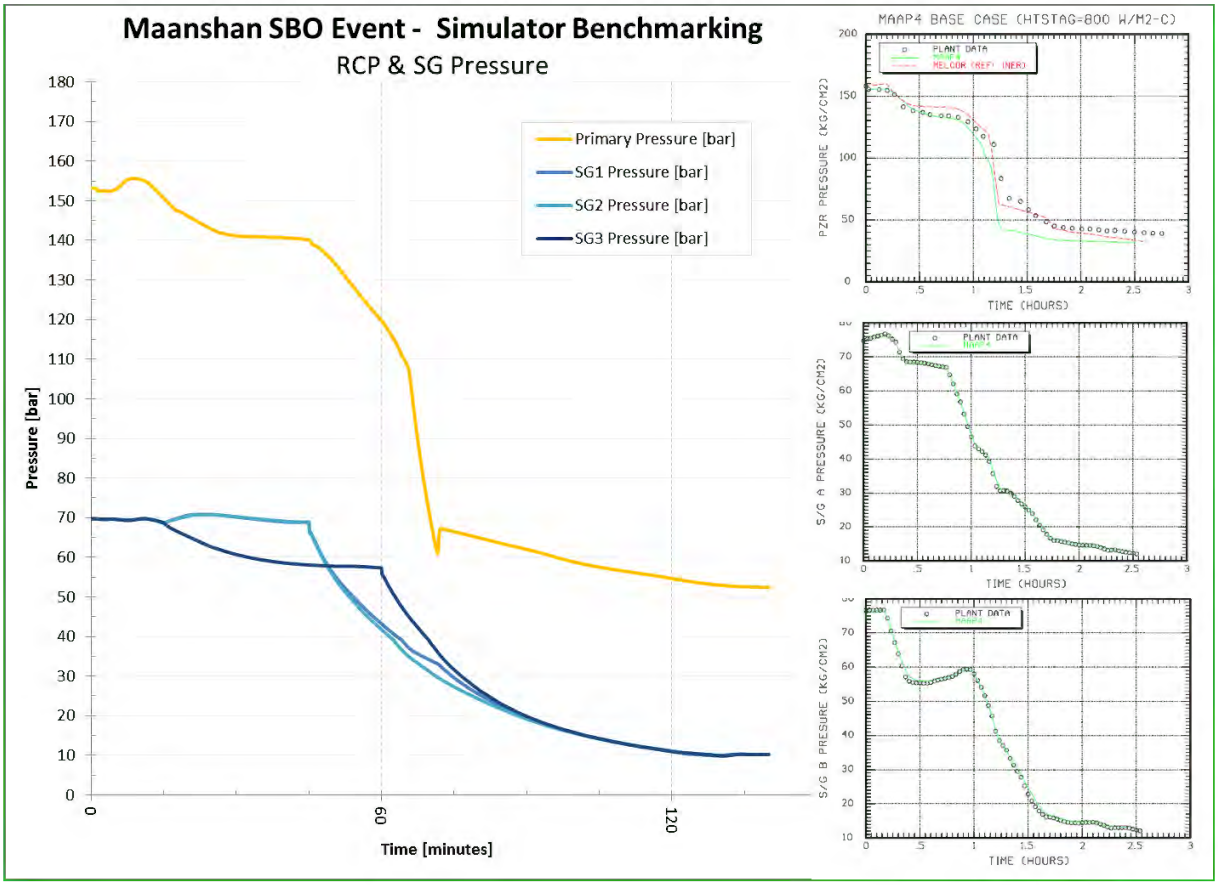


***Figure 18:*** *Maanshan SBO transient RCP pressure and SG pressure benchmarking*

A comparison between the Koeberg simulator results and the Maanshan event parameters showed a reasonable correlation. The only significant difference was the rate of depressurization of the reactor coolant system (RCP) system after steam bubble formation in the head. The actual event resulted in a faster primary system depressurization than the simulator run predicted. This is probably due to the model assuming lower thermal conductivity and heat transfer rate from the reactor head to the containment atmosphere, and/or potentially due to the reactor head cooling configuration. However, the simulated depressurization was delayed, which is penalizing, or conservative, regarding accumulator injection rate. Therefore this was considered acceptable while recognizing that there is a potential for refinement, if required later.

## List of Acronyms

| | |
|---|---|
| AC | Alternating Current |
| AIC | Silver, iridium and cadmium alloy |
| APOLLO2 | A code package for PWR neutronics calculations developed by CEA |
| APOLLO2-F | A customized code package of the SCIENCE Code used for Framatome PWRs |
| ASG | Auxiliary Feed-water System (Framatome System Abbreviation) |
| BDBA | Beyond Design Basis Accident |
| BEACON | Operational Core Support System Code developed for PWRs |
| BOL | Beginning of Life (Fuel Cycle) |
| BLX | Beginning of Life once Xenon has stabilized (Fuel Cycle) |
| BWR | Boiling Water Reactor |
| CEA | Commissariat a l'Energie Atomique |
| CFR | Code of Federal Regulations (US-NRC) |
| CPY | 900 MW Framatome PWR Design Identifier |
| DC | Direct Current |
| DBA | Design Basis Accident |
| DEC | Design Extension Conditions (similar to Beyond Design Basis Accident) |
| ECA | Emergency Contingency Procedures |
| ECCS | Emergency Core Cooling System |
| EDF | Électricité de France |
| EDG | Emergency Diesel Generator |
| ELAP | Extended Loss of All AC Power |
| EOL | End of Life (Fuel Cycle) |
| ESKOM | Electricity Supply Commission (Utility operating Koeberg NPP) |
| FSG | Functional Support Guidelines |
| FTC | Fuel Temperature Co-efficient |
| GCT | Secondary Steam Dump (Framatome System Abbreviation) |
| GDC | General Design Criteria (US-NRC) |
| HWR | Heavy Water Reactor |
| HZP | Hot Zero Power |
| IAEA | International Atomic Energy Agency |
| LHA | Essential Power Switchboard – Train A (Framatome System Abbreviation) |
| LHB | Essential Power Switchboard – Train B (Framatome System Abbreviation) |
| LOCA | Loss of Reactor Coolant Accident |
| LOOP | Loss of Off-site Power |
| LWR | Light Water Reactor |
| MAAP | Modular Accident Analysis Program |
| MAPS-L3 | Make of PWR Simulator |
| MOL | Middle of Life (Fuel Cycle) |
| MTC | Moderator Temperature Co-efficient |
| NNR | National Nuclear Regulator (South Africa) |
| NPP | Nuclear Power Plant |
| PDB | Koeberg Physics Data-books |
| PORV | Power Operated Relief Valve (Pressurizer) |
| PSA | Probabilistic Safety Assessment |
| PWR | Pressurized Water Reactor |
| PWROG | Pressurized Water Reactor Owners Group |
| RRA | Shutdown Cooling System (Framatome System Abbreviation) |
| RBMK | Russian Graphite-Moderated Nuclear Power Reactor Design |
| RCCA | Rod Cluster Control Assemblies |
| RCP | Reactor Coolant System (Framatome System Abbreviation) |

| | |
|---|---|
| RELAP | A Best-estimate Transient/Accident Simulation Code for LWRs |
| RSS | Root Sum Square |
| SBO | Station Blackout |
| SCIENCE | A Neutronics Code Package used for PWR neutronics calculations for Framatome PWRs. |
| SCRAM | Reactor Trip |
| SMART | A Code Package of the SCIENCE Code |
| SG | Steam Generator |
| SEBIM | Supplier and type of Power Operated Relief Valve (for Pressurizer relief) |
| SL-1 | Stationary Low-Power Reactor Number One, or the Argonne Low Power Reactor (ALPR) |
| TMI | Three Mile Island Nuclear Power Plant |
| US-NRC | United States Nuclear Regulatory Commission |
| VVER | Russian PWR design |
| WENRA | Western European Nuclear Regulators' Association |